UC Davis
UC Davis Electronic Theses and Dissertations

Title

Identifying the Biological Relevance of Fatty Acid Metabolites in Regulating or Promoting Disease

Permalink

Author

McReynolds, Cynthia

Publication Date

2021

Peer reviewed|Thesis/dissertation

Identifying the Biological Relevance of Fatty Acid Metabolites in Regulating or Promoting Disease

By

CYNTHIA BROWN McREYNOLDS
DISSERTATION

Submitted in partial satisfaction of the requirements for the degree of

DOCTOR OF PHILOSOPHY

in

Pharmacology and Toxicology

in the

OFFICE OF GRADUATE STUDIES

of the

UNIVERSITY OF CALIFORNIA

DAVIS

Approved:

_____

Bruce Hammock, Chair

_____

Heike Wulff

_____

Ameer Taha

Committee in Charge

2021

i

Contents

List of Figures

List of Tables

Acknowledgements

Many people have shaped and guided my path through graduate school, and I am grateful to all of the criticism and support along the way that has helped me become a better scientist. Deciding to go back to school after almost 15 years away was a big decision, and I could not have been successful without significant mentorship and emotional support along the way.

First and foremost, I would like to thank my PI, Bruce Hammock. I started working in his lab as a grant administrator, and without his initial encouragement, I would never have found the courage to embark on my life-long goal of becoming a PhD scientist. The exciting science, constructive criticism, and ideas for future research along the way were fun and very much appreciated.

All the members of the Hammock, especially Sean Kodani, Christophe Morisseau, Natalia Vasylieva, Candace Bever, Sung Hee Hwang and Jun Yang, were extremely supportive and patient as I reacquainted myself with lab work.

Academically, many classes and interactions helped inform and guide my research. Specifically, Drs. Aiming Yu, Heather Knych, and Sheila David guided my research interests in graduate school. My first rotation was in Dr. Yu's lab under the supervision of his graduate student, Joe Jilek. I was very nervous, but Joe was a great mentor, and I appreciated the welcoming and supportive environment that Dr. Yu provided in his lab. They both helped me develop a foundation in pharmacokinetics that I have incorporated in all areas of my research described here. Dr. Knych further helped me advance my interest and knowledge in PK. I especially appreciate all the resources she contributed especially to Chapter 2. By far the most challenging, but also my favorite, class in graduate school was Introduction to Chemical Biology, taught by Sheila David. I found Dr. David to be a great instructor and mentor, and I stive to have the passion and knowledge over subject matter that she displays through her teaching. And finally, to my dissertation

committee, Drs. Heike Wulff and Ameer Taha who have provided valuable guidance and suggestions along the way. I additionally want to thank Dr. Wulff for helping me prepare for my Qualifying Exam and additional scientific advice throughout my studies. She has really helped challenge my approach to experimental design and data review.

I have also been fortunate to collaborate with many wonderful scientists. From my colleagues at EicOsis, especially Drs. Glenn Croston, William Schmidt, Irene Cortes-Puch and Robert Gregoire, to co-authors on publications and grants, especially Drs. Alonso Guedes, Alan Buckpitt and Laura Carbone. I have gained valuable information and really enjoyed the times spent designing studies and writing grants. I look forward to more interactions in the future.

Most of all, my thanks and appreciation go out to my family. Without their support I could not have initiated or completed this process.

Dedication:

To Emmaline, Elliot, and Dave

Abstract

There is currently an urgent need for safe and effective treatment options for chronic diseases, especially pain, given that current medicines are accompanied by severe side effects. Bioactive lipid mediators resulting from the metabolism of polyunsaturated fatty acids (PUFA) are controlled by many pathways that maintain homeostasis and prevent disease, and regulation of this pathway presents a novel and safe approach for treating many diseases, including pain. Epoxygenated fatty acids (EpFA), formed through metabolism by cytochrome P450 enzymes, are regulatory lipids that demonstrate largely anti-inflammatory properties that reduce endoplasmic reticulum stress to help resolve disease; however, their utility is limited by rapid degradation by the soluble epoxide hydrolase (sEH) into corresponding vicinal diols. Inhibiting its activity increases concentrations of beneficial EpFA, and often disease states correlate to increased sEH activity that results in decreased concentrations of EpFA in the body.

Research described in this dissertation detail the pharmacological properties of EC1728, a novel soluble epoxide hydrolase inhibitor (sEHI), as an option for pain control in companion animals. The exposure and distribution are described in target animal species and demonstrate that there are differences in exposures between species that need to be considered for drug development. An efficacy study demonstrating pain relief after treatment with EC1728 in dogs with naturally occurring arthritis is also presented. Fundamentally, inhibition of the sEH is thought to offer therapeutic advantages by increasing EpFA; however, the last chapter explores lipidomics profiles in patients with severe COVID-19 disease to advance the idea that metabolism products of EpFA, specifically the diols resulting from linoleic acid metabolism, are also responsible for driving severe inflammatory disease. These studies demonstrate that sEH inhibition is beneficial by both increasing EpFA and decreasing inflammatory diol metabolites.

In summary, pharmacological properties of EC1728 demonstrate suitable properties for developing as a pain-relieving therapy in companion animals, and also validation of sEHI as a therapeutic target by demonstrating inhibition in natural disease in addition to laboratory models. The methods described here of characterizing detailed drug exposure, characterizing efficacy in companion animals with natural disease, as well as identification of biomarkers in disease settings represents a novel approach to drug discovery that may help advance selection of safe and effective treatments for multimodal diseases.

Chapter 1: Epoxy fatty acids are promising targets for treatment of pain, cardiovascular disease and other indications characterized by mitochondrial dysfunction, endoplasmic stress and inflammation.

Authors: Cindy McReynolds[1,2], Christophe Morisseau[1], Karen Wagner[1,2], Bruce Hammock[1,2]*

[1.] Department of Entomology and Nematology, and U.C. Davis Comprehensive Cancer Center, University of California Davis, Davis, CA 95616 USA

[2.] EicOsis, Davis, CA 95616 USA

* Corresponding author. Tel.: +1-530-752-7519

   E-mail address: bdhammock@ucdavis.edu

Introduction
1.1 Production of hormones and other chemical mediators

Lipids are an important component of human health, providing a source of energy, maintaining cellular integrity and acting as regulators of cell signaling. These bioactive lipids include steroids, diacyl glycerol (DAG), sphingolipids, phosphatidylinositol phosphate (PIP), phosphatidylcholine (PC), and polyunsaturated fatty acids (PUFA). They range in function from energy storage and generation through beta-oxidation (PUFA), cellular proliferation (PIP), insulin regulation (DAG), cellular protection (sphingolipids), pulmonary function (PC), and maintaining cell structure (cholesterol). However, the metabolism of these lipids often produces more potent biological mediators than the parent molecule. For example, PUFAs, which circulate through blood as triglycerides or as free fatty acids, can also be incorporated into adipose tissue or the membranes of cells that are further released upon insult or response to cell signaling, and their metabolism produces potent inflammatory and anti-inflammatory compounds that have profound effects on the body. Due to their potent effects, inhibitors that alter their metabolism represent one of the earliest drug targets of the pharmaceutical industry. For example, aspirin was discovered in the late 1800s although its mechanism of action as both a reversible and irreversible cyclooxygenase (COX) inhibitor that blocked the formation of prostaglandins (PG) was not identified until the early 1970s, and is still debated (1). Blocking COX activity and the formation of inflammatory PG compounds resulted in one of the largest selling classes of drugs, NSAIDs, on the market today. In addition to COX metabolism, PUFA are also metabolized by the lipoxygenase (LOX) and cytochrome P450 (CYP450) enzymes that have more recently attracted attention for their potential in modulating disease. LOX inhibitors are targeted for their ability to inhibit the formation of inflammatory leukotrienes, and zileuton, a 5-LOX inhibitor, is used for the treatment of asthma

(2) by blocking the formation of inflammatory leukotrienes. In contrast to COX and LOX metabolism, the CYP branch of PUFA metabolism results in the formation of both inflammatory hydroxylated metabolites as well as ant-inflammatory fatty-acid epoxides (Figure 1.1). Disease altering strategies targeting the CYP450 branch of the pathway focuses on increasing these beneficial epoxy fatty acids (EpFA). However, so far, few drugs specifically targeting this pathway have reached the market, although, several currently approved drugs alter EpFA concentrations through their action on enzymes and their metabolites in the CYP450 branch of the arachidonic acid cascade. This chapter will focus on the biological activity of these largely beneficial lipid epoxides, as well as strategies for developing pharmaceutical interventions to increase their concentrations in the body.

Figure 1.1. Metabolic fate of polyunsaturated fatty acids.

EpFAs biological activities
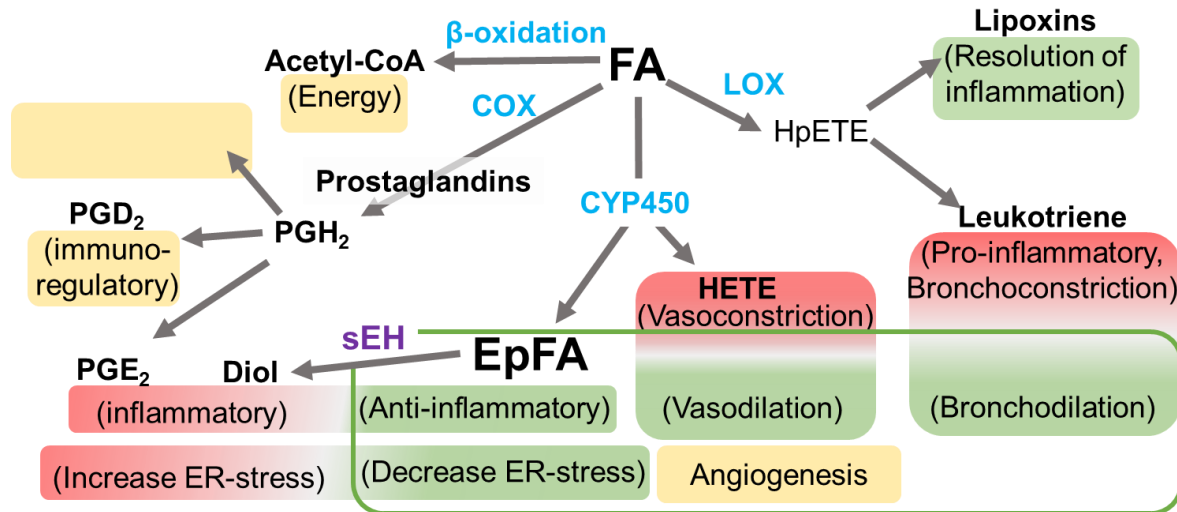
Free fatty acids are primarily metabolized through β-oxidation, Cyclooxygenase (COX), Lipoxygenase (LOX), and CytochromeP450 (CYP450). A simplistic overview of the biological action of the resulting metabolites is shown in parenthesis. **COX 1 and COX 2** metabolize PUFA to PGH2 which is the precursor to other inflammatory prostanoids and thromboxanes that regulate the immune system (PGD_2), increase pain and inflammation (PGE_2) and control platelet aggregation (PHI_2 and TXA_2). (3) **5-LOX** metabolizes PUFA to 5-HpETE or **15-LOX** to 15-HpETE, both are precursors to inflammatory leukotrienes and cytotoxic leukotoxins. These metabolites are important in exacerbating asthma by acting as powerful bronchoconstrictors, and they can also sustain inflammatory reactions through chemotaxis of inflammatory mediators. LOX metabolism of omega-3 fatty acids results in pro-resolving lipid mediators called resolvins, protectins and maresins. (4) **CYP450** metabolizes PUFA to anti-inflammatory epoxy fatty acids (EpFAs), n-terminal hydroxylated n-HETE, ω-1 oxidation, or allylic hydroxylations. 20-HETE regulates blood pressure by acting as a potent vasoconstrictor in kidneys and preventing sodium reabsorption in nephrons (5, 6). The biological significance of mid-chain hydoxylations is less well understood; however, biological significance has been observed with 12-HETE in corneal inflammation and neovascularization (7) (8). Formation of EpFA, particularly if induced, is primarily accomplished by CYP2C and CYP2J subfamily; however, other CYP enzymes can generate EETs. (9) The EpFA act as homeostatic regulators to other metabolites in this pathway by stabilizing mitochondria, reducing ROS, decreasing ER-stress (10) and inflammation (11), regulating the vascular endothelium (12) and increasing bronchodilation (13).

1.2 Polyunsaturated Fatty Acids: the essential fatty acids

PUFA are named for the presence of two or more double bonds in the mid-long chain carbon backbone that ranges in length from 16 to 24 carbons or longer. They are considered essential because the body cannot synthesize them naturally and must consume them in order to maintain health; however, with the proper precursors, PUFAs can be altered and interconverted. Depletion of either omega-3 or -6 PUFA result in serious side effects such as neuronal and vision impairment, skin anomalies, thrombocytopenia and intellectual disability (14). PUFA in the body are either circulating as free fatty acids or incorporated into glycerides and cellular membranes. Upon injury or stress, PUFA are released from cell membranes by phospholipase acetyltransferases (PLA) and other enzymes. PLA2 liberates PUFA from the triglycerides to release free fatty acid (FFA), but also PLC and PLD further act to increase FFA in circulation (Figure 1.2). Once freed from the plasma membrane, FFA are rapidly metabolized by β-oxidation or other enzymatic metabolism (15) (Figure 1.1). As mentioned above, the three main enzymes responsible for non-catabolic metabolism of PUFA are COX, LOX and CYP450. The COX and LOX enzymes form primarily inflammatory mediators, and therapeutic interventions focus on blocking the formation of these compounds. In contrast, the CYP450 metabolism results in the formation of both hypertensive and inflammatory hydroxylated compounds, as well as and anti-hypertensive and anti-inflammatory epoxide compounds. Therapeutic interventions discussed here focus on increasing the concentration of the anti-inflammatory epoxide metabolites.

Figure 1.2. Enzymatic Formation of EpFA.
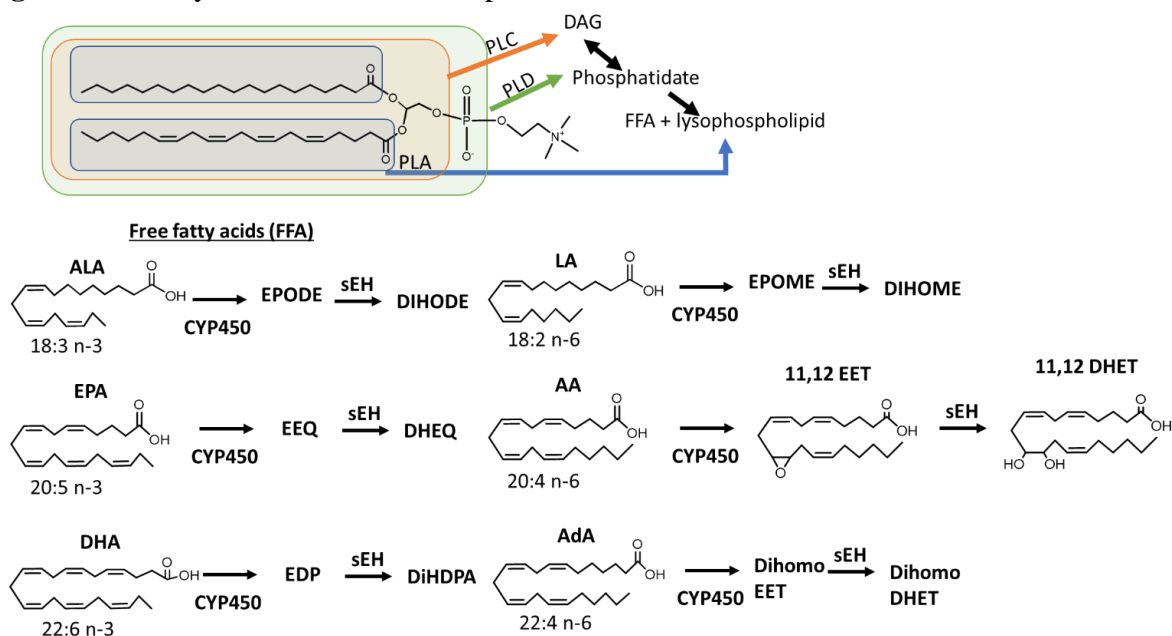
Figure 1.2. Polyunsaturated fatty acids (PUFAs) differ in both structure and function based on number of carbons and location of double bonds. They are incorporated as glycerides in fat cells, cellular membranes or circulating micelles and are liberated to free fatty acids by different phospholipases (PL) that act upon different areas of the glyceride or phospholipid (A). EpFA are formed through the oxidation of FFA by CYP450. The metabolism of Arachidonic Acid (AA, 20:4 n-6) by cytochrome P450 yields EpFAs, epoxyeicosatrienoic acids (EET), which are further degraded by the soluble epoxide hydrolase into dihydroxyeicosatrienoic acids (DHET). The epoxide and diol on the 11,12 position are shown, but similar regioisomers are possible on all the double bonds in the PUFA. The n-6 fatty acid linoleic acid, LA, has been attributed to largely inflammatory epoxides, EPOMES; however, studies show that they are only toxic in the presence of sEH, suggesting that the diols of LA, DIHOMES, are responsible for this inflammatory action. (16) The 18:3 omega-3 fatty acid, linolenic acid (ALA), does not seem to have this same inflammatory action. The omega-6 fatty Adrenic Acid, AdA, is named for its abundance in the adrenal gland. Less is known about this PUFA and its metabolites, although the AdA EpFA, dihomoEETs are thought to regulate blood flow to the adrenal gland.(17) n-3 fatty acids alpha eicosapentaenoic acid (EPA) and docosahexaenoic acid (DHA) form EpFA epoxyeicosatetraenoic acids (EEQs) and epoxydocosapentaenoic acids (EDPs) respectively. Omega-3 EpFA are largely beneficial with anti-inflammatory and pain resolving properties *in vitro* and *in vivo*. Little biological activity has been associated with the diols of Ada (dihomoDHET) or the diols of EPA and DHA, dihydroxyeicosatetraenoic acids (DHEQs) and dihydroxydocosapentaenoic acids (DiHDPAs) respectively. (see (18) for review)

2. Epoxy fatty acids are therapeutic targets for disease

2.1 Epoxy fatty acids (EpFA) are important signaling molecules that are regulated by their metabolism

EpFA are formed from the activity of CYP450, a large class of metabolizing enzymes that oxidize fatty acids as well as xenobiotics using heme as a co-factor. The addition of molecular oxygen results in the formation of compounds from the epoxidation of double bounds, end terminal hydroxylation or allylic oxidation (19) each with unique biologies and roles in disease. EpFA have beneficial effects on maintaining endothelium function, inflammation and cellular oxidative stress. As early as 1986 and continuing through present day, CYP450 metabolites were identified as influencing blood pressure and renal function by regulating vascular smooth muscle proliferation through MAP kinase signaling pathways (20), anti-aggregation of platelets by decreasing leukocyte adhesion to endothelial cells (21), and regulating vascular tone. Vascular tone, in part, is regulated by the balance of hydroxylated and epoxygenated CYP450 PUFA metabolites. The 20-hydroxy-fatty acids (20-HETE) act as vasoconstrictors by hyperpolarizing vascular smooth muscle cells through activation of the protein kinase C pathway, while the epoxy fatty acids hyperpolarize vascular endothelium through activation of voltage-gated potassium (BK) channels. In this way, the two metabolites act as homeostatic regulators to prevent pathological changes in vascular tone (22), (23). Although increased 20-HETE results in endothelium dysfunction and increased hypertension, increased EpFA decrease blood pressure, but has not been shown to cause hypotension (24), (25). This provides strong evidence that EpFA are homeostatic regulators of endothelium function (26, 27). EpFA also show other beneficial biologies, including potent anti-inflammatory effects and decreasing the endoplasmic-reticulum (ER) stress response pathway (28). EpFA act as anti-inflammatory agents by reducing the nuclear translocation of NF-kappaβ,

thereby preventing the transcription of several inflammatory cytokines and synthesis of inflammatory eicosanoids (11),(29). Furthermore, the diol metabolite of EpFA metabolism drives monocyte chemotaxis in response to monocyte chemoattractant protein, MCP-1. Thus, preventing the metabolism of EpFA by the sEH further regulates inflammation by decreasing monocyte infiltration (30). EpFA have demonstrated a wide range of beneficial effects in animal models of disease (31) which is not fully explained by anti-inflammatory or endothelial homeostasis, but possibly explained by the regulation of ER-stress by EpFA. ER-stress is a protective mechanism deployed by the cell to overcome cellular stress and prevent deleterious mutations. The ER-stress pathway is a homeostatic mechanism regulating cellular responses to the presence of increasing misfolded protein resulting from oxidative, physiological, or pathological stressors. Although a fundamental mechanism in maintaining homeostasis, this response is often upregulated in disease, and if not controlled, will result in increased inflammation or activation of cell death pathways. Preventing or reducing the inflammatory and apoptotic branches of ER-stress is associated with many beneficial disease treatments (32), and EpFA have demonstrated the ability to reduce ER-stress. (10) These ubiquitous mechanisms (inflammation, endothelial function, and ER-stress) underlie many diseases and are regulated by EpFA, which may explain why preclinical models investigating the role of EpFA indicate beneficial results in many different diseases when these lipid mediators are maintained.

In normal cell systems, and increasingly in disease, EpFA are rapidly removed from circulation either because they are re-incorporated back in cellular membranes, metabolized by beta-oxidation, or further degraded by epoxide hydrolases. (33) Metabolism enzymes generally increase polarity of compounds to aid in their elimination from the body, and the metabolism of PUFA are no different. After metabolism by the CYP450, the EpFA are further degraded by

epoxide hydrolases into the corresponding polar vicinal diols which diffuse from the cells or are rapidly conjugated and removed from the body. In many diseases, the sEH activity is upregulated compared to healthy controls, thus inhibiting its activity in disease settings indicate a potential target for increasing EpFA as a potential therapy.

The epoxide hydrolases are catalytically active dimers that convert xenobiotics or PUFA epoxides to corresponding diols through an exothermic, 2-step hydrolysis reaction (Figure 1.3) (34).

Figure 1.3. Mechanism of epoxide to diol metabolism by the soluble epoxide hydrolase (sEH).
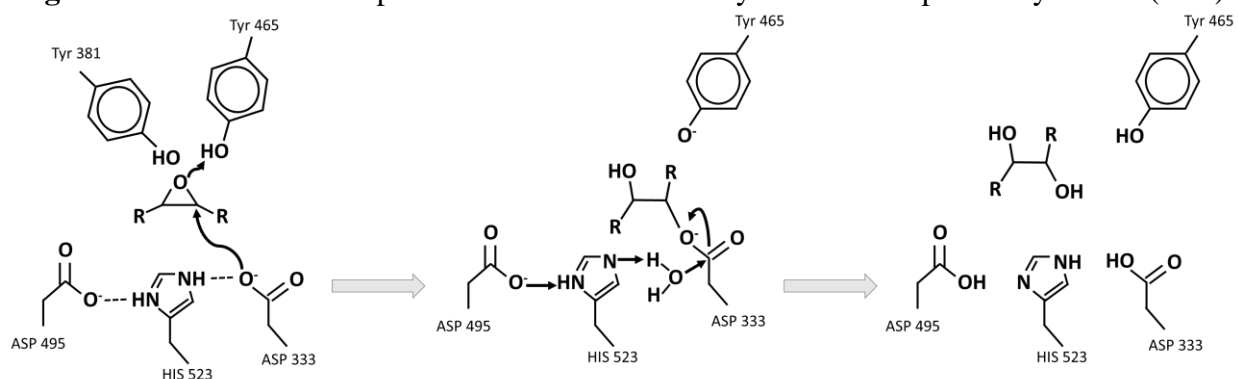
Figure 1.3. Two acidic tyrosines are oriented by pi-stacking to bind to and polarize the epoxide moiety. sEH inhibitors functionally mimic transient intermediates and the transition state of the enzyme (middle panel). The NH groups of the urea, amide, carbamate or other electronegative groups possibly encourage a salt bridge formation, for example between a polarized urea and the catalytic aspartic acid, likely stabilized by hydrogen bonds with the tyrosine. (35)

There are four structurally related isozymes in the epoxide hydrolase family of enzymes (EPHX1 – 4) in mammals, in addition to other enzymes that have hydrolase activity such as the leukotriene A4 hydrolase (LTA4H), cholesterol hydrolase, and Peg1/MEST. LTA4H metabolizes leukotriene A4 into the leukocyte recruiter, leukotriene B4, to help in the resolution of inflammation. While the functions of PEG/MEST and EPHX4 are not known, isozymes EPHX 1-3 are capable of metabolizing EpFA and differ in cellular location and substrate preference. EPHX1 (mEH), is named for its cellular location: it is found in microsomal membrane fractions in tissue and is active on polyaromatic hydrocarbons found in a variety of xenobiotic epoxides and is also capable of metabolizing EpFA. Conversely, EPHX2 is similarly named as the soluble epoxide hydrolase (sEH) after its predominant location in the cytosolic and peroxisomal fractions of the cell. The EH activity is located at the C-terminus portion of the protein, and the N-terminal portion of sEH has phosphatase activity while the N-terminus of mEH is anchored to the membrane. While mEH is capable of metabolizing both aromatic and aliphatic epoxides, catalytic turnover by the sEH is greater for mono and disubstituted epoxides, making EpFA a good substrate for this enzyme. However, trans, di, tri and even tetra-substituted epoxides can be turned over sometimes with a low Km. (36) Cholesterol epoxides and the squalene epoxide precursor to lanosterol are also substrates of mEH, although the cholesterol epoxide hydrolase and lanosterol synthase are the primary routes of metabolism for these compounds. (37) EPHX3 is also capable of hydrolyzing EpFA with similar efficiency (Kcat/Km) as that of sEH, but a >10x higher Km indicates that EpFA of arachidonic acid (AA) and presumably other PUFA are a weak substrate for EPHX3 compared to their affinity for sEH or mEH (38).

2.2 Human polymorphisms altering epoxide hydrolase activity affect EpFA concentrations and correlate epoxides with disease states.

Most EH related mutations in humans that are associated with disease states are associated with EPHX2 (sEH). There are four main mutations that affect enzyme activity, two that do not alter function, and as many as 20 less characterized non-coding mutations that can occur in up to 20% in human populations. (39, 40) The four most common coding mutations result in two gain of function mutations (K55R and C154Y) and two reduced function mutations (R287Q and R103C mutations results in decreased dimerization). These mutations affect the velocity of epoxide hydrolysis while leaving the selectivity for substrate binding and phosphatase activity apparently unchanged (41) (42). Considering that the concentration of the sEH enzyme (ranging from 3 nM in lung to 400 nM in liver) is often higher than that of the EpFA substrate (low nM in tissue (43-45)), and the concentration of EH enzymes, such as EPHX1 and 3, can convert epoxides to diols, it should be taken into consideration that mutations that only slightly affect enzyme efficiency may not significantly affect EpFA concentration. However, mutations in the sEH and prevalence of SNPs associated with different diseases suggest that this enzyme plays an important role in disease, as described below.

Mutations in sEH are biomarkers of anorexia nervosa

In a genome wide association study of patients with anorexia nervosa (AN), investigators identified rare mutations in non-coding regions of the EPHX2 that correlate with disease susceptibility. The activity of the mutations was not determined, but investigations in the levels of epoxide:diol ratios found they were decreased in ill AN patients compared to recovered AN or healthy populations, suggesting an upregulation in the conversion of epoxides to diols. Furthermore, the loss of function mutation, R287Q, occurred less frequently in AN patients

11

compared to healthy populations, further correlating increased sEH activity to higher risk of severe AN. (46-49) Although the exact mechanism for the involvement of EpFA in AN is unknown, considering the impacts of diet and aversion to food in this disease, understanding the role of altered lipid signaling in this disease is of increasing interest.

Reduced sEH activity protects against familial hypercholesterolemia

Familial hypercholesterolemia (FH) is a hereditary disease that causes increased plasma cholesterol concentrations resulting from a defective hepatic low-density lipoprotein receptor (LDLR). In a targeted analysis approach that studied the prevalence of the reduced function sEH mutation, R287Q, in 8 generations of families with FH, Sato et al. discovered that family members with the R287Q mutation had normal cholesterol levels compared to members with the normal 287R allele. Cholesterol was unchanged in healthy humans with the R287Q mutation. (50). Preclinical investigations further support the role that sEH has in reverse cholesterol transport through regulation of the ATP binding cassette transporter A1 (ABCA1), a membrane protein that regulates high-density lipoproteins (HDL) and delivers cholesterol from tissues to the liver for excretion and could possibly explain the protective effects on inhibiting its activity in LDLR related disease. For example, in Ldlr$^{-/-}$ mice that mimic the FH disease, treatment with the sEH inhibitor (sEHI), t-AUCB, decreased atherosclerosis plaques through increasing HDL synthesis and efflux of cholesterol from adipose lesions compared to vehicle treated controls. Further investigation demonstrated that sEHI treated mice had increased ATP binding cassette transporter A1 which is responsible for HDL synthesis through efflux of cellular cholesterol to extracellular apoA1 (51). Though the mechanism for this increase was not investigated, it is possible that the sEHI increases cholesterol in the cell (52), which can lead to upregulation of ABCA1 expression (53).

sEH mutations are associated with both positive and negative outcome measures in vascular disease

Impaired vascular function contributes to heart disease, age-related vascular decline, blood pressure and stroke. EpFA act as vasodilators by opening calcium-activated potassium channels that relax the vascular smooth muscle and are thought to mitigate vascular disease (54); therefore, it is hypothesized that decreased EpFA would contribute to heart disease, and in fact gain-of-function sEH polymorphisms are associated with increased cardiovascular diseases. For example, pregnant women with preeclampsia had higher frequency of the K55R gain of function mutation and lower methylation of the EPHX2 promotor region, causing higher expression, than healthy pregnant women (55). In another study that analyzed sEH polymorphisms with frequency of stroke in African American and Caucasian populations participating in the Atherosclerosis Risk in Communities study, investigators identified a rare EPHX2 mutation in African Americans that was not found in Caucasian populations. The mutation resulted in increased sEH activity and a 2-3-fold increased risk of stroke. Although the infrequency of the mutation complicated statistical analysis, and larger sample sizes were needed to determine significance. Additional haplotypes in the sEH gene correlated with both increased and decreased risk of stroke in both races. (39) Although the effect of these gene sequences on enzyme activity is not known, further studies analyzed site-directed mutagenesis on survival rates of ischemic cells *in vivo* and found that decreased sEH activity with the R287Q mutant conferred increased survival after inducing a simulated stroke environment of depleted glucose and oxygen. (56) This mutation was also associated with lower risk of stroke in Europeans. (57) Although a large Danish study failed to identify correlations in sEH SNPs and stroke, myocardial infarction or ischemic heart disease. (58) A large study in Swedish men found correlations between the gain-of-function mutation, K55R,

with increased risk of stroke. (59) Additionally, Hawaiian Asians with dementia but without prior ischemic injury compared to healthy age-matched controls had increased 14,15 DHET in cortical brain tissue from patients with dementia; however, heterozygous carriers of the reduced function R287Q SNP had increased markers for plaques compared to healthy patients. (60) These data are at odds for understanding if sEH activity protects or contributes to the progress of AD especially considering that dementia correlates with a decreased EET:DHET ratio, suggesting a negative role of sEH in this disease. However, because the R287Q mutation affects dimerization, it's possible that these heterozygous carriers still have functional sEH protein.

In addition to the sEH, the mEH also hydrolyses EpFA into corresponding diols, although with much less efficiency. As discussed later, the association of the mEH in the lipophilic endoplasmic reticulum membrane and with the cytochrome P450 that oxidize epoxy fatty acids may result in greater mEH contribution to diol formation than anticipated from the concentration and kinetic constants of the mEH. Mutations in mEH are also associated with several diseases, including cancer, preeclampsia, seizure, neurological disease, drug-dependence and COPD. However, because this enzyme is primarily responsible for metabolizing aromatic xenobiotic epoxides, it is uncertain if these associations are a result of decreased epoxides in the body, or from accumulation of toxic xenobiotics (reviewed in (61)). Interestingly, sEH expression in the brain is mostly localized in glial cells of the brain, while mEH is found more widely throughout the brain, suggesting either a specific role of sEH or more significant contribution of mEH to EpFA metabolism in the brain. (62) Recent studies demonstrate that sEH activity outside the brain can influence depression. In this study, overexpression of sEH in the liver resulted in increased depression in mice, and genetic deletion of sEH in the liver had a positive effect in treating stress-

induced depression. This study suggests that peripheral-acting EpFA can influence CNS diseases. (63)

2.3 Laboratory knockout models identify beneficial effects of increasing EpFA in treating preclinical models of disease.

A homozygous mouse model deleting EPHX2 stabilize EpFA and further demonstrate biological activity of increasing EpFA in disease. The first study using sEH$^{-/-}$ mice observed decreased blood pressure on a high-salt diet compared to wild-type mice (64), and sEH$^{-/-}$ mice were used to further demonstrate that increasing EpFA and decreasing diol formation resolves multiple disease states. For example, sEH null mice demonstrate beneficial effects in decreasing inflammation, maintaining the vascular endothelium, and resolving neuroinflammatory diseases. Specifically, sEH$^{-/-}$ mice demonstrated accelerated wound healing, reduced inflammation in inflammatory bowel disease and LPS-induced inflammatory models, improved insulin signaling in a Type II model of diabetes, reduced cisplatin-induced kidney damage, reduced niacin flushing, reduced arteriosclerosis, smaller infarct size in cerebral artery occlusion/reperfusion injury, decreased hepatic and arterial fibrotic disease, decreased autism, depression, and Parkinson's disease (see(65) and (66) for review). Recently, tissue specific sEH knockout models demonstrate the local effect that EpFA have on tissues. Mice with podocyte specific sEH knockout were protected from hyperglycemia-induced renal injury resulting from high fat diet or STZ-induced diabetic hyperglycemia (67). In further support of the importance of this pathway in disease, the analgesic effects of morphine were attenuated in CYP-null mice that lack the ability to generate EpFA, and in mice administered compounds that inhibit fatty acid oxidizing CYPs. (68) (69) (70) Thus genetic models that increase EpFA concentrations through deletion of their metabolism support the

beneficial effects of EpFA in treating disease, and models that decrease the ability of animals to form EpFA reduce these beneficial effects, suggesting an essential role of EpFA in disease.

3.Clinical approaches for increasing EpFA concentrations.

The EpFA to diol ratio is reduced in several disease states suggesting that increasing the EpFA concentrations in the body could provide beneficial effects in preventing or treating disease (Table 1). There are many different approaches for increasing concentrations of fatty acid epoxides for the treatment of disease. Strategies include direct administration of PUFA or EpFA, inhibition of EpFA metabolism through chemical inhibitors of sEH (sEHI), induction of EpFA formation through CYP modulators, or directly mimicking the fatty acid epoxide.

Table 1.1 Altered ratios of EpFA:diol correlate to disease outcomes

Alzheimers disease (AD) (71)

AD patients with and without Type 2 diabetes (T2D) had increased DHET compared to healthy controls. However, there were no effects following adjustments for multiple comparisons.

Arthritis (72)

In synovial fluid of arthritic vs. normal joints, 11,12-DHET and 14,15-DHET were higher in affected joints of people with unilateral osteoarthritis. In addition, these and 8,9-DHET were associated with worse progression over 3.3 years.

Anorexia Nervosa(47, 48)

Ill anorexia nervosa patients have higher DHA diol metabolites 19,20 DiHDPE:EpDPE compared to either recovered AN patients or healthy human subjects, while both ill and recovered AN patients have higher ALA diol metabolites 15,16 DiHODE:EpODE ratios compared to healthy subjects.

Peripheral arterial disease (73)

Increased 8,9 DHET correlated with increased risk of coronary and cerebrovascular events in patients with peripheral arterial disease.

Coronary artery disease (74)

Decreased EETs in patients with obstructive coronary artery disease compared to healthy controls

Depression(75)

In patients with major seasonal depression syndrome, sEH-derived oxylipins (12,13 DiHOME, 7,8- and 19,20 DiHDPE), in addition to other eicosanoids, increased in winter compared to summer-fall, while 14,15 EET and corresponding diol both decreased in the winter.

Preeclampsia(76)

In preeclamptic women 14,15-DHET was higher in urine samples compared to healthy pregnant women.

Vascular dementia (77)

In patients with cognitive impairment, an increase in 9,10- and 12,13 DiHOME: EpOME was associated with poor performance in function but not memory.

3.1 PUFA supplementation

Omega-3 supplementation is a widely investigated approach for improving health or treating disease, and the resulting fatty acid epoxides are thought to account for some of the beneficial effects observed with their supplementation. (44) However, randomized clinical trials often fail to support the efficacy observed in meta-analysis of diet behaviors and disease risk (78). Increased sEH activity in disease would increase EpFA metabolism, thus limiting efficacy and may account for the inconsistent therapeutic benefits reported with omega-3 supplementation. This is possibly due to lipid peroxidation products in some omega-3 lipids. Omega-3 lipids are inherently unstable and subject to oxidation, often as much as 200% increase in PUFA peroxides after only 22 days of storage (79), and further oxidation results in aldehydes that are not tested for in commercial settings (80). The oxidized products are associated with cellular stress and increased cellular toxicities and are hard to detect or control outside of sophisticated analytical labs and thus not a well-controlled approach for improving health or treating disease (81). Similarly, supplementation with EpFA is also subject to oxidation and provides further challenges because EpFA are also rapidly degraded by acid hydrolysis in the stomach or are eliminated through first-pass metabolism in the liver. An alternative administration route, for example direct application to affected tissue, would avoid first-pass metabolism; however, other metabolizing enzymes would still contribute to rapid elimination. For example, enteric coating to bypass the acid in the gut may provide options for treatment of intestinal diseases; however, metabolizing enzymes in the gut or microbiota containing epoxide hydrolases would further limit their effectiveness. Ocular therapy provides another application to avoid first-pass metabolism; however, recent studies have implicated increased sEH expression as contributing to disease progression in a mouse model of diabetic retinopathy as well as in samples from humans with diabetic retinopathy (82). Thus, ocular application to treat retinopathy would be susceptible to sEH metabolism possibly demonstrating that disease treatment by direct EpFA supplementation will be difficult due to sample stability and metabolic instability.

3.2 Increase formation of EpFA

Clinical and preclinical strategies for investigating biological activity of EpFA have focused on preventing their metabolism either through inhibition of the sEH enzyme or through synthesizing stable EpFA mimics. A third approach involves increasing their formation through CYP450 activity. Preclinical data indirectly suggests that increased CYP activity could reduce certain pathologies. In a mouse model of inflammatory pain, co-administration of a CYP modulator, omeprazole, and the sEHI, TPPU, resulted in increased efficacy compared to either compound administered alone. Omeprazole induces CYA1A1, 1A2, 2B1 and 3A1 and inhibits 2D2 and 2C. CYP2C is a more efficient at forming epoxides of AA (12/8 ratio of epoxidation/hydroxylation) compared to the other CYP isoforms which form hydroxylated metabolites in greater amounts than EpFA; however, because the other isoforms also form EpFA, increasing their activity would also increase EpFA as well as hydroxylated PUFA metabolites. (83) This is consistent with the results published in this study showing that the EpFA and hydroxylated metabolites were increased in the plasma of mice treated with both compounds. (84) Hydroxylated metabolites, especially hydroxylated metabolites of 18:2 linoleic acid (LA), are often associated with increased inflammation and oxidative stress (85-88), which brings up another complication with targeting CYP induction to increase EpFA in that it could also increase the production of inflammatory PUFA metabolites that could negate the beneficial effects of EpFA. Preclinical studies demonstrate that administration of ketoconazole, an inhibitor of CYP2A6, 2C19 and 3A4, reduces pain in an inflammatory mouse model by reducing the formation of hydroxy octadecadienoic acid (HODE), the mono-hydroxy metabolite of LA that causes hyperalgesia through activation of TRPV1 channels (83, 89). These studies demonstrate that increasing CYP activity is a complicated approach given the promiscuity of the CYP enzymes for forming both anti-inflammatory EpFA

19

and pre-inflammatory hydroxylated PUFA metabolites, as well as influencing the metabolism of other xenobiotics. Thus, increasing CYP activity does not present a viable strategy for clinical utility, and clinical approaches designed to increase EpFA should take into consideration drug-drug interaction potentially affecting EpFA formation if patients are currently taking CYP modulators.

3.3 Stabilizing EpFA through small molecule inhibitors of SEH

To overcome metabolic instability of EpFA, sEH inhibitors (sEHI) were identified that mimic the transition state of the epoxide ring opening. The pharmacophore of sEHI consist of a urea, carbamate, or amine heterocycle that mimic the interaction of the substrate and enzyme by forming one or more hydrogen bonds between the NH and aspartate (Figure 1.3.) The inhibitors contain hydrophobic regions that allow interaction with the enzyme and maintain high specificity over the mEH, while specifically placed polar side groups increase druggable properties such as water solubility, metabolic stability, and oral bioavailability. The first generation sEH inhibitor, 12-(3-adamantan-1-yl-ureido)-dodecanoic acid (AUDA) (90), was a small molecule designed to mimic to 14,15 EET with a dodecanoic acid to mimic the aliphatic chain and carboxylic acid present at the α end of the fatty acid, an adamantine to mimic the ω hydrophobic end of the fatty acid, and urea to act as a mimic to the epoxide and also inhibitor to the sEH enzyme. (91) AUDA is a potent sEHI, with an IC_{50} of 3-60 nM, but is short lived in the body ($T_{1/2}$ = 2.9 hrs. in canine PK) due to oxidation of the adamantine and beta oxidation of the alkyl chain, thus limiting its use *in vivo* to conditions where long half-life is not required. Since AUDA also mimics epoxy fatty acids, it shows biological activity in tissues lacking sEH. Such dual action may improve efficacy, but it complicates interpretation when AUDA is used to investigate physiology. (92) Second generation sEHIs replaced the adamantine with a more stable benzyl-trifluoromethoxy and alkyl chain with a benzenesulfonamide to maintain potency with the sEH enzyme while improving solubility and PK stability. ((93) for review). The most potent inhibitors of the sEH are reversible and tight binding with a slow off-rate from the enzyme and sub-nanomolar potency. They also show improvements in PK for increased

chances of testing clinical relevance for treating disease. Kinetic studies demonstrate optimization of new inhibitors by targeting drug occupancy time on the enzyme and demonstrate that inhibitors remain bound to the enzyme long after they are detectable by classical PK techniques. These data correlate with *in vitro* half-life measurements and provide novel techniques for selecting potent lead compounds for clinical development (94).

3.4 Mimics of EpFA
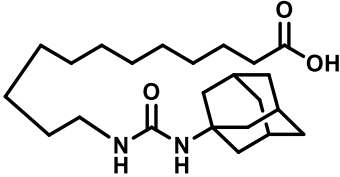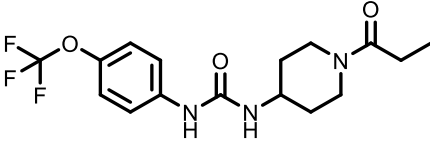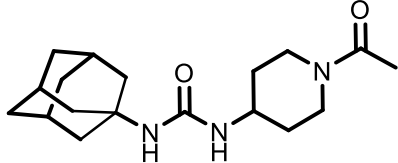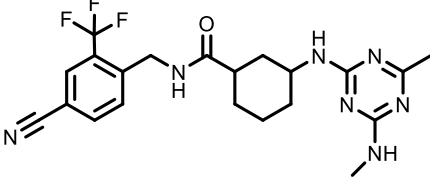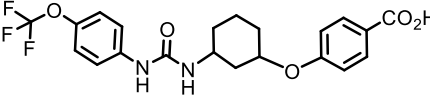
As an alternative to blocking the metabolism of EpFA in order to increase their concentrations, another strategy focuses on creating more stable mimics of EpFA while retaining the active moiety of the original compound. Epoxy fatty acid mimics investigated in clinical trials often replace the epoxide with functional groups that retain beneficial effects *in vivo* while also blocking β-oxidation by adding functional groups to the α-hydroxy portion of the fatty acid. Mimics of epoxy fatty acids remove the complexity of enzyme potency and off-rate kinetic parameters of small molecule sEHI that can complicate translation from the lab bench to clinical efficacy, but due to the unknown target for EpFA activity and complex structure diversity of EpFA, selecting one isomer for development could be overly simplistic. Many of the mimics were based on earlier studies in agricultural chemistry where various groups resistant to epoxide hydration were used to replace the epoxide of natural juvenile hormone while presumably retaining efficacy at the putative receptor. (95)

4. Clinical development of compounds that alter EpFA concentrations
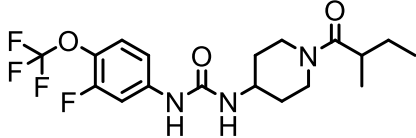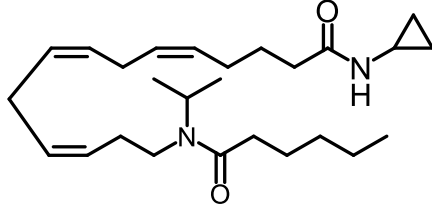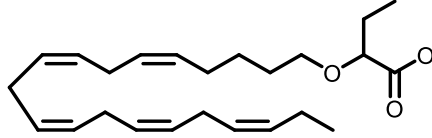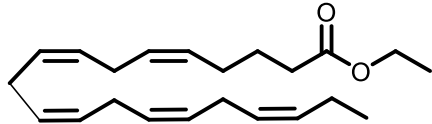
One of the first identified biological targets of EpFA action was modulation of the microvasculature and inflammation which underlies many pathological disease states. Clinical targets testing efficacy of increasing EpFA include hypertension, cardiovascular pulmonary disease, stroke, diabetes and pain. Preclinical studies provide evidence that altering concentrations of regulatory lipid mediators formed from metabolism of PUFA could provide beneficial effects in many other diseases, including neurological

disease and bone degeneration. Despite the unknown target, multiple clinical trials investigating the therapeutic potential of both small molecule inhibitors of the sEH as well as EpFA mimics have been initiated. These trials are highlighted in Table 1.2 and the mechanisms are explained in detail below along with the benefits and liabilities of these approaches.

Table 1.2. Clinical development candidates of small molecule sEHI and EpFA mimics.

Small molecule sEH inhibitors		Clinical Trials
AUDA		*Clinical trial NCT00654966: Microvessel Tone in patients with heart failure.* Status: Complete. Healthy humans and patients with heart failure challenged with topical urotensin II, a potent vasoconstrictor, and treated with sEHI. (96)
TPPU		This compound has not been investigated in clinical trials but is the most frequently used compound in preclinical research.
AR9281		*Clinical trial NCT00847899: Evaluation of sEHI in Patients with Hypertension and Impaired Glucose Tolerance.* Status: Complete. Single and multiple day testing up to 8 days at doses up to 1.2 g/day (400 mg every 8 hrs.) were well tolerated. (97) Data from Phase II clinical trials not published.
GSK2256294		*Clinical trial NCT01762774: A Study to Assess the Safety, Tolerability, PK and PD of Single and Repeat Doses of GSK2256294 in Healthy Volunteers and Adulate Male Moderately Obese Smokers.* Status: Complete. Doses were well tolerated and attenuated smoking related endothelial dysfunction.
EC1728 (*t*-**TUCB**)		Clinical trials are in being planned for companion animals.

EC5026		Clinical trials are in progress for the treatment of neuropathic pain in humans.
EpFA Mimics		**Summary of results**
CMX020		Clinical trial ACTRN12615000885594: A Study to Evaluate the Safety and Analgesic Efficacy of Oral CMX-020 in Subjects with Symptoms of Sciatica Resulting from Lumbosacral Radiculopathy. ACTRN12616001435471: A Phase 2 Study to Assess the Efficacy and Safety of CMX-020 in Treating Osteoarthritis. Status: Phase 1 studies complete. Enrolling for Phase 2.
OMT-28	structure not disclosed	*Clinical trial NCT03906799: Study on OMT-28 in Maintenance of Sinus Rhythm in Patients with Persistent Atrial Fibrillation.* Status: Enrolling
Icosabutate		*Clinical trial NCT04052516: A Phase 2b Study of Icosabutate in Fatty Liver Disease.* Status: Phase 1 studies complete. Enrolling for Phase 2b.
Vascepa (ethyl-EPA)		Status: approved for the treatment of hypertriglyceridemia.

4.1 Small molecule sEHI in clinical development

The clinical trials registry lists six clinical trials completed with small molecule soluble epoxide hydrolase inhibitors tested in diseases mostly affected by endothelial dysfunction. The following sections will highlight the small molecule sEHI investigated in these clinical strategies to increase EpFA as a mechanism for treating disease.

AUDA: Based on the observation that EpFA open potassium channels and hyperpolarize vascular endothelium resulting in vasodilation (54), investigators in Australia conducted clinical trial with NCT00654966 as an exploratory study in humans to determine if AUDA increases EpFA to protect against heart failure by increasing blood flow in the microvasculature. After topical challenge with a potent vasoactive peptide, urotensin II (UII), blood flow was measured in healthy humans or patients with heart failure (HF) treated with and without topical AUDA. UII causes vasodilation and increased blood flow in healthy humans but vasoconstriction and reduced blood flow in patients with HF. AUDA alone caused increase blood flow when administered at the intermediate dose of 0.1 μM in both healthy and HF patient populations. When administered with UII, AUDA was able to reverse the reduced blood flow observed in HF patients, although not back to levels observed in healthy subjects, and significantly increased blood flow in healthy subjects more than when UII was administered alone. (96) The increased vasodilation observed from this study indicate many potential benefits in addition to heart failure that increasing EpFA would have in patients; for example, diabetics and hypertensive patients would benefit from increased vasodilation; however, poor PK probably prevented this molecule from being a viable drug candidate.

AR9281 (UC1153): AR9281 offered some advantages as a clinical candidate including low IC_{50} on the rodent sEH, easy synthesis, a surprisingly high water solubility, high selectivity for the sEH,

and low mammalian toxicity; however, its poor target occupancy and the speed with which it was metabolized to synthetically complex metabolites were clear liabilities. In preclinical models, AR9281 reduced hypertension and renal injury in an angiotensin induced model of hypertension in rats (98). Multiple clinical trials were launched by Arete Therapeutics to test the safety and efficacy of AR9281 for treating hypertension. Published results from the Phase 1 study found that AR9281 was well tolerated at doses up to 1000 g/day but was rapidly cleared from the body, with a half-life of only 3-5 hrs. in humans. However, high plasma concentrations well above the IC_{50}, and *ex vivo* assays monitoring sEH activity showing 90% inhibition of the enzyme up to 24 hrs. at the top dose, justified advancing the compound to Phase 2 human efficacy studies. The results of the Phase 2 efficacy studies in hypertensive patients with glucose intolerance were not published, and Arete Therapeutics closed shortly after completing the study, so one assumes that the compound failed to show efficacy. One possible speculation for lack of efficacy was the high metabolic clearance of the compound. For example, the *ex vivo* determination of the IC_{90} was based on a 60-minute assay; however, AR9281 is a reversible inhibitor that has a kinetic $T_{1/2}$ on the enzyme of 6 min (99). Thus, the ex vivo data may not be representative of the *in vivo* environment where the inhibitor is rapidly metabolized and cleared from the body. Additional measurements of diols in the urine of subjects were combined from all treatments and compared to pretreatment levels and placebo treated subjects as a marker of target engagement. The diols of human subjects treated with AR9281 modestly decreased compared to pre-treated controls, while placebo treated subjects remained unchanged. Epoxide concentrations were not detectable in the urine; thus, the ratio of epoxide:diol change was not monitored and thus impossible to determine if the decrease in diol levels was due to treatment effect or other independent variables. Overall, the data from the Phase 1 trial did not demonstrate convincing data that AR9281 effectively

inhibited sEH activity, possibly explaining the lack of efficacy in phase 2 trials. There are situations where continuous IV administration can overcome the rapid clearance such as that demonstrated with adamantane containing compounds like AR9281 and AUDA; however, these have not been explored.

GSK225629A4: GSK225629A4 is a potent sEHI that attenuated leukocyte infiltration in mice after exposure to cigarette smoke.(100) Based on this information, clinical trials were initiated to test safety and endothelial dysfunction in both healthy humans and obese smokers at doses of 2-20 mg administered as a single or repeat oral dose for 14-days. Endpoints included safety and endothelial dysfunction measured by forearm venous occlusion plethysmography after intra-articular challenge with vasodilator, bradykinin. Overall, GSK225629A4 was well tolerated with favorable PK and $T_{1/2}$ equal to 19-30 hr. in healthy humans and 41-49 hr. in overweight smokers. One significant adverse event was reported, but ultimately considered non-drug related as the subject had a history of this event prior to the clinical trial. Otherwise, only mild-moderate adverse events of headache and contact dermatitis were reported. Headache occurred with similar frequency between the placebo and treated groups, and contact dermatitis around the site of ECG electrode placement was reported in 9 healthy patients receiving active compound and none in the placebo or obese smokers receiving active or placebo compound. Ex-vivo sEH activity was measured in the plasma of treated patients as a function of EET hydrolysis after 30-minute incubations with 14,15 EET, and investigators found that >80% inhibition of EET to diol hydrolysis was observed after repeat dosing in all dose cohorts. In obese smokers, vasodilation after bradykinin injection was reduced compared to healthy subjects, as expected. After administration of GSK225629A4 vasodilation improved in a dose and time dependent manner in obese smokers after 1 and 14-d administration compared to placebo control. Although some

limitations need to be considered, such as small sample size and non-smoking obese control subjects. Furthermore, as an added marker of safety, the sponsor measured VEGF and plasma fibrinogen after single and repeat dosing in response to potential safety concerns from increased angiogenesis (101, 102) and tumor metastasis (103) in preclinical settings. Both plasma VEGF and fibrinogen were similar across all treatment groups potentially indicating that preclinical angiogenesis observations may not be clinically relevant. Overall, these data suggest that GSK225629A4 is a safe compound with potential efficacy in patients with COPD, a disease exacerbated by cigarette smoke, or other disease affected by dysfunction of the microvasculature. Given the successful safety profile of GSK225629A4, independent investigators have secured rights to initiate clinical trials with the GSK compound to investigate insulin resistance and stroke as described below.

Insulin resistance: Preclinical data suggests that anti-inflammatory properties of EETs reduce inflammation in adipose tissue resulting in decreased insulin resistance in several, but not all, rodent models (104-106). Based on this information, a group at Vanderbilt University in Nashville, Tennessee initiated a Phase 2 clinical trial to investigate the therapeutic potential of GSK225629A4 ability to improve insulin sensitivity in response to glucose infusion. The study is currently recruiting patients, and there are no reported data from the study.

Subarachnoid hemorrhage (SAH): Numerous preclinical studies have investigated the role of soluble epoxide hydrolase in exacerbating stroke symptoms and the utility of inhibiting the sEH as a potential treatment option. (Reviewed in (107)) As a result of these data, investigators at the Oregon Health and Science University initiated a Phase 1 and 2 clinical trial with GSK225629A4 in patients with aneurysmal SAH to evaluate effects on length of hospital stay, incidence of new

stroke, disposition upon discharge and outcome measures. The study recently finished recruiting patients, but no results have been published.

Neuropathic Pain: As new mechanisms for explaining EpFA beneficial effects has been discovered, clinical activities are targeting diseases with complicated etiologies. For example, the newest clinical development programs that are scheduled to start at the end of 2019 focus on treating neuropathic pain, a disease attributed to pathological ER-stress. EC5026 is the newest sEHI being developed for clinical utility. Recent press releases announced FDA approval of an IND application from EicOsis to test their small molecule inhibitor, EC5026, for the treatment of neuropathic pain in humans, and EC1728 for treating inflammatory and neuropathic pain in companion animals. Many review papers have described the therapeutic potential of increasing epoxy fatty acids for the treatment of both neuropathic and inflammatory pain (reviewed in (18, 31, 108). Considering the devastating impacts of the opioid epidemic and lack of effective and safe pain medications, there is considerable interest in the outcomes of these clinical trials.

4.2 EpFA Mimics in Clinical Development

CMX-020 is a mimic similar to AUDA that is also designed around 14,15 EET. This compound maintains most of the original structure except the olefin on the 14,15 carbon is replaced with a dimethylcarbamoyl and the α hydroxy group is replaced with a cyclopropyl amine to prevent beta-oxidation. In preclinical studies, CMX-020 undergoes rapid elimination, with most of the drug eliminated one-hour after administration; however, the compound exhibits potent pain-relieving properties preclinically in the acetic assay writhing assay and tail flick assay, comparable to that of morphine. (109) It is unknown if CMX-020 metabolism results in epoxy-fatty acid mimics as a result of CYP450 epoxidation, or if CMX-020 acts to inhibit the sEH, similar to carbamates such as GSK225629A4. Based on the potent analgesic effects of CMX-020 and despite the rapid

elimination profile, multiple clinical studies were initiated to test the safety and efficacy of CMX-020 in treating painful conditions such as osteoarthritis and sciatic nerve pain in Australia. Results have not been published.

Focused mimics based on the structure of one regioisomer of one PUFA describe the challenges of developing a mimic to a fatty acid epoxide. While CMX-20 chose to mimic the omega-6 AA epoxides, other companies, described below, selected omega-3 fatty acids as the background for their mimics. The epoxides of omega-3 fatty acids are thought to account for some of the beneficial effects of omega-3 supplementation in the diet, and animal models show that they have more potent activity in *in vitro* and animal models than the omega-6 epoxides. (44) In addition to choosing which omega position of the fatty acids to model the mimic, further complications arise when identifying which regioisomer to target. For example, 11,12 and 14,15 EET are commonly associated with having vasodilator activity compared to the other regioisomers of arachidonic acid (12).

Omeicos is focused on developing another epoxy mimic by creating a transition state mimics of the 17,18 EPA omega-3 epoxide. Their lead compound, OMT-28, is actively recruiting patents for a Phase 2 clinical trial to treat atrial fibrillation. Although the exact structure is not disclosed, detailed structure activity relationship studies identified important characteristics needed to exert antiarrhythmic effects. Atrial fibrillation is a type of arrhythmia initiating from the top chambers of the heart and can lead to increased risk of blood clot, stroke, and heart failure. *In vitro* models using neonatal rat cardiomyocytes have been used to investigate the anti- or arrhythmic effects of certain drugs and demonstrate that omega-3 fatty acids and the R,S isomer of the 17,18 epoxide of EPA decreased the contraction rate in these cells(110), indicating a

potential ability to alleviate atrial fibrillation. These studies further demonstrate the complexity of EpFA biology that could potentially complicate the identification of an active mimic.

Other approaches that mimic the PUFA of omega-3 or -6 fatty acids have been developed. For example, Icosabutate, developed by Northsea Therapeutics, and Vascepa (icosapent ethyl, or ethyl-EPA), an approved product sold by Amarin, are structurally engineered fatty acids both being developed to lower triglycerides in the body. Icosabutate mimics EPA with the addition of 2-bromo butyric acid on the α end, while Vascepa adds a methyl group to the α end to prevent β-oxidation; otherwise, both structures are unaltered compared to EPA. Northsea data presented at the International Liver Congress in 2018 show the compound remains in the non-esterified form longer than EPA as expected, but was metabolized primarily by CYP2C enzymes, suggesting that epoxides are likely formed in the metabolism of this compound. (111) Multiple clinical trials were completed with Icosabutate testing the safety and potential drug-drug interactions with CYP inducers and inhibitors, as well as efficacy in hypertriglyceridemia (NCT01893515) and NASH (NCT04052516). Patients with hypertriglyceridemia receiving 600 mg once daily for 12-weeks had significantly lower triglyceride, very low-density lipoprotein cholesterol, and Apo C-III levels. (112) The NASH study recently started dosing and results are not yet available. There is more published information in icosapent ethyl considering that it is an approved drug for reducing the risk of cardiovascular disease in patients with hypertriglyceridemia. In a placebo controlled clinical trial enrolling 8179 patients, administration of 2g twice daily of icosapent ethyl significantly reduced ischemic events, including reduced incidence of death (113, 114).

Similar to risks in choosing a mimic to omega-3 or 6 fatty acid, identifying the regioisomer and stereoisomer to mimic further complicates the process. Omeicos is in a unique position by

having structure-activity relationship information for atrial fibrillation, but without knowing the target of EH activity, translating this information to other disease areas should not be assumed.

4.3 New therapeutic approaches targeting EpFA through polypharmaceutical approaches

Pharmaceutical targets to the COX and LOX enzymes focus on preventing the formation of inflammatory prostaglandins and leukotrienes, respectively. NSAID drugs inhibit COX-1 and-2 enzymes and are potent anti-inflammatory compounds by preventing the formation of inflammatory prostaglandins; however, these inhibitors are often accompanied by toxic side effects associated with enzyme distribution. COX-1 enzymes are in most cells and protect the GI mucosa by regulating acid secretion through the EP3 receptor. Inhibition of COX-1 increases gastric release, thus causing GI-toxicity and increased ulcer formation. COX-2 enzymes are found in lymphocytes, red blood cells and synovial cells and are thought to regulate pain and inflammation. Selectively inhibiting COX-2 was thought of as a desirable approach to reduce pain and inflammation while avoiding GI complications. However, while selective inhibition of COX-2 avoided gastro-intestinal ulcer formation, chronic use increased the risk of stroke and cardiovascular disease. Further investigation into the mechanism of this toxicity found that COX-1 inhibition decreases the vasoconstrictor thromboxane A2 synthesis; while COX-2 inhibition decreases the vasodilator, prostacyclin. Non-selective inhibitors would decrease both vasoregulators and maintain homeostasis, while selective COX-2 inhibitors would decrease only prostacyclin, resulting in platelet aggregation and vasoconstriction (115, 116). Vasodilatory effects of EpFA suggest further protection against endothelial dysfunction associated with COX-2 inhibition, but recent studies suggest an additional mechanism for decreasing COX toxicities results from the reduction of ER-stress. (117) NSAIDs increase ER-stress which has been attributed to the toxicities associated with NSAID use, including cardiovascular toxicity (118-120).

ER-stress also increases COX transcription, which creates a feedback inflammatory mechanism perpetuated by COX-2 activation of IRE1a, a key protein involved in activating the ER-stress pathway. Blocking ER-stress, as has been demonstrated with EpFA, prevent the upregulation of COX, and dual inhibition of sEH and COX are an attractive therapeutic strategy for increasing the benefit of NSAIDs while reducing their toxicity. Many preclinical studies demonstrate the advantages of dual COX-sEH inhibition. For example, the sEH inhibitor, t-AUCB, or NSAID inhibitor, Celecoxib, administered alone do not affect tumor volume or metastasis in a Lewis lung carcinoma mouse model of cancer while treatment with both significantly reduced both tumor volume and metastasis. Previous studies demonstrated that sEH null mice have increased metastasis and tumor volume (121), presumably through increased angiogenesis and VEGF expression; however, clinical trials with GSK's sEHI failed to show translation of VEGF increases in mice to human patients (122). Furthermore, preclinical studies identify that EETs are angiogenic and induce endothelial cell proliferation (123-125) through metabolism by COX that produces a potent angiogenic metabolite (126). Thus, dual inhibition would prevent the formation of this metabolite and could explain the added benefit in tumor models. Additional benefits have been observed in improving survival after tumor-induced cytokine surge in mice. Inflammation is a protective mechanism to eliminate foreign toxicants from the body; however, an intense and rapid inflammatory response, as occurs in sepsis, can be deadly. CAR-T therapy is a promising treatment of cancer that activates the body's immune system to recognize tumor cells as foreign material. The body mounts an aggressive immune attack to eliminate these tumor cells; however, if too effective, the outcomes also result in sepsis and death. Preclinical studies demonstrate that the dual COX/sEHI, p-TUPB, improves survival rate in a cancer cell debris model of cytokine-surge in mice. (127)

Dual inhibition with COX and sEH is an attractive target for treating disease by minimizing the toxicities associated with NSAIDs while also increasing the efficacy of both compounds (128). Many NSAIDs and coxibs lead to mitochondrial dysfunction, which in turn increases the production of reactive oxygen species. They have also been shown to increase ER-stress (120), which can induce the transcription of COX2 and prostaglandin synthase (3) leading to an increase in inflammatory eicosanoids and cytokines. Thus, the most widely used drugs in the world are themselves inflammatory. Anti-inflammatory sEHI block this inflammation axis both at the level of the mitochondria and the endoplasmic reticulum. Thus, when used with NSAIDS and coxibs should make these drugs not only safer but also improve their anti-inflammatory activity. Multiple rodent studies have shown that sEHI synergize with NSAIDs and coxibs to reduce inflammatory pain and extend the utility of NSAIDs and coxibs to include neuropathic pain. The sEHI also reduce gastrointestinal and cardiovascular side effects of cyclooxygenase inhibitors. Since prescription and over the counter COX inhibitors are so commonly used in pain management, this interaction is likely to be seen in the clinic if patients in trials are continued on standard of care treatment.

Exploiting this interaction commercially will be more complex. Regulatory pathways require that novel therapeutics demonstrate stand-alone efficacy before being combined with other targets, thus the pathway toward human treatment with NSAID-sEHI combinations is complicated. A polypharmaceutical approach: where one compound inhibits both COX and sEH, such as PTUBP, would lessen this challenge; however, the FDA closely monitors NSAID cardiovascular toxicity and requires extensive cardiovascular safety studies and lengthy clinical trials prior to testing in humans, thus developing this dual target under the current regulatory environment would likely be more expensive and risky than other targets. For example, this regulatory scrutiny

resulted in the FDA not approving a potent NSAID, etoricoxib, after the FDA advisory committee recommended further cardiovascular risk assessment, despite etoricoxib approval in other countries. (129)

Other targets in the fatty acid metabolism pathway provide attractive opportunities for treatments. For example, inhibition of LOX is currently approved for the treatment of asthma. Leukotrienes, the main target of LOX metabolism, are potent inflammatory agents that potentiate bronchoconstriction and exacerbate an asthma attack. Inhibiting LOX activity through direct inhibition (e.g. Zileuton) or through the inhibition of 5-lipoxygnase activating protein (FLAP) is an approved treatment for asthma. (130) sEHI has also shown efficacy for treating asthma. (131) Interestingly, Zileuton and the FLAP inhibitors, Zafirlukast and Montelukast, also have weak activity for inhibiting the sEH (0.9 – 1.95 µM), but at concentrations likely achieved at therapeutic doses. (132) Identifying improved dual LOX-sEHI with greater potency for the sEH is an attractive target for improving asthma treatments.

The fatty acid amide hydrolase enzyme (FAAH) is a complicated target for drug therapy. The endocannabinoids, a bioactive class of lipids formed through the addition of an amide to the carboxylic acid of PUFA. For example, N-arachidonoyl phosphatidylethanolamine (NAPE), and related amides are associated with beneficial effects in a variety of disease models including inflammation, pain, asthma, epilepsy, neurological disease, among others (see (133) for review). Because FAAH metabolizes endocannabinoids, therapeutic approaches of inhibiting this enzyme were considered for treatments of some diseases. Over ten clinical trials have been initiated to test efficacy of FAAH inhibitors, but after significant toxicities and one death were reported in a Phase 1 study of a claimed FAAH inhibitor in France, all clinical trials were put on hold. Although the exact cause of the toxicity is unknown, recent reports suggest that off-target effects on lipases

caused the toxicity (134). Renewed interests in FAAH as a target for pain came after a case study identified a woman with a knock-out mutation in FAAH were thought to result in her inability to feel pain (135). Administration of both sEH and FAAH inhibitors show synergistic effects in animal models of pain (136) and continued efforts to develop a dual inhibitor suitable for clinical development are ongoing. (137)

sEH inhibitors are more effective in reducing pain in the presence of cAMP. Dual phosphodiesterase 4 (PDE4) and sEH inhibition also show synergistic effects in decreasing pain in animal models. (138) PDE inhibitors (PDEi) have been developed for the treatment of inflammation by preventing the metabolism of cyclic adenosine monophosphate (cAMP); however, increasing cAMP has also been associated with increased pain states. Interestingly, PDE4 and 5 inhibitors increase EpFA through lipase activity, releasing arachidonate and possibly EETs from phospholipids, and could possibly explain the mechanism for analgesic effects of PDEi despite increases in cAMP. (138) In laboratory settings, investigators demonstrated that decreasing EpFA concentrations through CYP450 inhibition while treating with PDEi resulted in increased pain states. Conversely, increasing EpFA concentrations through sEHI resulted in synergistic increases in pain relief. Efforts are ongoing to identify dual inhibitors of PDE4 and sEH, and recent advances identified MPPA, a compound with potent inhibition on both enzymes that is also efficacious in an LPS model of inflammatory pain. (139)

While some compounds are synthesized specifically to inhibit an enzyme, others are identified after approval as having off-target effects against desirable or undesirable enzymes. For example, sorafenib and regorafenib are receptor tyrosine kinases that have anti-angiogenic properties by inhibiting VEGFR-2 and other kinases. They are approved for the treatment of hepatocellular carcinoma and renal cell carcinoma, and both are potent inhibitors of the sEH (12

and 0.5 nM IC$_{50}$, respectively). The other approved small molecule inhibitor of VEGFR, sunitinib, is not an sEH inhibitor. Although the biological relevance of this dual activity is difficult to compare with other kinases that do not affect sEH because kinases are in general promiscuous inhibitors of many kinases. Both sorafenib and regorafenib are known for being difficult to formulate and for often serious side effects of their use. Clinical doses of these Raf-1 and pan-kinase inhibitors are likely to inhibit most sEH activity and increase EpFA *in vivo.* It is likely that without the sEH inhibition, these kinase inhibitors would have even worse side effects. It follows that the side effects of these two kinase inhibitors could be dramatically reduced by increasing dietary ω-3 and limiting dietary ω-6 lipids. The kinase inhibition is not ubiquitous to the urea pharmacophore that inhibits sEH; however, Sorafenib and regorafenib are unique compared to other published sEH inhibitors used in preclinical or clinical studies in their ability to inhibit kinases, as can be predicted from structure activity relationships. (140)   Although recent publications indicate that TPPU is a weak inhibitor of p38 kinase (IC$_{50}$ = 0.98 µM). The p38 kinase is a mitogen-activated protein kinase and activates inflammatory cytokines, and inhibition of this kinase would explain many of the beneficial effects seen in the preclinical studies using this compound; however, p38 is also regulated by oxidative stress, and the study failed to show if the activity was an indirect result of reducing oxidative stress vs. direct inhibition of the kinase given that the *in vitro* assays were conducted below the IC$_{50}$ of 100 nM. (141)

5. Summary and future directions for targeting EpFA as treatments for disease.

The newest innovations in inhibiting the sEH focus on identifying natural compounds with inhibitory activity, or polypharmaceutical approaches targeting multiple enzyme pathways. The inhibitors being tested for sEH inhibition focus on a central pharmacophore of either a urea, amide, or carbamate, and few new patents have been filed with different pharmacophores. Instead, new

technologies focus on identifying new targets of disease, poly-pharmaceutical approaches developing a single compound to inhibit multiple targets (142), or inhibitors isolated from natural products. Inhibiting the sEH affects a regulatory pathway, ER stress, and is a relatively safe target that could offer benefits when combining with other targets. In some cases, efforts for developing dual targets to provide added benefits or safety have been intentional, while others have been discovered as off-target effects after developments. Both approaches are described below.

Current clinical approaches are focused on developing small molecule inhibitors or EpFA mimics; however, future approaches are investigating polypharmaceutical approaches, thus capitalizing on the low toxicity of alerting this pathway. Yet despite widespread interest in targeting this pathway, few new pharmacophores are identified that lack a carbamate or urea as the active moiety. Recently, natural products have been identified as a new source of sEH inhibitors that hold promise for future nutraceutical development; however, these products have relatively poor potency, with $IC_{50}s$ (in the µM range), which would require g/day amounts of dosing. Techniques are being considered to improve production and isolation of natural sEHI or identify more potent natural sEHI. (143) (144)

Many early sEHI, such as AUDA, were designed as mimics of specific EpFA. This dual action was clearly demonstrated in earlier publications. (145) Subsequent synthesis led to compounds that inhibited the EH without mimicking EpFA or compounds that mimicked specific EpFA without inhibiting sEH. Shen and Hammock discussed the advantages and limitations of each of these approaches. (146) The resulting molecules made biological data much easier to interpret when they were used as physiological probes, and likely simplified patent positions as well. Possibly it is worth reconsidering dual acting compounds. For example, one could have an sEHI pharmacophore which would increase EpFA systemically, while also targeting mimicry of

17,18 EEQ or 19,20 EDP to control atrial fibrillation. (147) Such compounds would offer the advantages of stabilizing all EpFA while allowing direct action of the EpFA mimic in tissue with a reduced ability to epoxidize PUFA.

In summary, lipid epoxides and their mimics or stabilizers are of increasing interest in treating disease due to their many beneficial and homeostatic functions as well as limited observed toxicities. However, their multimodal mechanism of action, including effects on angiogenesis and cancer, raises caution for monitoring safety in clinical trials. Furthermore, few studies report toxicities associated either with direct supplementation of EpFA, or inhibition of sEH; however, one study reported that sEH null mice displayed reduced survival in a cardiac arrest model compared to wild type mice(148) demonstrating one of the few examples of increased toxicities in preclinical models modulating the sEH. While the most recent advances are focused on investigating the polypharmaceutical advantages of increasing EpFA, other approaches that could increase EpFA include altering the release and reincorporation into the cell membrane and could provide attractive benefits to the current clinical approaches being investigated (Figure 1.4.). Currently small molecule inhibitors of sEH are being tested in clinical settings to investigate the effects of increasing EpFA concentrations in the body as a way of treating pain, diabetes, and reducing the symptoms of subarachnoid hemorrhage. Other strategies focus on mimicking the beneficial EpFA and are targeted in clinical investigations for treating pain, fatty liver disease, hypertriglyceridemia, and atrial fibrillation. Overall, previous clinical trials targeting strategies to increase EpFA lack on-target toxicities, and most studies using sEH knock-out animals lack toxic side effects, which increases confidence in the safety of increasing EpFA concentrations in the body. The combined safety profile and wide-ranging efficacy in treating disease encourage continued investigation in the beneficial effects of this pathway as a treatment option.

Figure 1.4. Possible ways of increasing natural epoxy fatty acid chemical mediators to prevent and treat disease.
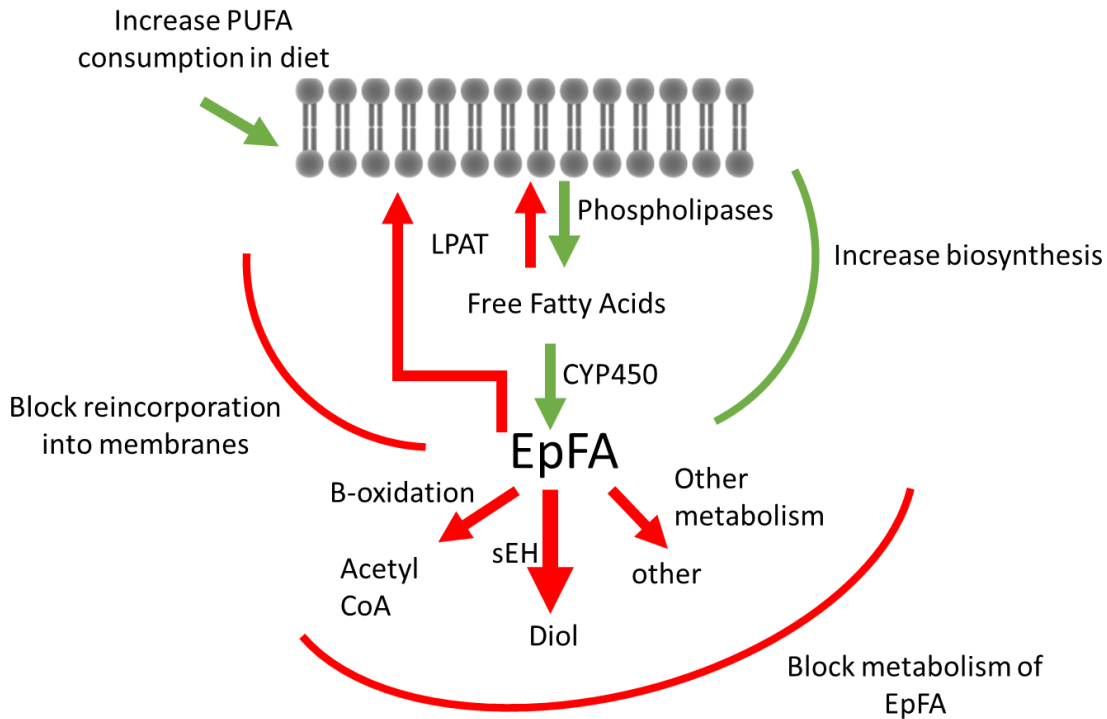
Increasing EpFA concentrations in the body have been associated with treating many diseases. This figure demonstrates potential pathways of increasing their concentrations through increasing their biosynthesis or through preventing their metabolism. EpFA can be increased by increased PUFA consumption, increasing release from lipid membranes, or increased formation through CYP450 activity. Inhibiting the metabolic enzymes that convert EpFA to more polar compounds that are rapidly eliminated from the body, or supplementing the diet with EpFA mimics that prevent degradation by β oxidation are other ways in increasing the concentrations of the beneficial fatty acids.

Chapter 2. Species differences in metabolism of soluble epoxide hydrolase inhibitor, EC1728, highlight the importance of clinically relevant screening mechanisms in drug development.

Cindy McReynolds[1,2], Jung Yang[1,2], Alonso Guedes[3], Christophe Morisseau[1], Roberto Garcia[4], Heather Knych[5,6], Sung Hee Hwang[1,2], Karen Wagner[1,2], Bruce Hammock[1,2]*

[1]Department of Entomology and Nematology, UC Davis Comprehensive Cancer Center, University of California, Davis, Davis, CA, United States,

[2]EicOsis, Davis, CA, United States

[3]Department of Veterinary Clinical Sciences, College of Veterinary Medicine, University of Minnesota, St. Paul, MN 55108, USA.

[4]Dechra Development LLC,, 1 Monument Sq, Portland, ME 04101.

[5]K.L. Maddy Equine Analytical Pharmacology Laboratory, School of Veterinary Medicine, University of California, Davis, USA.

[6]Department of Veterinary Molecular Biosciences, School of Veterinary Medicine, University of California, Davis, USA.

*Correspondence: bdhammock@ucdavis.edu; Tel.: (530) 752-8465

Abstract: There are few novel therapeutic options available for treating companion animals, and medications rely heavily on repurposed drugs developed for other species. Considering the diversity of species and breeds in companion animal medicine, comprehensive PK exposures in the companion animal patient is often lacking. The purpose of this paper was to assess the pharmacokinetics after oral and intravenous dosing in companion animal species (dogs, cats, and horses) of a novel soluble epoxide hydrolase inhibitor, EC1728, being developed for the treatment of pain in animals. Results: Intravenous and oral administration revealed that bioavailability was similar for dogs, and horses (42 and 50 %F) but lower in mice and cats (34 and 8%, respectively). Additionally, clearance was similar between cats and mice, but >2x faster in cats vs. dogs and horses. Efficacy with EC1728 has been demonstrated in mice, dogs and horses, and despite the rapid clearance of EC1728 in cats, analgesic efficacy was demonstrated in an acute pain model after intravenous but not oral dosing. Conclusion: These results demonstrate that exposures across species can vary, and investigation of therapeutic exposures in target species is needed to provide adequate care that addresses efficacy and avoids toxicity.

Keywords: soluble epoxide hydrolase; companion animals; pharmacokinetics, feline drug metabolism.

1. Introduction

Companion animal medications are often repurposed drugs approved for human use or for use in species other than the patient being treated (149). Although more research is being conducted to understand exposures in companion animals, information is still lacking, and limited understanding of the distribution and pharmacokinetic profiles of compounds in the intended species can result in failed efficacy from conservative dosing strategies used to avoid toxicities. Due to the paucity of data, dose recommendations are often based on allometric scaling and *in vitro* metabolic stability in microsomes; however, this may not capture true metabolism if other mechanisms of elimination, such as intestinal transporters or phase II metabolism, are involved (150). The broad generalizations of exposure based on human data or data in other species are especially problematic for cats. Cats are obligate carnivores and have fewer mechanisms for xenobiotic metabolism as a result (151, 152). Court (2013) (153) compared the elimination rate of 25 therapeutics among humans, cats and dogs and found that human elimination rates poorly predicted metabolism in cats and dogs; however, cats and dogs had similar elimination profiles when compounds were excreted unchanged vs. compounds metabolized by CYP450 oxidation or phase II conjugation mechanisms.
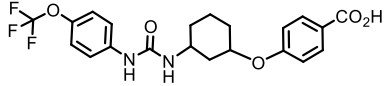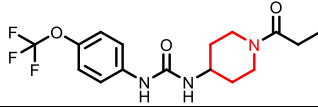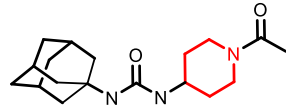
This lack of understanding of drug exposures in companion animals often leads to limited treatment options for fear of overdosing, particularly where side effects are a significant concern. This is especially true for pain relief in companion animals (154, 155). Options for pain control in companion animals are limited to a few options, such as NSAIDs, opioids or repurposed seizure medications. While opioids are effective analgesics in companion animals, their use is accompanied by the same severe side effects seen in humans, including respiratory depression at high doses (156), and gastric stasis (157); however, it is commonly assumed that cats and horses

respond to opioids with increased activity, termed opioid mania, but this is only present at higher doses (158, 159). In addition, tolerance and hyperalgesia after chronic dosing further limit their long-term use (156). NSAIDs are often used as pain relieving options in companion animals despite being one of the 10 most common causes of unintentional overdose in dogs and cats (160). Dogs and horses tend to tolerate NSAIDs at higher doses than cats due to limited glucuronyl transferase in cats, but even dogs and horses are not exempt of potential adverse events when using long-term NSAIDs due to gastro-intestinal toxicities and liver damage (161, 162). Recently anti-seizure gabapentinoids, such as gabapentin, are being used to treat pain and seizures in companion animals, and despite being the most commonly prescribed pain medications for chronic musculoskeletal pain in cats (163) and highly used in other companion animal species including horses (164), gabapentin has not been approved for use in companion animals and assessments are on-going to determine safety and efficacy. Sedation and somnolence are the most frequently described dose-limiting side effects, and withdrawal symptoms, such as rebound pain and agitation which are observed in humans, could further complicate their use in companion animals (165-167).

Due to limited safe and effective long-term pain-relieving options in companion animals, improved analgesic drugs with a novel mechanism of action are greatly needed. EC1728 is currently under development for treating pain in companion animals based on inhibition of the soluble epoxide hydrolase (sEH) to increase beneficial and natural analgesic epoxy fatty acids (EpFA). Essential polyunsaturated fatty acids (PUFAs) are metabolized primarily through three enzymatic mechanisms, cyclooxygenase (COX), lipoxygenase (LOX) and cytochrome P450 (CYP450) enzymes, that results in the formation of both inflammatory and inflammation-resolving regulatory lipid metabolites. While the COX and LOX pathways form largely inflammatory

products, the EpFA formed from CYP450 have been shown to reduce pain and inflammation (for review see (31)). However, the biological relevance of EpFA is limited by their rapid degradation by the sEH into corresponding vicinal diols that are inactive or pro-inflammatory (168). In contrast to NSAIDs that inhibit the COX enzymes to prevent the formation of inflammatory prostaglandins, inhibition of sEH is being developed as an analgesic option by largely preventing metabolism of beneficial EpFAs. By effecting a response through increasing concentrations of safe endogenous compounds, the on-target toxicity of sEH inhibitors is expected to be less than those of other drug targets. There are many efforts to identify a therapeutic strategy targeting this pathway (for review see (169)), and the primary inhibitors and their physiochemical properties are identified in Table 2.1. Interestingly, compounds containing a piperidine moiety are significantly less active on the sEH enzyme of dogs and cats. In contract, EC1728 is a selective sEH inhibitor nominated for use in dogs, cats and horses based on its potency, solubility, and stability *in vitro* (170). It has shown efficacy in treating both natural disease in horses (171) and dogs (172), and murine models of neuropathic and inflammatory pain (173, 174).

Table 2.1. Summary of solubility and potency of main sEH compounds

Compound	Solubility (µg/mL)a	Melting Point (°C)	cLogP b	Potency (Ki) (ng/mL)c			
				Mouse	Cat	Dog	Horse
EC1728 (t-TUCB)	5	240-244 (242)	4.7	11	0.18 ± 0.004	0.39 ± 0.02	25.87
Piperidine series							
UC1770 (TPPU)	60	198.2-200.8 (199.5)	1.5	2.9 ± 0.72	155 ± 80	1,138 ± 696	25 ± 9
AR9281 (UC1153, APAU)	277	205-206 (205.5)	0.8	2.8	144	160	39

aThe solubility of the drugs were measured in 0.1M Sodium Phosphate Buffer at pH 7.4
bcLogP was calculated using ChemBioDraw (v 19.1 CambridgeSoft)
cIC50 was calculated using CMNPC at 5 µM as previously described (175)

EC1728 is a potent inhibitor of the sEH (38), and stable in microsomes, with 100% remaining after 30 min, indicating that the compound is not substantially metabolized by CYP450 enzymes (170). EC1728 has been evaluated for efficacy and PK in several preclinical species (94, 172, 176, 177); however, comprehensive PK in target companion animal species has not been specifically characterized. The purpose of this study was to determine exposure of EC1728 after intravenous (IV) and oral dosing in target companion animal species (dogs, cats and horses) to evaluate comparative pharmacokinetics and exposures based on existing literature and new data presented in this paper. Plasma protein binding and *in vitro* phase II metabolism studies were conducted to further characterize elimination pathways of EC1728.

2. Results
2.1. Pharmacokinetic profiles in companion animals

EC1728 exposure supports once daily oral dosing in mice, dogs and horses, with a T1/2 of >12 hour and bioavailability between 42-50% (Table 2). Dogs showed the longest exposure described

by a 2-phase absorption with a rapid alpha phase (T1/2 0.09 ± 0.08 h) followed by long beta phase (T1/2 47.00 ± 10 h) (Table 2, Figure 2.1). Cats showed significantly higher clearance (6x higher than dogs and horses and 3x higher than mice) and lower volume of distribution (Vss) (3.9, 6.7, and 2.9x lower than mice, dogs and horses, respectively) at a low dose of 0.1 mg/kg IV and PO. Cats often display longer exposures to compounds due to fewer Phase I and II metabolizing enzymes, and a low dose was selected initially as a safe dose to characterize PK. However, due to rapid elimination, only early timepoints had detectable drug concentrations. The last collection timepoint (Tlast) in cats was 8 h for IV and 12 h for PO; however, the last timepoint with detectable concentration (Clast) was 3 h for IV and 4 h for PO. For this reason, a higher dose of 1 mg/kg IV and 3 mg/kg PO were administered to better characterize PK. At higher doses (1 mg/kg IV and 3 mg/kg PO), the Cl was lower, although still faster than observed in dogs and horses (3.5 ± 1.1 vs. 0.45 ± 0.38 and 1.2 ± 0.33 mL/min*kg in cats, dogs and horses respectively after accounting for hepatic blood flow rate). The Vss was higher at higher doses in cats (2.0 ± 0.8 vs. 0.4 ±0.2 L/kg at the 0.1 mg/kg dose) and consistent between all species 1.5-2.6 (L/kg for all animals tested). The higher IV dose likely represents a more adequate PK profile and was used to calculate bioavailability. Oral dose exposure studies determined that bioavailability decreased with higher doses (17 ± 8, 8 ± 0.6 and 3 ± 0.3% for 0.1, 3 and 10 mg/kg PO dose, respectively) without appreciable changes to the terminal elimination rate 0.64 ± 0.4, 0.28 ± 0.05 and 0.32 ± 0.06 L/hr (Figure 2.2 and Table 2.3).

Figure 2.1. General overview of PK profiles of EC1728 in different animal species.
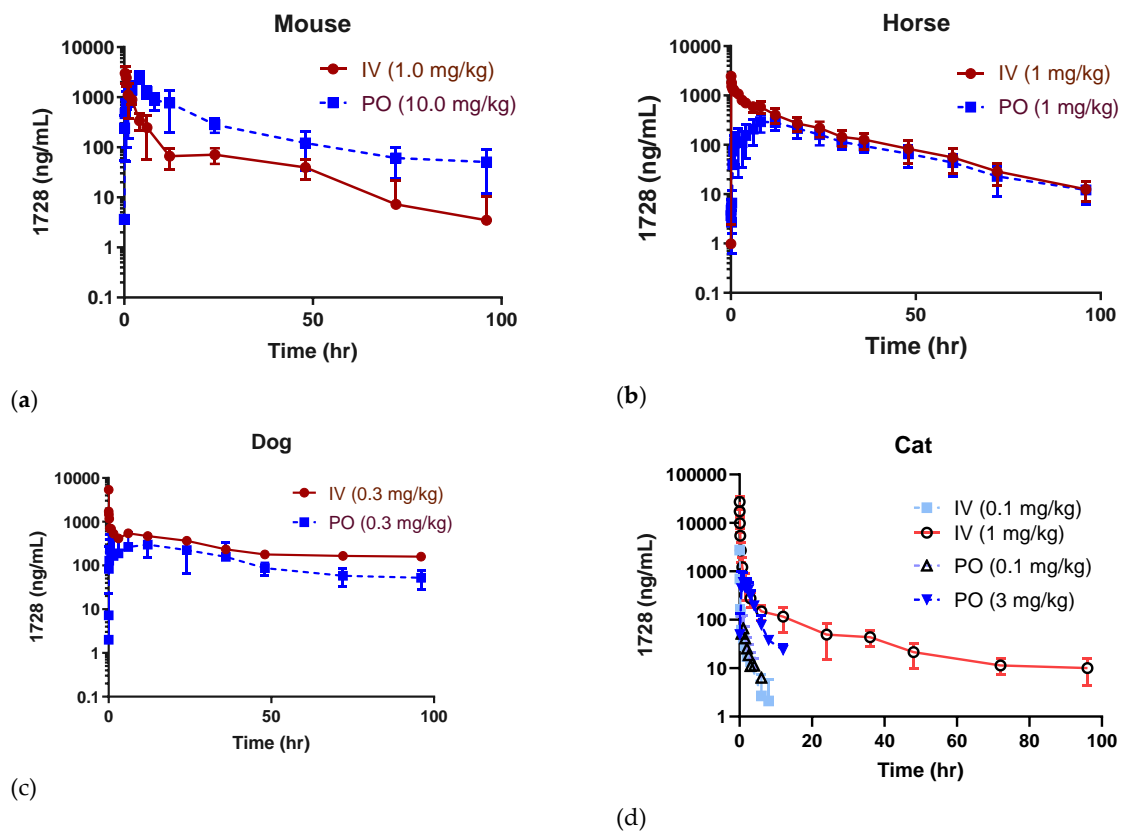
General overview of PK profiles of EC1728 represented as semi log-linear plots of concentrations after dosing IV or PO in mice (n=4) (a), horses (n=8) (b), dogs (n=5) (c) and cats (n=3-6) (d). T_{last} in cats at 0.1 mg/kg iv and PO was 8 hour for IV and 12 hour for PO; however, the C_{last} in the low dose cat group dosed IV was observed at 3 hour and 4 hour for PO. Linear representation of graphs through 12 h are plotted in Supplementary Figure S1.

Table 2.2 Summary of EC1728 PK parameters between species.

Parameter[1]	Mouse	Cat		Dog	Horse
Dose (mg/kg)					
IV	1	0.1	1.0	0.3	1
PO	10	0.1	3.0	0.3	1
Cmax (ng/mL) /dose					
IV					
PO	3,087 ± 1,089	2,076 ± 1,194	27,241 ± 8,114	1,566 1128	2,436 ± 304
	2,570 ± 670	91.5 ± 14.6	802 ± 241	403 232	336 ± 83
IV-Dose adjusted (Cmax/dose)	3,087 ± 1,089	20,760 ± 11,942	27,241 ± 8,114	5,219 ± 3,761	2,436 ± 304
PO-Dose adjusted (Cmax/dose)	257 ± 67	915 ± 146	267 ± 80	1,343 ± 772	336 ± 83
AUC (hr*ng/mL) /dose					
IV					
PO	8,488 ± 1,319	271 ± 88	8,182 ± 3,083	12,662 ± 8,309	16,604 ± 4,535
	28,624 ± 6,008	140 ± 62	2,081 ± 137	14,443 ± 4,852	9,190 ± 2921
IV-Dose adjusted (AUC/dose)	8,488 ± 1,319	2,716 ± 878	8,182 ± 3,083	96,388 ± 63,239	16,604 ± 4,535
PO-Dose adjusted (AUC/dose)	2,862 ± 601	1,402 ± 619	693 ± 46	48,142 ± 16,173	9,190 ± 2921
Tmax (h)					
IV	0.38 ± 0.14	0.04 ± 0.04	0.025 ± 0	0.04 ± 0.03	0.08 ± 0
PO	4.0 ± 0.0	0.8 ± 0.6	1.2 ± 0.8	10.3 ± 9.3	10.6 ± 3.8
Cl$_{int}$ (mL/min*kg)	2.0 ± 0.3	6.6 ± 2.1	2.3 ± 0.8	0.7 ± 0.6	1.0 ± 0.3
Vss (L/kg)	1.5 ± 0.9	0.4 ± 0.2	2.0 ± 0.8	2.6 ± 2.0	1.2 ± 0.2
%F	34 ± 8	52 ± 51	8 ± 0.6	42 ± 14	50 ± 8
T$_{1/2}$ (h)					
IV α	α = 1.20 ± 0.34	1.4 ± 0.4	α = 0.23 ± 0.13	α = 0.10 ± 0.08	16.5 ± 2.3
β	β = 44 ± 23		β = 20.5 ± 7.4	β = 47 ± 10	
PO	16.3 ± 2.8	0.9 ± 0.2	4.6 ± 4.1	42 ± 20	18.0 ± 4.3
PPB (%)	96.04 ± 0.99	98.32 ± 0.61	98.32 ± 0.61	98.0 ± 1.4	98.75 ± 0.24
Cl(hep) (ml/min*kg)	7.30 ± 0.97	8.60 ± 2.12	3.5 ± 1.1	0.45 ± 0.38	1.2 ± 0.33
Body weight (kg)	0.032 ± 0.002	3.9 ± 0.3		12.9 ± 1.6	554 ± 22

Numbers represent mean ± STDEV. PPB (Plasma Protein Binding), IV (intravenous), PO (oral gavage in mice (n=4) and per os for cats (n=3-6), dogs (n=5) and horses(n=8)), Cl$_{int}$ (intrinsic clearance), %F (oral bioavailability), T$_{1/2}$ (half-life), Cl(hep) (hepatic clearance). Hepatic blood flow rates used to calculate Cl(hep) are 30, 40, 35, 24 mL/min in mouse, cat, dog and horse, respectively (178, 179). Gender and animals dosed/group are described in Table 2.5 of the methods section.

Figure 2.2. Dose dependent exposure of EC1728 after oral dosing in cats.
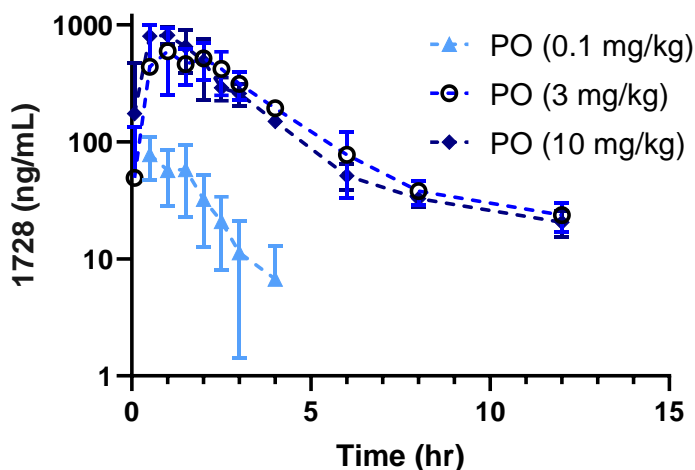
Fasted cats (n=3) were dosed with increasing concentrations of EC1728. The maximum exposure was achieved at 3 mg/kg, and bioavailability decreased at the high dose without affecting terminal elimination (table 3).

Table 2.3. Summary of EC1728 PK parameters after oral and IV dosing in cats

Route	PO		
Parameter[1]			
Dose (mg/kg)	0.1	3.0	10.0
Cmax (ng/mL)	92 ± 15	803 ± 241	1,115 ± 541
AUC (hr*ng/mL)	140 ± 62	2,369 ± 517	2,278 ± 245
%F			
Based on 0.1 mg/kg	52 ± 23.0 17 ± 7.6	29 ± 6.0	8 ± 1.0
Based on 1 mg/kg		8% ± 0.6	3 ± 0.3
$T_{1/2}$ (h)	0.89 ± 0.2	4.62 ± 4.1	4.50 ± 2.2
Tmax (h)	0.83 ± 0.6	1.17 ± 0.8	0.83 ± 0.3
Cl_{int} (mL/min*kg)	14.4 ± 8.4	24.1 ± 1.6	73.7 ± 7.8
Kel (1/h)	0.64 ± 0.35	0.28 ± 0.05	0.32 ± 0.06

[1]Numbers represent mean ± STDEV of 3 cats. IV (intravenous), PO (per os), Cl_{int} (intrinsic clearance), %F (oral bioavailability), $T_{1/2}$ (half-life)

Metabolism profiles were investigated to determine why cats display rapid elimination of EC1728. Plasma protein binding (PPB) was evaluated between species to determine if there was higher free drug available for metabolism and elimination in cats versus other species, however PPB was similar (>96%) among all species tested (Table 2). Phase II metabolism mechanisms are often responsible for differences in elimination and are not usually tested during early screening programs **(150)**. Even though cats are considered poor at glucuronidation compared to other species due to a lack of two UGT enzymes (UGT1A6 and UGT1A9), Lautz et al. described cats as having a 'peculiar expression and activity' of phase II metabolism enzymes **(180)** because they have other UGT and Phase II enzymes that efficiently metabolize xenobiotics. For this reason, stability of EC1728 was assessed in each species with UDPGA, PAPS and GSH, the necessary co-factors for the main phase II metabolism mechanisms. The S9 liver fraction was used for these experiments in order to capture enzymes located in the microsomes and cytosol. These experiments revealed that EC1728 was equally stable in all species tested (98 ± 2.2, 94 ± 4.7, 105 ± 2, $94 \pm 1.2\%$ remaining after 1 hour incubations in mouse, cat, dog and horse liver S9 fractions, respectively, Supplementary Table S2.2). Neither mechanism of PPB nor Phase II metabolism explained the rapid elimination by cats compared to other species. Despite this, hepatic clearance accounting for free drug unbound to proteins and hepatic blood flow rates between species further highlighted the differences in clearance between cats (3.5 mL/min/kg) versus dogs (0.57 mL/min/kg) and horses (1.2 mL/min/kg) (Table 2).

Mouse PK was included to correlate multiple published efficacy studies to PK values and relate those values to efficacy in companion animal species. Previously published data evaluated EC1728 after a single oral dose of 0.1, 0.3, 1 and 3 mg/kg and reported dose-dependent increases in AUC and Cmax (181). An oral dose of 10 mg/kg and IV of 1 mg/kg was selected for novel

evaluation in this study and to support previously published studies showing efficacy in a diabetic pain model at increasing subcutaneous doses from 1 to 10 mg/kg, with only 10 mg/kg showing statistical significance (174). The Cmax and AUC reported here were consistent with previously published data and were only slightly higher than expected (2.6 and 1.3-times higher Cmax and AUC, respectively) based on Liu et al (181). Mice also demonstrated 2-phase absorption with a rapid alpha phase ($T_{1/2}$ 1.2 ± 0.34 h) followed by long beta phase ($T_{1/2}$ 43.8 ± 23 h) (Table 2). As expected from rodent species, particularly from mice with exceptionally high heart rates, intrinsic clearance of EC1728 in rodents was more rapid than larger animal species (Table 2).

2.2 Predictions of clearance based on allometry

Allometric scaling based on estimated body surface area was determined for Cl to assess expected vs. observed values. The 1 mg/kg IV dose in cats was used for comparisons to IV hepatic clearance in mice, dogs and horses. Due to the slow Cl in dogs vs. high Cl in cats, there was a high variability in plotting clearance vs. body weight for all species (r^2 =0.51) (Figure 2.3). Accuracy (calculated/predicted) of predicting clearance values based on body weight was calculated from the allometry constant and coefficient determined from all animals or based on calculations where either the cat or dog data was excluded. Based on allometric scaling of mice, dogs and horses, dog clearance was lower than would be predicted based on body weight ($r^2 = 0.54$), whereas clearance in cats compared to mice and horses was as expected based on body weight ($r^2 = 0.99$). Although the rapid clearance in cats suggests they are unique in their metabolism, body weight calculations suggests that in fact dogs may be unique in their slow elimination profile.

Figure 2.3. Relationship between clearance vs. body weight in animals dosed with EC1728.

(a) Mice Cats Dogs Horses
Y = -0.2157*X + 0.4441
r^2 = 0.51
--- Projected Cl

(b) Mice Cats Horses
Y = -0.1852*X + 0.6091
r^2 = 0.99
···· Projected Cl

(c) Mice Dogs Horses
Y = -0.2109*X + 0.3644
r^2 = 0.54
···· Projected Cl
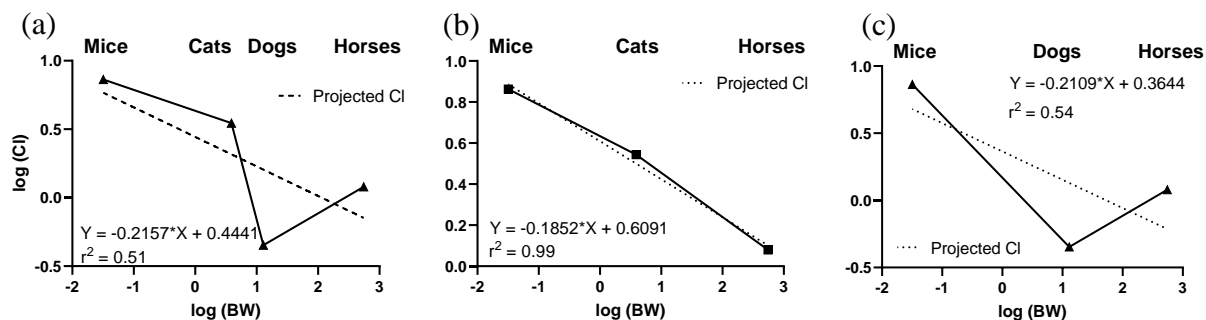
The accuracy of observed clearance was compared to the predicted clearance based on body weight. Clearance was predicted based on the graphing observed clearance values vs. body weight for mice, cats, dogs and horses (a), excluding dogs (b) or excluding cats (c). Excluding dog clearance improved the accuracy of allometric scaling.

2.3. Efficacy of EC1728 in a monosodium urate model of inflammatory pain

EC1728 is a potent inhibitor of cat sEH with an IC_{50} of 0.4 nM (170), and despite rapid clearance, concentrations in cats still exceeded 10x above the IC_{50} for at least 3-hours even at the lowest dose tested. Because of these favorable characteristics, short-term pain models were assessed in spite of the rapid clearance in the PK profile. In a monosodium urate crystal model (MSU) of synovitis, two pain observations were monitored as described in the method section after administration of EC1728. EC1728 at 0.1 mg/kg IV one hour after MSU injection into the stifle joint significantly decreased pain (Figure 2.4); however, a single oral dose of 3 mg/kg EC1728 after MSU injection failed to show a difference in the pain response (Figure 2.4). Clinical observations and physical exam found no serious adverse events related to test article administration. Body weights did not deviate from -2 to 7% over the course of the study, and there was no test article related effect on appetite (cats routinely ate 67-100% of food offered). All cats returned to normalcy for all parameters tested 6-days after MSU injection (data not shown).

Figure 2.4. Analgesic activity of EC1728 and meloxicam in cats after MSU injection
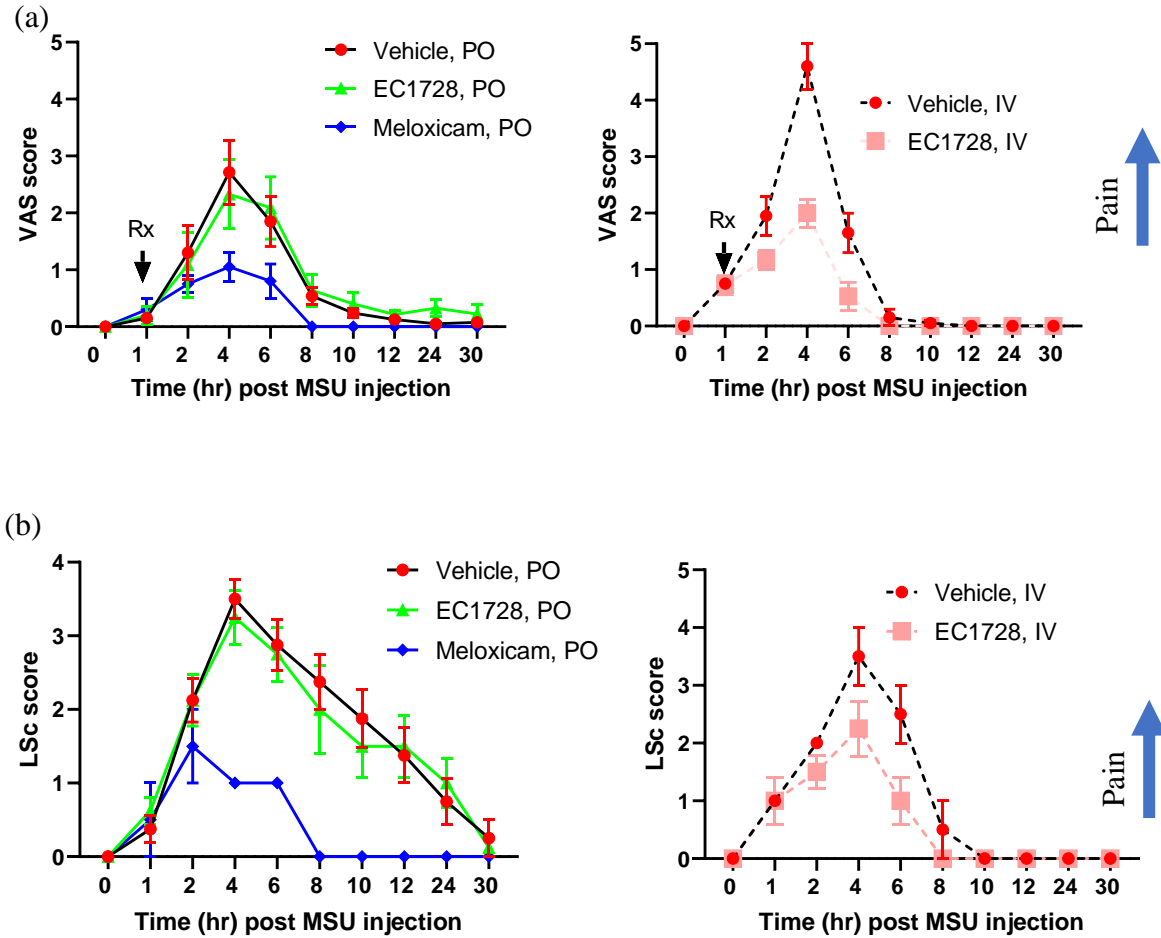
EC1728 was administered once orally at 3 mg/kg or IV at 0.1 mg/kg 60 min after MSU injection. Meloxicam served as a positive control and was administered once orally at 0.1 mg/kg 60 min after MSU injection. Pain response was recorded by (a) visual analog scale (VAS) or (b) lameness score (LSc) and represented as mean ± SEM. A vehicle control matched each dosing regimen (IV, PO). Oral administration of EC1728 did not alter the pain response after MSU injection, but a single IV dose significantly decreased pain in both recorded pain measures ($p < 0.05$). N=8 for vehicle and EC1728, IV, and n=4 cats were used for EC1728, PO. An n=2 cats were used for IV vehicle and meloxicam since the response was consistent with previous results (not shown) this was deemed sufficient for comparison.

Discussion

Understanding PK parameters in target animal species is important for identifying a safe and efficacious dose for treatment; however, few publications have analyzed differences in companion animal PK between species, and treatment options often rely upon human drugs repurposed for animal use. Therefore, there is an urgent need for species specific understanding of PK due to lack of detailed literature in companion animals.

Among the urea based sEH inhibitors potency was initially optimized based on the murine and human recombinant enzyme (182) and then the library rescreened to find potent inhibitors of the canine and equine enzymes (170). The IC_{50}'s of two of the potent sEHI's commonly used in the field compared to EC1728 are shown in Table 2.1 along with some of their properties. Both compounds are high melting suggesting stable crystal structures as expected of the urea pharmacophore. When the property of high melting point is combined with lipophilicity as indicated by the log P values the materials must be administered in a formulation that will present the inhibitors in true solution because they will dissolve very slowly in biological fluids. Fortunately, as indicated by the low IC_{50}'s on the target enzyme, the potency can be very high making the compounds attractive as pharmaceuticals in spite of their challenging physical properties. A surprise in examining the piperidine structures such as EC1770 and AR9281, an sEH inhibitor previously administered in human clinical trials for hypertension (97), was that although these structures were very potent inhibitors of rodent and primate enzymes their potency fell off dramatically in other species, particularly the cat (170). Thus, when EC1728 was selected as an Investigational New Animal Drug candidate for canine and equine use, we evaluated it for use in felines.

In our assessment of EC1728 exposures in selected animal species, we observed unique PK profiles demonstrating that extrapolations of exposures between species is not the most accurate for this compound. The most notable variability between species was between cats and dogs, with cats displaying faster clearance of EC1728 vs. dogs, and dogs demonstrating much slower clearance than would have been predicted by allometric scaling (Figure 2.3). Cats are reported to metabolize compounds more slowly than other animals due to having lower levels of CYP450 enzymes, and lack of two glucuronidation (UGT1A6 and UGT1A9) and one ATP-binding cassette transporter (ABCG2) ((153, 179, 183). While faster metabolism typically represents less risk of toxicity, it makes identifying effective concentrations more challenging. Due to differences in clearance observed in cats and dogs, several obvious elimination pathways were analyzed to understand these differences. Free drug in the plasma can increase elimination due to the availability of the drug to metabolic mechanisms; however, the PPB of EC1728 is consistent across species, and the drug is highly stable in assessments of both Phase I and II elimination mechanisms *in vitro*. Given the stability of EC1728 after incubation with phase I and II metabolic enzymes from cats with added co-factors, elimination by efflux transporters or failed binding to absorptive transporters remained as possible explanations as to why clearance rates are more rapid in cats. Additional observations suggest that transporters highly influence cat PK. For example, lower bioavailability in general and at higher oral doses without altering clearance, as observed in a dose escalation study in cats, suggests that transporters, specifically ones with high kcat and poor (high) Km that would be more active at higher concentrations, are responsible for elimination (184). Additionally, the Biopharmaceutics Drug Disposition Classification System (BDDCS), proposed by Wu and Benet (185) to predict absorption and elimination based on physical properties, identify EC1728 as a Class IV drug with low solubility and low metabolism. Based on this BDDCS

classification, EC1728 would be highly absorbed but also influenced by transporters. There is limited information available on specific transporters in cats besides a lack of ATP-binding cassette G2 transporters (153, 179, 183); however, based on the stability *in vitro* in liver microsomes and S9 fractions, a unique species-specific interaction with a transporter may explain the low oral bioavailability in cats and increased exposure in dogs. Due to the use of dogs as the preferred tox species in the development of human drugs, much more is known about the expression of dog transporters; but even in dogs, little is known about the functional role these changes play in the absorption or elimination of xenobiotics (186, 187). It is possible that other factors influenced PK. For example, precipitation in the gut after dosing could contribute to poor bioavailability in cats; however, further studies are needed to confirm this. Future studies comparing the differences in the expression of dog and cat transporters, testing alternate dosing routes that would avoid first pass metabolism in the gut (e.g. topical or IP dosing), or testing different formulations to improve bioavailability would allow for focused investigations on transporter involvement and improvements with formulation.

Despite rapid elimination, EC1728 was effective in reducing pain after a single IV administration, indicating excellent intrinsic potency and validating the target. However, no significant analgesia was seen after oral administration in cats. Efficacy in a short-term pain model is expected considering that EC1728 is a transition state mimic inhibiting the sEH enzyme at low concentrations and with high affinity and high target occupancy due to slow kinetic off-rate from the target enzyme (99). sEH inhibitors with these characteristics often demonstrate target-mediated drug disposition (TMDD) that results in observed efficacy independent of PK due to elimination largely resulting from the inhibitor binding the intracellular sEH enzyme with high affinity and thus removing it from detection in the plasma while still retaining a high level of enzyme

inhibition. Similar sEHI have demonstrated TMDD properties, and these properties are often characteristic of drug classes (188). Interpretation of efficacy results in compounds demonstrating TMDD are often more complicated than simple correlations of drug exposure translating to efficacious effects and may explain why low exposures of EC1728 after IV dosing results in acute analgesia in an inflammatory pain model in cats. It is harder to explain why oral dosing of EC1728 was not efficacious despite plasma coverage above the IC_{50} during the course of the study. It is possible that Cmax is an important parameter for driving efficacy of EC1728, and the low Cmax after single oral doses was not adequate for driving the compound into target compartments and loading the sEH target with inhibitor. Additional studies investigating target engagement (for example monitoring EpFA:diol ratios in target tissues and not just plasma) would help address this question.

In drug development, both human and animal, translation of efficacious concentrations is often based upon rodent PK data or correlations from other species. Therefore, the data in this publication serve as a warning that PK cannot be assumed based on general assumptions of body weight and hepatic blood flow rates. While an understanding of companion animal PK can advance safety and efficacy for companion animal drugs, it can also advance an understanding of fundamental PK parameters since unique differences in animal species aid to better characterize chemical classes as they relate to metabolism, and intrinsic characteristics that affect distribution and elimination. Although EC1728 is in development as an oral analgesic for canines, for inflammatory pain for equine arthritis, and IV analgesic for equine laminitis (neuropathic pain) its use at this point for felines is likely to be limited to IV administration unless a unique formulation can be found to increase prolonged blood levels of the drug. Possibly an understanding of the low blood levels and the mechanism for rapid elimination of the drug in cats will provide a pathway.

Ultimately, the rapid clearance of EC1728 provides a unique opportunity to investigate differences in PK between species and, understand important PK parameters required for efficacy, or unique handling challenges that need to be taken into consideration when working with feline pain models.

4. Materials and Methods

4.1 Solubility and potency

Solubility and potency were determined as previously described (170). Briefly, solubility was determined at saturation conditions by dissolving 0.25-2g of compound into PBS (0.1M, pH 7.4) for 30°C for 24 hours, filtering through a 0.22 uM filter and analyzing the dissolved compounds by LC/MS/MS. Potency was determined using a fluorescent based assay in purified enzymes at a final concentration of 17, 99 and 208 µg/mL for horse, cat and dog, respectively and a final CMPC concentration of 5 µM. Reactions were incubated at 30°C for 5 minutes. These conditions were optimized in each species to ensure linear product formation over the course of the experiment. Melting points were determined on an OptiMelt melting point apparatus.

4.2 Test Article and preparation of dosing solution

EC1728 (*t*-TUCB) and internal standard, deuterated 1728 *trans*-4-(4-[3-(4-trifluoromethoxy-phenyl)-ureido]-cyclohexyloxy)-benzoic-2,3,5,6-d4 acid, also referred to as 3049, *t*-TUCB-d4), was synthesized as previously described (175, 189). IV dosing solutions were dissolved in DMSO and filtered through a 0.2 micron sterile filter. For mouse (IV) and cat (IV and PO) formulations, PEG400 and saline were added after the compound was dissolved in DMSO and then filtered through a 0.2 micron sterile filter. Oral dosing solutions were dissolved in PEG400 by heating to 50°C for 10 minutes followed by 1 minute of sonication. Dosing volumes and concentrations are described below.

Table 2.4. Concentration and dosing volumes of dosing solutions in EC1728 PK studies

	Vehicle	Dose (mg/kg): concentration (mg/mL)
Mouse	IV: DMSO:PEG300:Saline (2:25:73) PO: PEG400 (100%)	1.0 mg/kg: 0.06 mg/mL, IV 10 mg/kg: 1 mg/mL, PO
Cat	IV and PO: DMSO: PEG400 (20:80)	0.1 mg/kg: 2 mg/mL, IV and PO 3.0 mg/kg: 60 mg/mL, PO 10 mg/kg: 100 mg/mL, PO
Dog	IV: PEG400 (100%) PO: PEG400 (100%)	0.3 mg/kg: 1 mg/mL, IV 0.3 mg/kg: 1 mg/mL, PO
Horse	IV: DMSO (100%) PO: PEG400 (100%)	1 mg/kg: 20 mg/mL, IV 1 mg/kg: 20 mg/mL, PO

4.3 *In vitro* metabolism and plasma protein binding.

Plasma protein binding: frozen plasma, pooled mixed gender, was purchased from Biochemed Services for all species tested. Plasma protein binding was tested using the Plasma Protein Binding Equilibrium Dialysis (RED device) from ThermoFisher Scientific following manufacturer's instructions (176). Briefly, 100 µL of plasma was spiked with EC1728 (final concentration 1µM in 0.1% DMSO) and loaded in the sample chamber. A negative control containing spiked dialysis buffer was loaded into the sample chamber and used to validate the assay. 350 µL of dialysis buffer (PBS containing 100mM sodium phosphate and 150mM sodium chloride) was added to the buffer chamber. Plates were sealed and samples were incubated at 37°C on an orbital shaker at 250 rpm for 4 hours. To terminate the reaction, a sample of the buffer and sample side were removed and added to an equal volume of sample or buffer, respectively. A 6x volume of ice-cold methanol containing internal standard,

t-TUCB-d4, was added to each tube and centrifuged for 10 minutes at 13,000 x g before analysis by LC/MS/MS as described below.

In-vitro metabolism studies: Liver S9 fractions, pooled mix gender, were purchased from Sekisui Xenotech and used at a final concentration of 1 mg/mL. Metabolism studies were executed following methods published by Richardson et al. (150). Briefly, 200 mM Tris buffer containing 2 mM magnesium chloride, pH 7.4 was used for dilution. EC1728 was dissolved in DMSO at 0.2 mM for final concentration of 1 μM. Activating cofactors included phase 1 (NADPH regenerating system) (190) and phase 2 (UDPGA, PAPS, GSH) reactions. S9 fractions and EC1728 were incubated at 5 min before addition of activating co-factors or buffer (control). A separate control without S9 was included to monitor inhibitor stability. Reactions were run in a shaking water bath at 37°C for 60 min and terminated with an equal volume of ice-cold methanol containing internal standard, *t*-TUCB-d4, centrifuged for 10 minutes at 13,000 x g, and stored at -80 before analysis by LC/MS/MS as described below.

4.4 *In Vivo* studies

All animal procedures were preapproved by the Institutional Animal Care at each institute conducting the in vivo study (dose administration and blood collection was conducted at University of California at Davis for horses and mice, University of Minnesota for dogs and cats administered PK doses at 1 mg/kg, IV. Kingfisher International conducted all other studies in cats reported here). Concomitant medications were withheld for a minimum of two weeks prior to administration of EC1728. Dogs, cats and horses were fasted 12-hour prior to receiving IV or oral EC1728. Otherwise, animals received *ad libitum* water and routine animal chow throughout the study. Cats, dogs and horses were confirmed healthy by complete blood count, serum biochemistry, and physical exam. Mice were confirmed healthy by visual examination.

Animal disposition are described below (additional data in Supplementary Table S2.1)

Mice: Four male swiss-webster mice (6–8-week-old from Charles River) with an average ± SD weight of 31 ± 0.1 g were used in each IV and PO arm, for a total of 8-mice.

Cats: Three separate studies comprised the cat data. For the PK studies at 0.1 mg/kg and all PO dosing, twelve adult domestic short-hair cats (9 neutered male and 3 intact female) aged 8 – 33 months with an average ± SD weight of 3.9 ± 0.3 kg were enrolled in this study. Six adult spayed female cats were used for IV dosing at 1 mg/kg, weights were not recorded. Eight cats were enrolled in efficacy studies with MSU injection (7-35 months with an average ± SD weight of 4 ± 0.2.

Dogs: Five adult University owned dogs of unknown age and gender with an average weight of 12.92 ± 1.6 kg

Horses: Eight University owned horses (four sexually intact females and four castrated males) aged 4–23 years with an average ± SD weight of 555 ± 34.4 kg were used in a cross-over exposure design in this study. IV injection was administered by slow injection (30-60 sec) via catheter in each species. For oral dosing, mice received liquid oral dosing solution by gavage; cats and dogs received liquid dosing solutions via capsule (Torpac capsule, size 3), and horses by per os.

Blood samples were collected by venipuncture or pre-placed central line in the jugular vein in dogs, cats and horses into EDTA (K_2) tubes and plasma was isolated by centrifugation and stored at -70°C until analysis. In mice, blood was collected by tail nick and stored in 0.1% EDTA water frozen at -70°C until analysis. Blood sampling after IV was collected in a dedicated catheter or separate location from injection to avoid residual compound from injection confounding results.

Timepoints of blood collection are listed in table 2.6. Concentrations of EC1728 were measured by LC-MS/MS as previously described (172, 176).

Table 2.5: Blood samples times post EC1728 dose in companion animals

Species	Time (hr)
Mouse	IV: 0.25, 0.5, 1, 2, 4, 6, 8, 12, 24, 48, 72, 96 (n=4)
	PO: 0.25, 0.5, 1, 2, 4, 6, 8, 12, 24, 48, 72, 96 (n=4)
Cat	IV (0.1 mg/kg): 0.017, 0.08, 0.25, 0.5, 0.75, 1, 1.5, 2, 3, 6, 8 (n=3)
	IV (1 mg/kg): 0.025, 0.05, 0.1, 0.2, 0.38, 0.75, 1.5, 3, 6, 12, 24, 36, 48, 72, 96 (n=6)
	PO: 0.08, 0.5, 1, 1.5, 2,2.5, 3, 4, 6, 8, 12 (n=3)
Dog	IV: 0.025, 0.05, 0.1, 0.2, 0.38, 0.75, 1.5, 3, 6, 12, 24, 36, 48, 72, 96 (n=5)
	PO: 0.025, 0.05, 0.1, 0.2, 0.38, 0.75, 1.5, 3, 6, 12, 24, 36, 48, 72, 96 (n=5)
Horse	IV: 0.083, 0.167, 0.25, 0.5, 0.75, 1, 2, 3, 4, 6, 8, 12, 18, 24, 30, 36, 48, 60, 72, 96 (n=8)
	PO: 0.083, 0.167, 0.25, 0.5, 0.75, 1, 2, 3, 4, 6, 8, 12, 18, 24, 30, 36, 48, 60, 72, 96 (n=8)

4.5 Feline efficacy studies

A masked, crossover design was implemented. Eight cats were randomly allocated to two sequence groups to evaluate efficacy after EC1728 IV and oral administration (Table 6). Monosodium urate (MSU) crystals (20 mg in 1 mL suspension) were injected into the stifle joints in cats (left stifle for the first period and right stifle for the second). EC1728 was administered by IV injection (period 2) or oral capsule (period 1) 1 hour after MSU injection. Meloxicam was included as a positive control and administered at a dose of 0.1 mg/kg 1-hour after MSU injection. A vehicle control matched each dosing regimen. Analgesia was assessed by a Visual Analogue Scale (VAS) and Lameness Score (LSc) along with clinical observations, body weight, and physical examination. VAS was scored first and assessed through observation on a scale of 0 (no pain) to 10 (most severe pain). LSc was rated on a scale of 0 (no observable lameness) to 4 (unable to bear weight). Cats were monitored at 0, 1, 2, 4, 6, 8, 10 and 12 hour and 7, 14, and 21 days post injection,

as well as days 6, 13 and 20 to ensure cats returned to normalcy after MSU injection. Statistics were determined using repeated measure ANOVA mixed effect model using time and dose as variables in Graph Prism version 9.1.

Table 2.6. Efficacy study design in cats administered monosodium urate and treated with EC1728

Sequence Group	Period 1	Wash-out	Period 2
S1 (n=4)	Vehicle$^\epsilon$		Test Article$^\pounds$
S2 (n=4)	Test Article*	7 days	Reference Article$^\alpha$ or Vehicle$^\beta$

* One oral dose of EC1728 at 3.0 mg/kg (between 50 and 60 min post MSU injection);
€ Equivalent frequency, timing, and volume to the respective test article counterpart;
£ One IV dose of EC1728 at 0.1 mg/kg (between 50 and 60 min post MSU injection);
α Cohort 1 (n=2) received one oral dose of METACAM at 0.1 mg/kg as a positive control (between 50 and 60 min post MSU injection);
β Cohort 2 (n=2) received one IV dose of vehicle (between 50 and 60 min post MSU injection).

4.6 Pharmacokinetic parameter estimation

Individual parameters were calculated by fitting blood concentrations to a non-compartmental analysis using Kinetica software (ThermoFisher version 5.1). Using the log-linear trapezoidal method, the area under the curve were calculated and were extrapolated to infinity using the last measured plasma concentration (C_{last}), defined as the timepoint collected 72 hours after the last dose or 8 hours after the first dose on day 1, divided by the terminal slope (λz).

The following PK parameters were estimated, if sufficient data was available:

AUC_{total}: Area under the plasma drug concentration curve over time. Calculated as mixed log-linear AUCtlast + (Clast/kelim). If the AUCtlast/AUC0-∞ was at least 0.80, the sampling profile was deemed adequate.

Cmax and **Tmax**: Highest observed dose (Cmax) at the given time (Tmax). Obtained from experimental observations.

$T_{1/2}$: Estimated as the amount of time it takes to eliminate half of the maximal drug concentration. Calculated as ln(2)/ kelim.

k_{elim}: Elimination rate constant. Estimated using linear regression on the terminal phase of the semilogarithmic

concentration-time curve. Values below the LLOQ which occur after Tmax were excluded from calculation of the terminal regression line. A minimum of three data points were used for the calculation of kelim.

F(%): Absolute oral bioavailability was calculated as ([AUC (PO)_dose (IV)]/[AUC (IV)*dose (PO)])*100.

Cl(int): Apparent total clearance of the drug from plasma is calculated as: $CL = Dose/AUC_{total}$

Cl(hep): Measure of the maximal clearance in the absence of protein binding or blood flow differences between species is calculated as: Q [(f x Cl(int)/(Q+ f x Cl(int)], where Q is the hepatic blood flow rate (mL/min/kg) and f is estimated fraction of EC1728 unbound to plasma proteins.

PK values were evaluated for non-compartmental analysis using the Akaike Information Criterion (AIC) in Graphpad Prism. Multiple compartmental modeling was conducted if the AIC was>0 using a semilog-linear simpler model compared to a segmental regression alternative model.

Allometric Scaling: The log value of all pharmacokinetic values was plotted against the log body weight and the linear regression was calculated in Graphpad Prism and used to calculate predicted clearance. The efficiency ratio was determined by the predicted values/observed values. (191).

Supplementary Chapter 2 Table S.1. EC1728 individual PK parameters in animal species

Mouse

IV Unit	Dose mg/kg	Cmax ng/mL	Tmax h	TLast h	AUCtot ng/mL*h	Kel 1/h	$T_{1/2}$ h	MRT h	Clearance mL/min/kg	Vss L/kg
Animal										
1.00	1	3401	0.50	48	8615	0.35	1.96	7.02	1.93	0.81
2.00	1	3988	0.25	96	10305	0.26	2.70	12.65	1.62	1.23
3.00	1	3456	0.25	48	7598	0.17	4.05	9.57	2.19	1.26
4.00	1	1503	0.50	72	7433	0.24	2.93	21.01	2.24	2.83

PO Unit	Dose mg/kg	Cmax ng/mL	Tmax h	TLast h	AUCtot ng/mL*h	Kel 1/h	$T_{1/2}$ h	MRT h	F %
Animal									
1.00	10	1802	4.00	96	36251	0.04	15.78	22.38	42
2.00	10	3431	4.00	96	24129	0.05	13.42	20.55	23
3.00	10	2594	4.00	96	30596	0.03	20.17	26.39	40
4.00	10	2453	4.00	96	23523	0.04	15.87	16.65	32

Cat

IV Unit	BW kg	Dose mg/kg	Cmax ng/mL	Tmax h	TLast h	AUCtot ng/mL*h	Kel 1/h	$T_{1/2}$ alpha h	$T_{1/2}$ beta h	MRT h	Clearance mL/min/kg	Vss L/kg
JAJ31[nm]	3.6	0.1	708	0.080	3	192.53	0.59	1.18	n.d.	1.05	8.66	0.55
JEC2[nm]	4.5	0.1	2910	0.017	8	366.11	0.38	1.82	n.d.	1.41	4.55	0.38
LAU4[nm]	3.8	0.1	2610	0.017	3	256.02	0.57	1.22	n.d.	0.66	6.51	0.26
1[sf]	n.r.	1.0	37,267	0.025	96	10131.1	0.02	0.21	21.22	11.2	1.65	1.77
2[sf]	n.r.	1.0	29,028	0.025	96	13344.8	0.03	0.35	19.62	12.8	1.25	1.20
3[sf]	n.r.	1.0	31,399	0.025	96	6820.16	0.04	0.12	12.69	9.0	2.44	1.61
4[sf]	n.r.	1.0	29,751	0.025	96	7355.12	0.03	0.44	34.10	8.0	2.27	1.69
5[sf]	n.r.	1.0	21,948	0.025	96	6817.12	0.03	0.12	15.32	11.3	2.44	1.93
6[sf]	n.r.	1.0	14,055	0.025	96	4622.26	0.03	0.13	19.85	12.6	3.61	3.60

PO Unit	BW kg	Dose mg/kg	Cmax ng/mL	Tmax h	TLast h	AUCtot ng/mL*h	Kel 1/h	$T_{1/2}$ h	MRT h	F %
EAB2[nm]	3.5	0.1	80.3	0.5	2.5	69.26	0.92	0.67	1.19	8%
EAQ4[f]	3.7	0.1	86.2	1.5	4	168.00	0.75	0.92	1.849	21%
LBB3[nm]	3.8	0.1	108	0.5	4	183.27	0.25	1.07	1.859	22%
CBD2[f]	4.1	3	642	1.0	12	1944.23	0.32	2.16	3.41	8%
LBA3[nm]	3.6	3	1080	0.5	12	2217.88	0.30	2.30	2.52	9%
LBB2[nm]	3.7	3	686	2.0	12	2083.26	0.22	3.13	4.47	8%
CBD3[f]	4.1	10	1720	0.5	12	2535.76	0.28	2.48	2.48	3%
JEH2[nm]	4.2	10	677	1	12	2048.27	0.29	6.91	5.12	3%
LAQ1[nm]	3.8	10	948	1	12	2250.28	0.38	4.11	3.10	3%

nr = not recorded; n.d. = not determined; nm = neutered male; sf = spayed female; f = female

Dog

IV Unit	Dose mg/kg	Cmax ng/mL	Tmax h	TLast h	AUCtot ng/mL*h	$T_{1/2}$ alpha h	$T_{1/2}$ beta h	MRT h	Clearance mL/min/kg	Vss L/kg
1	0.3	2358	0.025	96	15268	0.05	55.13	38.95	0.33	1.61
2	0.3	685	0.1	96	14183	0.25	48.47	35.10	0.35	1.27
3	0.3	1024	0.025	96	6337	0.07	41.03	36.56	0.79	3.06
4	0.3	617	0.025	96	3164	0.05	33.55	33.08	1.58	6.00
5	0.3	3145	0.025	96	24359	0.05	58.04	38.84	0.21	1.30

PO Unit	Dose mg	Cmax ng/mL	Tmax h	TLast h	AUCtot ng/mL*h	Kel 1/h	thalf h	MRT h	F %
1	0.3	197	12.00	96	11,825	0.02	33.05	54.69	34
2	0.3	387	24.00	96	12,969	0.02	31.74	46.69	40
3	0.3	157	12.00	96	8,877	0.01	49.82	70.51	61
4	0.3	621	3.00	96	21,212	0.03	21.97	29.80	*294**
5	0.3	656	0.38	96	17,330	0.01	72.89	101.87	31

* Not included in %F average.

Horse

IV	Dose	Cmax	Tmax	TLast	AUCtot	Kel	thalf	MRT	Clearance mL/min/	Vss
Unit	mg/kg	ng/mL	h	h	ng/mL*h	1/h	h	h	kg	L/kg
Animal										
Flora	1	2506	0.08	96	22249	0.04	16.10	22.34	0.75	1.00
Kitty	1	2284	0.08	72	16242	0.06	11.02	18.02	1.03	1.11
Rice	1	2151	0.08	96	17120	0.04	15.44	20.89	0.97	1.22
Curtis	1	2182	0.08	96	19598	0.04	18.81	22.83	0.85	1.17
George	1	2812	0.08	96	14188	0.04	17.77	15.92	1.17	1.12
Que	1	2910	0.08	96	24562	0.04	18.81	22.66	0.68	0.92
Robin	1	2304	0.08	96	14106	0.04	17.38	19.57	1.18	1.39
Ketchup	1	2406	0.08	72	10388	0.06	12.47	14.27	1.60	1.37

PO	Dose	Cmax	Tmax	TLast	AUCtot	Kel	thalf	MRT	F
Unit	mg/kg	ng/mL	h	h	ng/mL*h	1/h	h	h	%
Animal									
Flora	1	311	8.00	96	10176	0.03	21.96	33.90	
Kitty	1	341	8.00	96	7637	0.04	18.50	27.50	55.13
Rice	1	459	8.00	96	9585	0.04	19.70	28.04	48.47
Curtis	1	244	12.00	96	7480	0.06	11.09	26.90	41.03
George	1	262	18.00	96	6884	0.04	16.07	31.15	33.55
Que	1	437	12.00	96	15198	0.05	14.94	29.77	58.04
Robin	1	295	8.00	96	7372	0.03	23.91	36.96	
Ketchup	Not detectable								

Supplementary Data Chapter 2. Figure S1. EC1728 PK exposures up to 24-hours post dose

(a)

(b)

(c)

(d)
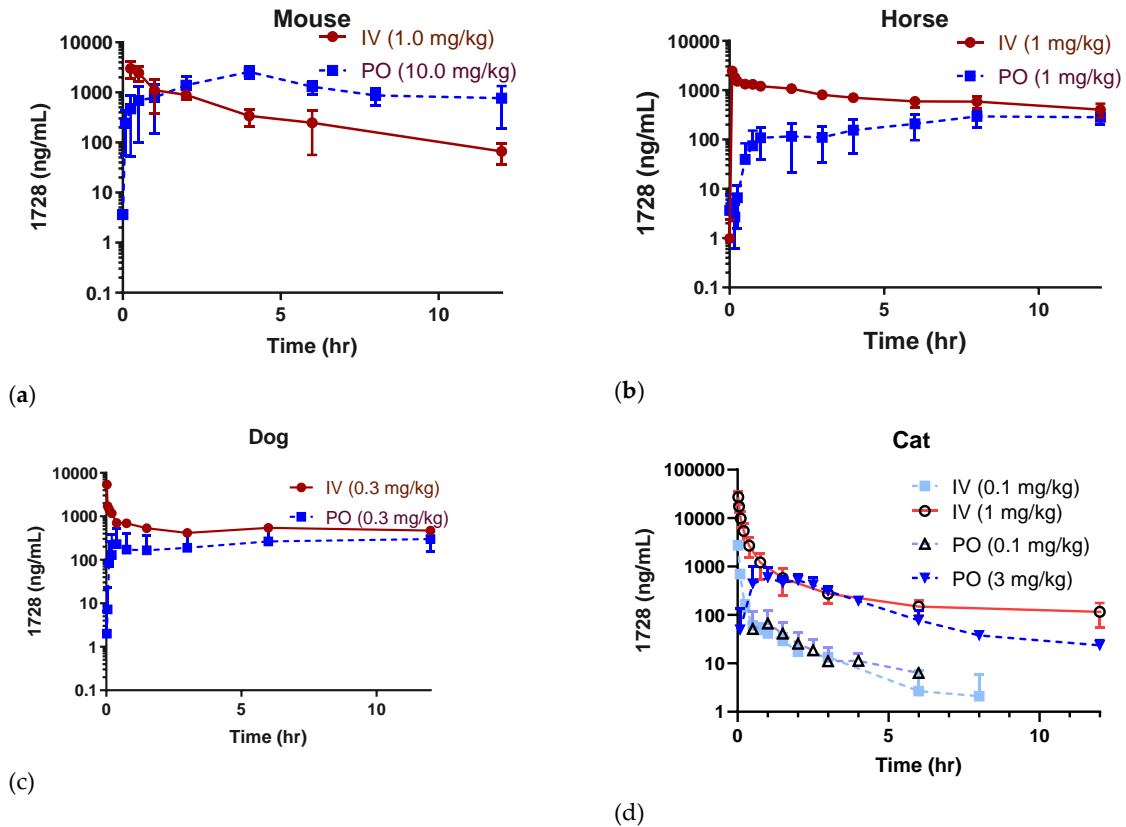
Main figure 2.1 regraphed to emphasize the first 12 hours of distribution and elimination. General overview of PK profiles of EC1728 represented as semi log-linear concentrations after dosing IV or PO in mice (n=4) (a), horses (n=8) (b), dogs (n=5) (c) and cats (n=3-6) (d). T_{last} in cats at 0.1 mg/kg iv and PO was 8 hour for IV and 12 hour for PO; however, the C_{last} in the low dose cat group dosed IV was observed at 3 hour and 4 hour for PO.

Supplementary Data Chapter 2. Table S2.2. Stability of EC1728 in liver s9 fractions isolated from different species

	S9+NADPH+Cofactors (Phase 2 metabolism)	S9+NADPH (Phase 1 metabolism)	S9 (blank)
Mouse	25.08	24.56	25.95
	25.86	24.52	25.45
	24.83	24.93	
% remaining	98 ± 2%	95 ± 0.1	100 ± 1
Cat	23.99	25.08	27.03
	25.90	25.61	26.77
	26.07	27.02	
% remaining	94 ± 5	94 ± 1	100 ± 0.1
Dog	25.17	25.34	24.28
	26.14	25.87	24.66
	25.46	22.57	
% remaining	105 ± 2	107 ± 4	100 ± 1
Horse	22.76	22.86	22.62
	23.10	24.13	26.30
	23.34	24.56	
% remaining	94 ± 1	95 ± 3	100 ± 11

Numbers represent the peak area of EC1728 divided by the internal standard (deuterated-EC1728). Negative control samples were included without microsomes (25.12, 24.165, 24.49, or 101% remaining). Percent remaining was calculated by dividing average values by average values of s9 sample without cofactors (NADPH, UDPGA, PAPS, GSH).

Supplementary Data Chapter 2. Table S2.3. Calculated clearance and accuracy based on body weight

Species for calculation*	Predicted Values Cl(hep) (ml/min*kg)		
	MCDH	MCH	MDH
Mouse	5.84	7.69	4.78
Cat	2.07	3.16	1.74
Dog	1.60	2.53	1.35
Horse	0.71	1.26	0.61
	Accuracy		
Mouse	125%	95%	153%
Cat	169%	111%	202%
Dog	28%	18%	33%
Horse	169%	95%	197%

*M: Mouse, C: Cat, D: Dog, H: Horse

Chapter 3. Pharmacological effects of inhibiting the soluble epoxide hydrolase in dogs with naturally occurring arthritis

Osteoarthritis (OA) is a degenerative joint disease that causes pain and bone deterioration driven by an increase in prostaglandins and inflammatory cytokines. Current treatments focus on inhibiting prostaglandin production, a pro-inflammatory lipid metabolite, with NSAID drugs; however, other lipid signaling targets could provide safer and more effective treatment strategies. Epoxides of polyunsaturated fatty acids are anti-inflammatory lipid mediators that are rapidly metabolized by the soluble epoxide hydrolase (sEH) into corresponding vicinal diols. Interestingly, diol levels are increased in the synovial fluid of humans with OA, warranting further research on the biological role of this lipid pathway in the progression of OA. sEH inhibitors (sEHI) stabilize these biologically active, anti-inflammatory lipid epoxides, resulting in analgesia in both neuropathic and inflammatory pain conditions. Most experimental studies testing the analgesic effects of sEH inhibitors have used experimental rodent models, which do not completely represent the complex etiology of painful diseases. In the publication described below, published in Frontiers in Pharmacology (172), we tested the efficacy of sEHI in aged dogs with natural arthritis to provide a better representation of the clinical manifestations of pain. Two sEHI were administered orally, once daily for five days to dogs with naturally occurring arthritis to assess efficacy and pharmacokinetics. Blinded technicians recorded the behavior of the arthritic dogs based on pre-determined criteria to assess pain and function. After five days, EC1728 significantly reduced pain at a dose of 5 mg/kg compared to vehicle controls. Pharmacokinetic evaluation showed concentrations exceeding the enzyme potency in both plasma and synovial fluid. *In vitro* data showed that epoxyeicosatrienoic acid (EETs), epoxide metabolites of arachidonic acid, decreased inflammatory cytokines, IL-6 and TNF-α, and reduced cytotoxicity in canine chondrocytes

challenged with IL1β to simulate an arthritic environment. These results provide the first example of altering lipid epoxides as a therapeutic target for OA potentially acting by protecting chondrocytes from inflammation induced cytotoxicity. Considering the challenges and high variability of naturally occurring disease in aged dogs, these data provide initial proof-of-concept justification that inhibiting sEH is a non-NSAID, non-opioid, disease altering strategy for treating OA warranting further investigation.

Chapter 3. Pharmaceutical Effects of Inhibiting the Soluble Epoxide Hydrolase in Canine Osteoarthritis

Cindy B. McReynolds[1,2,] Sung Hee Hwang[1,2], Jun Yang[1,2], Debin Wan[1], Karen Wagner[1,2], Christophe Morisseau[1], Dongyang Li[1], William K. Schmidt[2], Bruce Hammock[1,2*]

[1]Department of Entomology and Nematology and UC Davis Comprehensive Cancer Center, University of California, Davis, USA.

[2] EicOsis, Davis, CA, USA

*Correspondence: Dr. Bruce Hammock, bdhammock@ucdavis.edu

Keywords: Soluble Epoxide Hydrolase, Osteoarthritis, Epoxyeicostrienoic Acids, Analgesic, non-opioid analgesic, non-NSAID analgesic

Introduction

Arthritis is a collective term used to describe joint disease and pain; however, there are many types of arthritis with very different etiologies. The two most common forms of arthritis are rheumatoid arthritis (RA), an autoimmune disease, and osteoarthritis (OA), a degenerative disease that results in breakdown of cartilage between bone leading to joint pain, swelling, reduced mobility and bone degradation. Cartilage is comprised of chondrocyte cells that are responsible for generating the extracellular matrix and maintaining healthy cartilage tissue. Upon injury or disease, inflammatory cytokines lead to chondrocyte cytotoxicity and if not resolved, cartilage destruction. Recent medical advances for RA target immune suppression through monoclonal antibodies. These treatments have shown promise in effectively treating RA (192); but OA, remains largely untreated, and patients often turn to NSAIDs and opioids to alleviate pain with no benefit to treating or stopping the progression of the disease (193). In addition, these treatment options have serious side effects. For example, over 100,000 people are hospitalized each year for NSAID complications, and addiction to opioids has become a national health crisis affecting over 2 million people. Considering these serious side effects, safer and more effective options are needed for patients suffering from OA.

OA is characterized by an increase in both inflammatory cytokines and inflammatory metabolites of arachidonic acid (AA) (72). AA is an omega-6 polyunsaturated fatty acid (PUFA) that is metabolized primarily by three main enzyme systems: cyclooxygenases (COX), lipoxygenases, and CYP450s. COX metabolism of AA produces proinflammatory prostaglandins (PGs) that increase inflammatory cytokines and drive the progression of OA. Blocking PG production with NSAIDs that inhibit COX function has been an important approach to treating the disease (194). However, despite the prevalent use of NSAIDs prescribed to OA patients, the efficacy and side-effects vary widely among patients, and long-term NSAID use is associated with

76

increased risk of life-threatening toxicities (195). Targeting other lipid mediators, such as the CYP450 branch of the arachidonic acid cascade instead of the COX branch may provide better treatment alternatives. CYP450 epoxide metabolites of AA, or epoxyeicosatrienoic acid (EETs) prevent the translocation of Nf-κB into the nucleus thereby resulting in decreased inflammatory cytokines (11). Additionally, EETs reduce ER-stress to help maintain homeostasis and have been effective in reducing neuropathic pain (196). For these reasons, EETs are viewed as largely anti-inflammatory compounds thought to resolve inflammation and ER-stress and reverting disease states back to physiologically normal conditions, but are often limited in efficacy due to their rapid degradation by the sEH into diol metabolites for excretion (197) (Figure 3.1). Recently, the sEH products of EET metabolism (specifically 11,12 and 14,15 dihydroxyeicosatrienoic acid (DHET)) were found in higher concentrations in arthritic joints compared to healthy or unaffected joints (72). Chemical inhibitors of sEH increase the concentration of EETs and other epoxides of omega-3 and -6 fatty acids in the body by decreasing the formation of corresponding diol metabolites (43). Increasing epoxy-fatty acid (EpFA) concentration through inhibition of the sEH resolves a variety of disease states in laboratory settings, and efforts are ongoing to evaluate inhibition of sEH as an effective treatment for pain in clinical applications (31).

Figure 3.1: Arachidonic acid metabolism
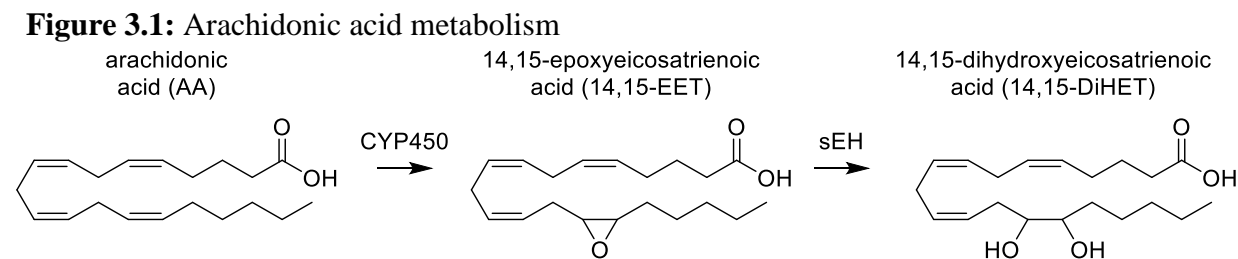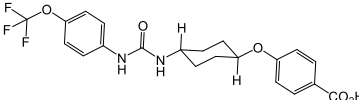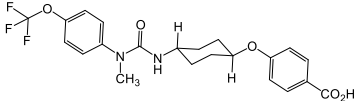
Figure 3.1: Metabolism of arachidonic acid (AA) by cytochrome P450 (CYP450) generates anti-inflammatory fatty acid epoxides (EETs) that are degraded by the soluble epoxide hydrolase (sEH) to the corresponding 1,2 diols (DHETs). DHETs are more polar and diffuse out of the cells and are readily conjugated and excreted. The omega-6 fatty acid, arachidonic acid and representative metabolite, 14, 15 DHET is depicted below. Similar vicinal diols are formed on the double bonds, and other omega-3 and 6 PUFAs are metabolized in a similar fashion.

The sEH inhibitor, EC1728 (*trans*-4-(4-[3-(4-trifluoromethoxy-phenyl)-ureido]-cyclohexyloxy)-benzoic acid, also referred to as *t*-TUCB), is a potent sEHI that has shown efficacy in several animal models (198) and in treating a natural, neuropathic pain condition in horses called laminitis (171). Although EC1728 has been effective in multiple models of pain, it has poor physical properties, such as a high melting point (212.2°C) and low water solubility (5 mg/L in PBS), that limit its formulation and bioavailability. Efforts were made to develop new sEHI with improved physiochemical properties. Because optimization of sEH inhibitors demonstrated that carbamates and amides are generally less active than urea pharmacophores (199), new compounds focused on keeping the urea pharmacophore. Attempts at improving the physicochemical characteristics of EC1728 identified EC3039 (*trans*-4-(4-[3-methyl-3-(4-trifluoromethoxy-phenyl)-ureido]-cyclohexyloxy)-benzoic acid, also referred to as t-MTUCB) as a structurally similar compound that differs only in the addition of a N-methyl group to the urea pharmacophore (Table 1). The results below describe the evaluation of these two sEHI in a preclinical, randomized and blinded study for their ability to alleviate pain in dogs with natural osteoarthritis. *In vitro* studies tested the hypothesis that sEH inhibition reduces pain by increasing EETs that decrease inflammation in the chondrocytes.

Table 3.1: EC1728 and EC3039 are potent sEH inhibitors. EC3039 has a lower melting point and higher solubility but is less potently inhibiting the canine sEH enzyme compared to EC1728.

Structure	Mol. Wt. (g/mol)	Melting Point (˚C)	Cal. LogP[1]	canine sEH IC$_{50}$ (ng/mL)[2]	Solubility (mg/mL)[3]	
					PBS pH 7.4	PEG300
EC1728	438.40	240 244	-5.0	0.4 ± 0.1	0.005 ± 0.001	97 ± 2
EC3039	452.43	92.4 94.7	-5.0	2.0 ± 0.3	0.130 ± 0.015	99 ± 1

[1] LogP was calculated using ChemDraw Professional version 18.0.0.231
[2] IC$_{50}$ was measured using PHOME ([S] = 50 µM) as fluorescent substrate with partially purified canine sEH from dog liver (200). The residual esterase activity was completely inhibited with paraoxon (100 µM) in assay buffer.
[3] Solubility was measured at 40°C as described (189).

Materials and Methods
sEHI (EC1728 and EC3039): EC1728 was synthesized in-house as previously described (189),

synthesis of EC3039 and deuterated 1728 *trans*-4-(4-[3-(4-trifluoromethoxy-phenyl)-ureido]-

cyclohexyloxy)-benzoic-2,3,5,6-d_4 acid, also referred to as 3049, *t*-TUCB-d_4) is described in the

Supplementary Materials.

IC$_{50}$ was determined as previously described. (200) Briefly, canine enzyme was partially purified

on a Q-sepharose column from liver cytosol (~10-fold purification) as described in (92). The

residual esterase activity was completely inhibited with paraoxon purchased from Chem Services

Inc (West Chester, PA, catalog number 42417404) at a concentration of 100 µM in assay buffer.

EET mixture: EETs (5,6 EET, 8,9 EET, 10,11 EET and 13,14 EET) were purchased from Cayman

Chemicals (catalog numbers 50211, 50351, 50511, and 50651) and diluted 1000-fold for a final

concentration of 0.1 µg/mL for each EET (0.4 µg/mL total). **Meloxicam** iv injectable was

purchased from the UC Davis veterinary pharmacy at 5 mg/mL. Stock solutions were diluted to 1 mg/mL in ethanol and added to cell cultures at a final concentration of 1 µg/mL and 0.1% ethanol.

Solubility of sEHI: solubility was determined by shaking the compounds in phosphate buffered saline (pH 7.4) at 40 ˚C for 24h in glass tubes. The non-dissolved compounds were filtered through a 0.22 µm centrifuge filter at 40˚C and the supernatant was further diluted 10 times with methanol. The samples were analyzed by LC/MS-MS. Conditions are based on previously published methods in the lab and kept consistent in order to compare compounds (189).

HPLC/MS-MS method: Concentrations of EC3039 and EC1728 were determined by LC/MS/MS analysis as previously described (92) and defined in detail in the supporting materials section S2 and optimized parameters listed in supplementary table S3.1.

In vitro model of chondrocyte cytotoxicity

     Cell culture: Canine chondrocytes (CnC) were purchased from Cell Applications, Inc (catalog number Cn402-05). Cells arrived at Passage 1 and were cultured in complete growth media (Canine Chondrocyte Growth Medium supplemented with 10% Canine Chondrocyte Growth Supplement (CGS), both from Cell Applications, Inc.) and maintained at 37°C in a 5% CO_2 atmosphere. Once cells reached 80% confluence, they were passaged by removing the media, washing with PBS (warmed to room temperature) before adding 0.05% Trypsin-EDTA (Gibco Life Technologies, catalog number 25300) also warmed to room temperature. Cells were kept at room temperature and monitored for detachment (~2 minutes). Detached cells were added to 3x volume of full growth media and centrifuged to remove trypsin. Cells were reseeded at a concentration of 15,000 cells/cm^2 to reach 80% confluence in 3 days. Cells were expanded and

frozen at the 3rd passage in CGS containing 10% DMSO. For individual experiments, fresh cells were thawed and used at passage 5.

Chondrocyte cytotoxicity in vitro: CnC cells were plated in 96-well plates at a density of 15,000 cells/cm^2. Optimal cell number was predetermined by a cell seeding experiment outlined in O'Brien et al. (201) Cells were treated with recombinant canine IL1β (Novus Biologicals catalog number 3747-CL-025) in CGS-free media for 2 hours at 37°C. After two hours, the IL1β treated media was aspirated and replaced with complete growth media supplemented with either vehicle (0.1% ethanol), regioisomers of epoxyeicosatrianoic acid, or meloxicam for 48-hours before assessing inflammatory cytokines and cytotoxicity. Cells were also pretreated with meloxicam or EET mixture 30 min prior to adding IL1β treatment for 2-hours. After IL1β was removed, treatments were added to complete growth media for 48-hours as described above. Treatment conditions are described in the results section.

Cytotoxicity assay: After the CnC cells were treated for 48-hours under conditions described above, the media was removed and replaced with complete media containing 10% Alamar Blue (Life Technologies, catalog number DAL1025). The Alamar Blue assay relies on the metabolism of non-fluorescent resazurin to the highly fluorescent resorufin by healthy cells. Fluorescent intensity can be used to track cytotoxicity after xenobiotic treatments (202). After the addition of Alamar Blue, plates were protected from light and incubated at 30°C in a 5% CO_2 atmosphere for 8 hours. The conversion of resazurin was monitored by reading fluorescence at 570 excitations and 585 emission on a plate reader (Tecan M1000 Pro) and cytotoxicity was calculated as the ratio of fluorescence from treated cells to non-treated controls.

ELISA determination of IL-6 and TNF-α: ELISA determination of canine IL-6 and TNF-α: DuoSet ELISA kits (R and D Systems, RRID:SCR_006140) were used to quantify

inflammatory cytokines, IL-6 (catalog number DY1609) and TNF-α (catalog number CATA00) in the media collected after 48-hour of EET or vehicle treatments. Manufacturer's instructions were followed with adaption to improve the assay sensitivity using polymeric horseradish peroxidase (PolyHRP) according to previous work (203). The following adaptions were conducted: the original two separate steps of adding standards\sample and biotinylated detection antibody with each incubated 2 hours were changed to one-step simultaneous addition of both reagents with incubation time shortened to 1 hour. After washing, the addition of streptavidin conjugated to horseradish peroxidase (Streptavidin-HRP) from the kit was replaced with streptavidin PolyHRP40 conjugate (25 ng/mL, 30 min) from SDT GmbH (Baesweiler, Germany). All incubations above were performed at room temperature with shaking (600 rpm, MTS 2/4 digital microtiter shaker, IKA, Germany).

Microsomal stability: Male and female dog liver microsomes (Xenotech) were diluted in potassium phosphate buffer (0.1M, pH 7.4), MgCl2 (3.15mM), sodium EDTA (1.05 mM) to a final protein concentration of 1 mg/mL. Compounds were added at 0.1mM in methanol at 1% and microsomes were activated with 5% (v/v) NADPH regenerating system (100 µL sodium phosphate buffer (0.1M, pH 7.4), 50 µL, glucose-6-phosphate in sodium phosphate buffer (0.1M, pH 7.4), 50 µL NADP+ in sodium phosphate (0.1M, pH 7.4) and 50 µL of 100 Units/mL of glucose-6-dehydrogenase). Compounds were incubated for 60 minutes at 37°C and quenched with 4x volume of ice-cold methanol containing deuterated EC1728 as an internal standard. Compounds were incubated without microsomes or NADPH as negative controls.

Pain assessment in arthritic dogs

In vivo **studies:** Studies were contracted with InterVivo Solutions, Toronto, Canada to assess pain and pharmacokinetics of E1728 and EC3039 in aged beagle dogs with osteoarthritis. This study was conducted in accordance with InterVivo's approved IACUC protocol, in compliance with the Animal Welfare Act (AWA) and Public Health Service Policy on Humane Care and Use of Laboratory Animals.

Drug Administrations: There were five groups in total (placebo, 1 mg/kg EC1728, 5 mg/kg EC1728, 1 mg/kg EC3039 and 5 mg/kg EC3039). The placebo group contained 8 osteoarthritic dogs. The four drug-treated groups contained 8 osteoarthritic dogs and two satellite dogs (1 male and 1 female) of similar age and weight for PK blood sampling. Time 0 served as the pretreatment control. A total of 48 animals were on study.

PK analysis: Eight satellite dogs (2 per each group) had whole blood collected for PK analysis on study Days 0 through 4. On Day 1, blood was collected immediately prior to dosing, and again at 0.25, 0.5, 1, 2, 4, 6, 8 ($\pm$ 5 minutes) after dosing. On Day 2 through 4, blood was collected 0.5 hours ($\pm$ 5 minutes) after dosing. On Day 5 blood was collected immediately prior to dosing, and again at 0.25, 0.5, 1, 2, 4, 6, 8 ($\pm$ 5 minutes), 24, 48 and 72 hours ($\pm$ 30 minutes) post treatment. The exact sampling time was noted in the study file. For all blood samples, a minimum of 3mL of whole blood was collected from a suitable vein as per written and approved standard operating procedures. The blood was transferred to K_2EDTA (spray dried) blood tube and inverted gently multiple times to ensure proper mixing of the blood and anticoagulant. On study Day 5, synovial fluid was collected by arthrocentesis immediately after the subject completed the questionnaire (approximately 3 hr after dosing). Subjects were anesthetized as per written and approved Standard Operating Procedures. A minimum of 0.1mL of synovial fluid was collected

from each subject. Samples were frozen in an upright position and stored at -80°C ±4°C before being shipped to UC Davis for analysis.

For PK analysis in the satellite group, individual parameters were calculated by fitting blood concentrations to a non-compartmental analysis using Kinetica software (ThermoFisher version 5.1). Using the log-linear trapezoidal method, the area under the curve were calculated and were extrapolated to infinity using the last measured plasma concentration (C_{last}), defined as the timepoint collected 72 hours after the last dose or 8 hr after the first dose on day 1, divided by the terminal slope (λz).

Efficacy: The study was conducted as a blinded, parallel matched-group design. Dogs were randomized into groups based on pretreatment pain scores and each group was randomly assigned a treatment. Prior to randomization, each dog was assessed for arthritis by radiograph to assess the severity of OA by presence of osteophytes, subchondral sclerosis or joint effusion each scored on a scale of 0 (least) to 3 (worst) for each of 12 joints. Severity of the radiograph score was included in the randomization protocol and distributed between the groups, and there were no statistical differences between the averages of each group. Individual radiograph scores can be found in Table S3.2 of the supplementary material. Treatment groups consisted of vehicle control, 1 mg/kg EC3039, 5 mg/kg EC3039, 1 mg/kg EC1728, and 5 mg/kg EC1728. Compounds were dissolved in PEG300 to a concentration of 2.4 mg/mL (1 mg/kg) and 12 mg/mL (5 mg/kg) and administered as approximately 5 mL in size 12 gelatin capsules (Torpac) administered once daily on days 1 through 5. Vehicle group consisted of 5 mL PEG300 in capsule. Concurrent medications were not allowed and not needed during the study.

Pain and Function Assessments: Pain and function were assessed by a questionnaire answered by blinded technicians based on observation of study animals housed at Intervivo. The

survey was adapted from the canine brief pain inventory (CBPI), which was developed based on clinical questionnaires in which owners score the function and pain level of their pets with existing pain conditions (204). Modifications to the questionnaire attempted to account for differences between owner pain evaluation of pets and pain evaluation of laboratory dogs by technical staff. For survey administration, blinded technicians attempted to elicit objective behavior-specific measures of function and pain level across a variety of normal canine behaviors (e.g. walking, trotting, galloping, rearing, stair-climbing, etc.). For this, one technician was responsible for soliciting the relevant behaviors from a dog using encouragement and/or food rewards, while the evaluating technician scored function and observable pain using the modified CBPI questionnaire. Subjects were tested daily on Days -7 through -3, to develop baseline scores, and again on Days 1 through 5 administered 1.5 hours after dosing. Dosing occurred in the morning, and observations were recorded 1.5hr after dosing, to limit time-of-day variability. Questions are listed in Supplementary Table S3.3. Animals in treatment groups had blood and synovial fluid collected ~2 hour after the last dose on day 5 (immediately following the study questionnaire) to confirm plasma concentrations in treated animals. Full pharmacokinetic assessments were collected from a satellite group of animals so as not to interfere with pain assessment.

Statistical Analysis: Canine pain and function data were analyzed using ANOVA, linear mixed effects model, with Tukey adjustment in R and repeated measures ANOVA. Correlations coefficients were calculated in Graphpad Prism using the nonparametric Spearman correlation coefficient. *In vitro* experiments were analyzed using ANOVA in Graphpad Prism. Data are reported significant if $p < 0.05$.

Results

sEHI physicochemical characteristics. EC3039 was synthesized and designed to have favorable physiochemical properties relative to EC1728. As crystals or larger particles, lipophilic

urea compounds have poor oral availability. Also, Chu and Yalkowksy showed an association between lower melting point and increased absorption (205). Thus, improving the aqueous solubility and lowering the melting point were prioritized to improve the potential for efficacy in future *in vivo* studies. EC3039 had improved solubility and lower melting point compared to EC1728 but had a slightly less potent IC_{50} (5-times less potent than EC1728, Table 3.1). To assess the metabolic stability, both compounds were tested for stability after incubation in dog liver microsomes. Both compounds were relatively stable with EC1728 having over 95% remaining, and EC3039 having over 90% remaining in male liver microsomes and 85% remaining in female liver microsomes after 60-minute incubations (Table 3.2).

Table 3.2. EC3039 and EC1728 are stable after 60-minute incubations with male and female dog liver microsomes.

Compound		% Parent	
		+ NADPH	- NADPH
EC3039*	Males	90 ± 7	97 ± 4
	Females	85 ± 2	93 ± 5
EC1728	Males	103 ± 6	108 ± 8
	Females	98 ± 6	106 ± 9

* A small amount of EC1728 higher than the LOD (0.3 ng/mL) but lower than the LOQ (3 ng/ml) was detected in microsomes incubated with EC3039. Values represent mean ± of 3 replicates.

In Vivo **arthritis evaluation:** To evaluate the PK of both EC1728 and EC3039 and the ability to alleviate pain in dogs with natural arthritis, two dose levels of EC1728 and EC3039 were administered orally for five consecutive days to aged dogs with arthritis.

PK analysis: In the satellite PK group (n=2, 1 male and 1 female), concentrations of EC3039 and EC1728 increased through day 5 (Figure 3.2). Based on the reported half-life of both compounds (24 – 40 hr, Table 3.3), it is expected that concentrations reported on day 5 represent the steady state values (206). Systemic exposure (C_{max} and AUC) increased in a more than dose

proportional manner for EC3039 in both the male and female satellite PK dogs. On day 1, a 5-fold increase in dose resulted in a 30 to 40-fold increase in C_{max} and approximate 18-fold increase in AUC for EC3039 (Figures 3.2A and B). Alternatively, a 5-fold increase in dose for EC1728 resulted in a less than dose dependent increase in systemic exposure (3.25-fold increase in both C_{max} and AUC after 5-fold dose increase) (Figures 3.2C and D). As the compounds reached steady-state, dose proportionality for EC1728 was less pronounced, with EC1728 having similar C_{max} and AUC for both doses (Table 3). This is likely due to the poor solubility of EC1728 where intestinal absorption is dependent upon the amount of drug that is in a true solution. A small portion (<10%) of 3039 was metabolized by demethylation to form EC1728 (Figure 3.2A and B).

Efficacy: Dogs tolerated all treatments well, with no treatment related adverse events reported (a list of events recorded for the study can be found in Supplementary Table S3.4). Body weights were recorded on the day prior to dosing and again on day 5 of dosing. No dogs gained or lost more than 5% of their body weight in any of the treatment groups. Dogs were assessed for pain and function based on a 12-question survey. The survey was administered for 5 days prior to dosing: the first two days were defined as an acclimation period and the final three days were averaged to provide baseline scores. One two days prior to treatment, and after establishing baseline measurements, each dog was randomized based on age, radiograph score, and survey response. Prior to treatment, all groups averaged a score of 20 out of 24 for pain, and 14 out of 48 for function, except for the 1 mg/kg EC3039 group which averaged 15 for function. There were no significant differences between the baseline assessments of each group. One-way ANOVA analysis indicates that over the five days of treatment, EC1728 administered at 5 mg/kg significantly reduced pain in dogs with osteoarthritis (Figure 3.3A). The maximum effect was observed on day 4 with an average of 44% reduction in pain compared to predose values. Vehicle

treated animals were reported to have only a 7% reduction on this day. While there were no statistical differences between function scores for each of the treatment groups, dogs treated with EC1728 at 5 mg/kg tended to have increased function scores compared to the other groups (Figure 3.3B). After 5-days of dosing, dogs showed a 16% increase in function compared to a 3% decrease in function reported in the vehicle treated animals. Both pain and function scores showed high variability throughout the course of treatment. In addition, we did not observe significant association between pain and function in our data when analyzed by a nonparametric Spearman correlation coefficient.

Table 3.3. PK parameters of EC3039 and EC1728 administered to a satellite group of n=2 dogs for 5 days by oral gavage.

	Gender	Compound Detected	C_{max} (ng/mL)		AUC_{last} (h*ng/mL)		$T_{1/2}$ (h)
			Day1	Day5	Day1	Day5	Day5
EC3039 (1 mg/kg)	M	EC3039	400	2,300	2,490	72,100	33
		EC1728[1]	5	101	26	6,370	-
	F	EC3039	568	17,300	3,940	361,000	40
		EC1728	4	404	24	25,200	-
EC3039 (5 mg/kg)	M	EC3039	16,900	32,100	46,500	463,00	27
		EC1728	54	772	295	50,200	-
	F	EC3039	18,000	30,900	67,200	589,000	25
		EC1728	50	606	298	39,000	-
EC1728 (1 mg/kg)	M	EC1728	330	1,900	1,690	32,000	27
	F	EC1728	308	4,660	1,350	155,000	33
EC1728 (5 mg/kg)	M	EC1728	1,100	1,930	3,760	96,300	25
	F	EC1728	1,160	4,990	4,940	53,200	23

[1] EC1728 was detected in animals treated with EC3039, presumable from N-demethylation by CYP450; however, the T1/2 could not be calculated because it could not be fitted to a PK model.

EC3039 had improved PK properties compared to EC1728. EC3039 had higher systemic exposure (C_{max} and AUC) compared to EC1728, and exposure increased in a more than dose proportional manner for EC3039 and less than dose proportional manner for EC1728. Exposure for both compounds increased over the 5-days of dosing.

Figure 3.2: Concentrations of EC3039 and EC1728 in the blood exceeded the IC50 for sEH for all treatment groups for the duration of the study.
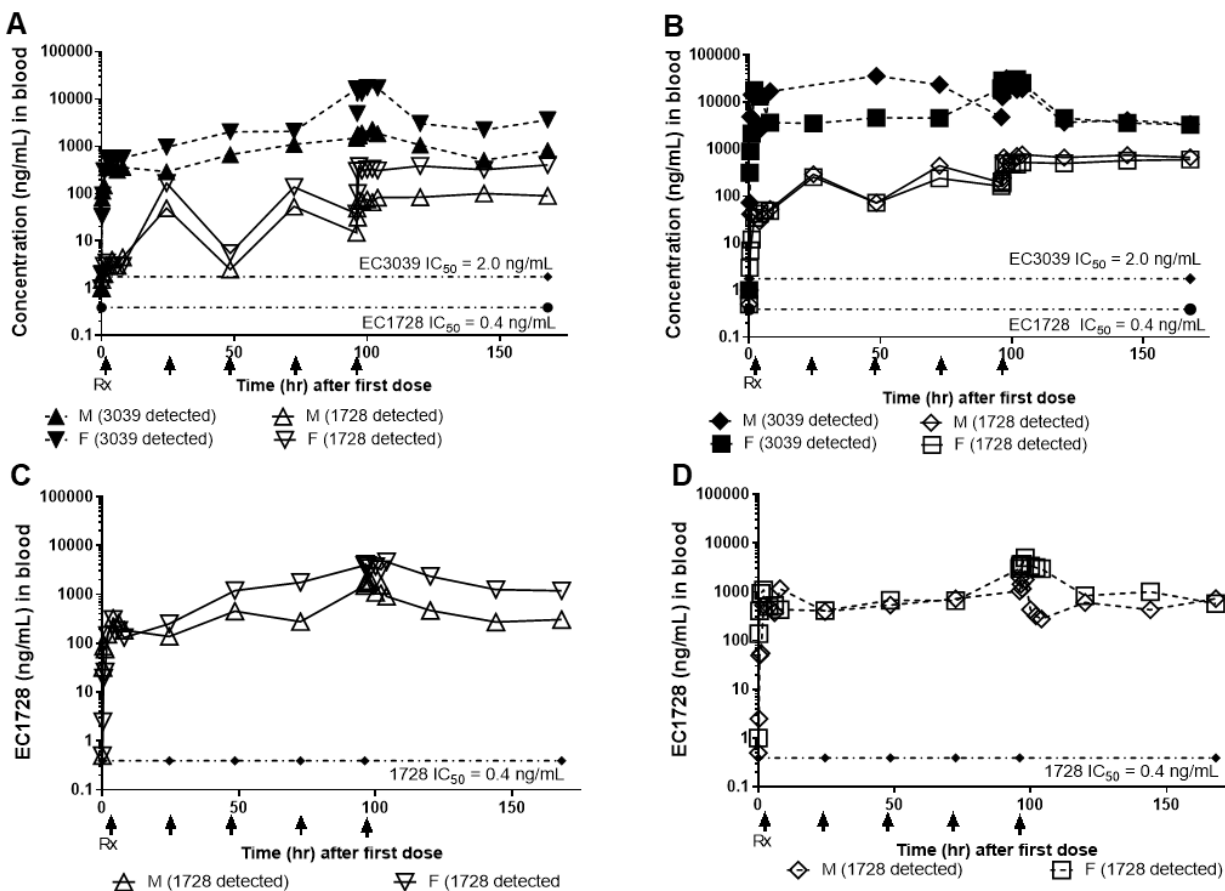
Figure 3.2. The PK profile of animals treated with EC3039 (A and B) or EC1728 (C and D) in a satellite group of n = 2 dogs administered 1 mg/kg or 5 mg/kg orally once daily for 5 consecutive days is shown below. Blood was collected at 0.25, 0.5, 1, 2, 4, 6, 8 hours after dosing on Day 1, and again on days 2 through 4 at 0.5 hours after dosing. On Day 4, blood was collected immediately prior to dosing, and again at 0.25, 0.5, 1, 2, 4, 6, 8 ($\pm$ 5 minutes), 24, 48 and 72 hours ($\pm$ 30 minutes) post treatment. Concentrations of EC1728 and EC3039 were well above the EC_{50} for the study duration. Blood concentrations increased over the 5 days of dosing in all treatment groups, and $T_{1/2}$ calculated from the parent concentration predicts that steady-state is reached by day 5 for EC1728 and between days 5-8 for EC3039.

Figure 3.2A and 2B. Dogs administered EC3039 at 1 mg/kg (**2A**) and 5 mg/kg (**2B**) had detectable amounts of EC1728 in their blood presumably from demethylation of the urea by CYP450. The amount was proportional to EC3039 levels and above the EC_{50} for sEH, although approximately 3x lower than the dogs in the EC1728 treatment groups. A model could not be fitted for EC1728 detected from dogs administered EC3039 and $T_{1/2}$ were not calculated.

Figure 3.2C and 2D. Dogs administered EC1728 at either 1 mg/kg (**2C**) and 5 mg/kg (**2D**) had no detectable amounts of EC3039 in their blood. Drug concentrations did not show a clear dose response for dogs treated with EC1728, and dogs treated with 1 mg/kg of EC1728 (**2C**) had approximately half the AUC as dogs treated with 5 mg/kg EC1728 (**2D**).

Figure 3.3: Treatment with sEHI EC1728 but not EC3039 reduced pain but did not significantly increase function in arthritic beagle dogs compared to placebo control.

Figure 3.3: EC1728 at 5 mg/kg reduced pain and increased function in dogs with osteoarthritis.
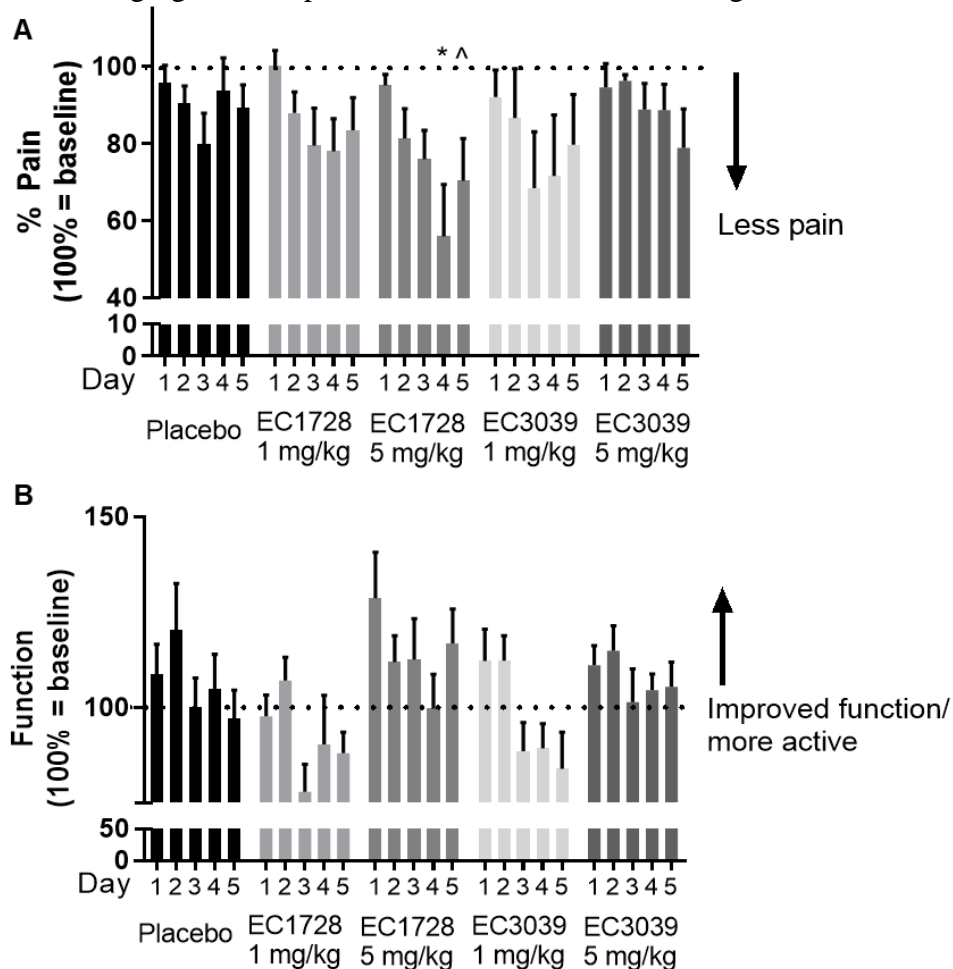
In order to assess pain, technicians blinded to treatment answered a predetermined questionnaire based on observed dog behavior (on a scale of $0 - 2$) and activity (on a scale of $0 - 5$) of aged beagle dogs (n=8/group). Score 0 was classified as least pain and most function. The composite score was normalized for each individual dog to their predose score for pain (A) and function (B) are presented below. (A). Dogs treated orally, once daily with EC1728 at 5 mg/kg for five days had significantly less pain compared to the placebo group. Placebo control consisted of administration of an empty 100% PEG300, size 12 capsules from Torpac. Statistical significance was reached on day 4. After 5-days of dosing, EC1728 significantly reduced pain compared to vehicle control when analyzed by repeated measures ANOVA. There were no statistical differences identified for other treatment groups. **(B)** While no statistical significance was observed for improvement in function with any treatment group, dogs treated with EC1728 tended to have higher function scores than other treatment groups (p<0.05 for treatment effect when analyzed by repeated measures ANOVA, but there was no statistically significant interaction between treatment groups). * p < 0.05 compared to placebo and ^ p<0.05 for cummulative treatment effects when analyzed by repeated measure ANOVA. Figures represent mean ± STDEV.

Concentrations of EC3039 and EC1728 were assessed in the whole blood and synovial fluid of dogs in each treatment group (n=8). No compounds were detected in the placebo treated group. Most animals had compound concentrations measured above the IC_{50} for enzyme inhibition in both blood and synovial fluid indicating that the compound was able to penetrate into the target tissue (Table S5 in Supplementary Materials). Dogs treated with EC3039 had higher C_{max} and AUC concentrations of sEHI in their blood and synovial fluid than dogs treated with EC1728 (approximately 2x more in the low dose group and 10x more in the high dose group). Dogs treated with EC3039 also had detectable levels of EC1728 in their blood and synovial fluid, presumably due to demethylation of the urea. However, these concentrations were lower than dogs administered parent EC1728, indicating that EC3039 is acting largely as a direct sEHI, and EC3039 is a poor prodrug for EC1728. Of note, one dog (dog 2.4, Table S3.5 in Supplementary Materials) treated with 5 mg/kg EC1728 had lower amounts of compound detected in the blood and synovial fluid (34 ng/mL in the blood on day 5 compared to 395 ng/mL average for the remainder of the group, and 80-95 ng/mL in the synovial fluid vs. 988 ng/mL averaged for the group on day 5). Due to low exposure levels, this dog was removed from analysis.

In vitro **model of chondrocyte cytotoxicity:** To elucidate the role of increasing EET concentrations in arthritic animals, EET mixtures were evaluated for their ability to decrease inflammatory cytokines and protect chondrocytes against IL1β induced cytotoxicity. CnC cells treated with IL1β showed a significant and dose dependent increase in cytotoxicity (Figure 3.4A) that was eliminated when the chondrocytes were pretreated with either meloxicam or EETs, or treated post-IL1β with a mixture of EETs (Figure 3.4B). The *in vitro* model evaluated two concentrations of IL1β, 10 and 100 ng/mL, to simulate osteoarthritis conditions in patients. A dose dependent reduction in cytotoxicity was observed (Figure 3.4A), and 10 ng/mL was selected as

the concentration for continued experiments to better replicate *in vivo* conditions (0.288 ng/mL reported in the synovial fluid of humans with OA (207)). Interestingly, treating CnC cells with meloxicam after IL1β did not result in significant improvement in cytotoxicity. IL1β induces COX activity and an increase in prostaglandins such as PGE2 (208); thus, it is no surprise that post treatment with a COX inhibitor would fail to attenuate inflammation in the presence of prostaglandins (209). Conversely, the anti-inflammatory action of EETs act downstream of PGE2 (138); therefore, it is expected that EETs would work to counter PGE2 induced inflammation post IL1β treatment when the NSAID, meloxicam, did not. Protein measurement of inflammatory cytokines IL-6 and TNF-α were reduced in chondrocytes treated with a mixture of EETs (Figure 3.5); confirming that EETs protect chondrocytes through an anti-inflammatory response.

Figure 3.4: EETs reduced cytotoxicity in a dog chondrocyte cell line after IL1β exposure.
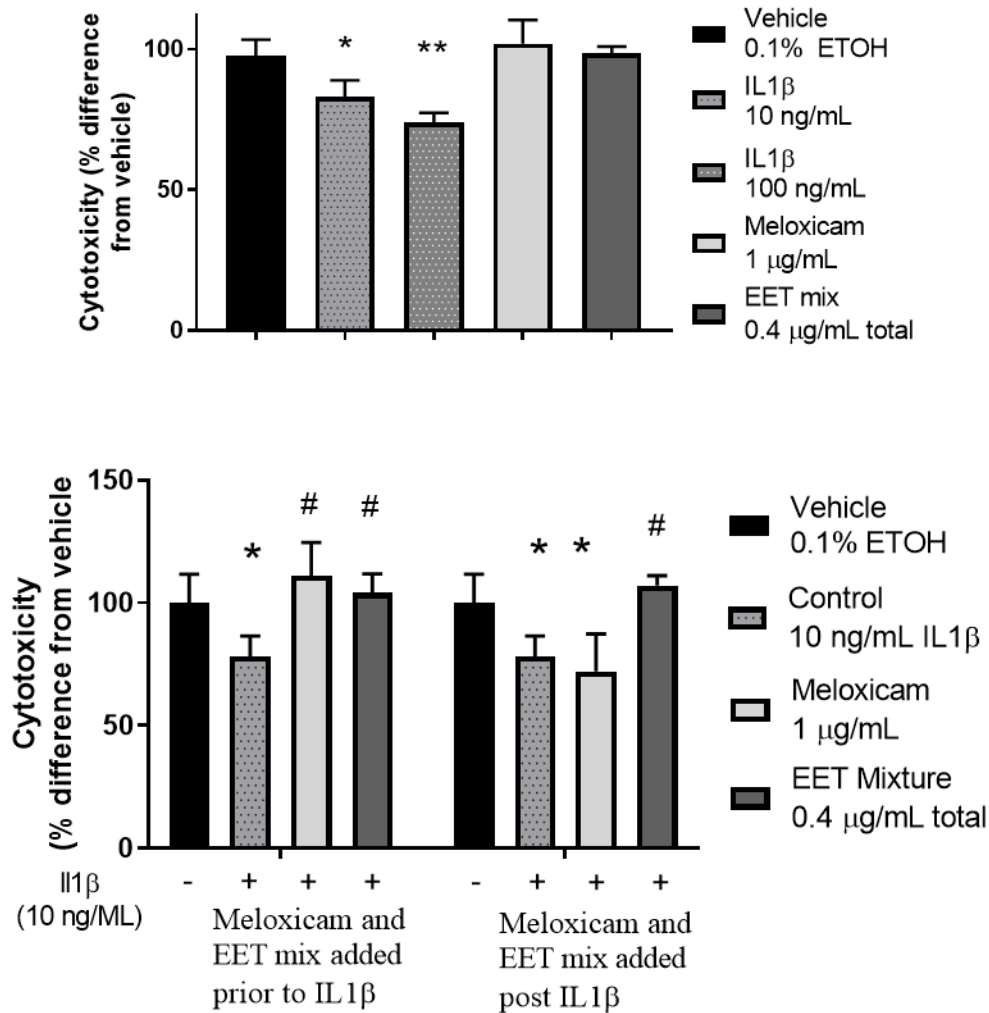
Figure 3.4: IL1β induced cytotoxicity was alleviated by meloxicam or EET mixture in an *in vitro* model of OA. **(A)** CnC cells treated two hours with IL1β showed a dose dependent increase in cytotoxicity measured by Alamar Blue. The meloxicam or EET mixture, treated for 48 hours, in the absence of IL1β, had no effect on healthy CnC cells. **(B)** Chondrocytes treated with IL1β for 2 hours before or after treatment with meloxicam (1 µg/mL) or a mixture of EETs (5,6 EET, 8,9 EET, 11,12 EET and 14,15 EET each at 0.1 µg/mL for a total EET concentration of 0.4 µg/mL). Meloxicam (added before the addition of 10 ng/mL of IL1β) or EET mixture, added either before or after a 2-hour IL1β treatment significantly reduced IL1β induced cytotoxicity. Meloxicam added after IL1β did not result in significant reduction in cytotoxicity.
* $p < 0.05$, **$p < 0.005$ compared to vehicle not treated with IL1β; # $p < 0.005$ compared to vehicle treated with IL1β. Figures represent the average ± STDEV of a minimum of 3 separate experiments. Each experiment tested a minimum of 3 wells.

Figure 3.5: EETs reduced inflammatory cytokines, TNF-α and IL-6, in a dog chondrocyte cell line after IL1β exposure.
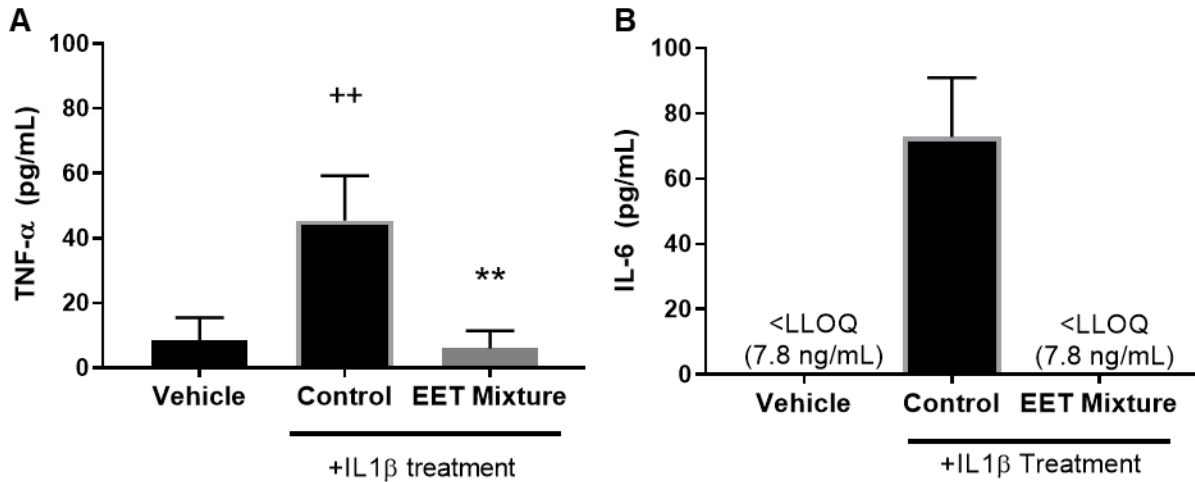
Figure 3.5: EET mixture (0.4 µg/mL) significantly reduced inflammatory cytokines, TNF-α and IL-6 after a 2-hour treatment of IL1β (10 ng/mL).

Inflammatory cytokines, TNF-α (**Figure 3.5A**) and IL-6 (**Figure 3.5B**), protein levels were measured by ELISA 48-hour after a 2-hour treatment of IL1β or vehicle. Treatment with IL1β significantly increased both cytokines. When a mixture of EET regioisomers (0.1 µg/mL of each for a total of 0.4 µg/mL total) was added to the media after IL1β was removed, IL-6 and TNF-α decreased to levels comparable to cells not treated with IL1β. $P < 0.005$ between IL1β treated and not-treated (++) and post IL1β treated vehicle vs. EET (**). There was no significant difference between cells not treated with IL1β and cells treated with EET mixture after a 2-hours after IL1β. Figures represent the average ± STDEV of a minimum of 3 separate experiments. Each experiment tested a minimum of 3 wells.

Discussion

To assess the effects of sEHI on treating pain in animals with OA, arthritic dogs were treated orally with either of two sEHI (EC3039 or EC1728) for five days, and pain and function were measured compared to untreated placebo animals as a measure of efficacy. Although a potent inhibitor, EC1728 has poor solubility in both water and common organic solvents as well as a high melting point. EC3039 was synthesized to improve solubility without significantly altering the structure: by adding a methyl group to the urea pharmacophore, potency only slightly decreased but water solubility improved by almost 30-times and melting point was reduced from 240°C to 92.4°C. Additions of N-methyl groups on the urea of sEHI are generally less active because the two hydrogens on the urea are needed to bond to the catalytic aspartic acid in the active site of the enzyme (210). EC3039 was ~5x less potent than EC1728 presumably due to the addition on the urea pharmacophore; although more active than most other compounds with N-methyl additions on the urea. Improved solubility and lower melting resulted in improved PK as evident by the increase C_{max} and AUC of EC3039 compared to EC1728, and it was hypothesized that improvements in PK would compensate for decreased potency. Despite the less than ideal physiochemical properties of EC1728, the compound displayed favorable PK, and both EC3039 and EC1728 had concentration measured in the plasma and synovial fluid well above the IC_{50} of sEH. Only EC1728 at 5 mg/kg was effective in reducing pain associated with OA in dogs. While a full PK profile was conducted in satellite animals, in order to not interfere with pain assessments, study animals only had synovial fluid collected on days 1 and 5 after pain assessments were complete. Because a full timecourse of distribution in the synovial fluid was not feasible without interfering with efficacy measurements, it is unknown if EC1728 remained in the synovium longer than EC3039. It is also possible that EC1728 is more effective in penetrating the cells and interacting with the target enzyme than EC3039. In addition to differences in potency and

distribution, target occupancy, or amount of time the drug is bound to the enzyme, could also influence the efficacy of the compounds. Target occupancy is a predictor of efficacy, and although the exact resonance time of the drug on the enzyme is unknown, the decrease in potency suggests an increase in K_{off}; thus, improved efficacy observed with EC1728 could be a function of potency and target occupancy (211). Further investigation is needed to test this and understand the additional benefits provided by EC1728.

The sEHI work to inhibit the metabolism of the anti-inflammatory EpFA, thereby increasing their biological concentrations. In the *in vitro* cytotoxicity assay, EETs proved to be anti-inflammatory and decreased the inflammatory cytokines, IL-6 and TNF-α, after canine chondrocytes were incubated with IL1β. The primary effect is hypothesized to be independent of prostaglandin production since efficacy was achieved after IL1β incubation and reported stimulation of PG (212). Furthermore, treatment with the NSAID, meloxicam, was only effective in protecting chondrocytes from IL1β induced cytotoxicity if added prior to IL1β stimulation (Figure 3.4B); however, in the longer term, EETs have been shown to down regulate induced COX-2 protein and message (128). Chondrocytes are cells in joint cartilage that produce cartilage and regulate cytokine release in response to stress stimuli, and decreased chondrocyte viability in response to injury or inflammatory stimuli has been associated with the progression of osteoarthritis (213). IL1β has been associated with pathological changes in osteoarthritis by increasing matrix metalloproteases and inflammatory cytokines such as IL-6 and TNF-α (214, 215). Chondrocytes express the receptor for IL1β and are considered the main cellular target of this proinflammatory cytokine in cartilage (216). Thus, *in vitro* data predict that increased EET concentrations will reduce synovial inflammation *in vivo* and protect chondrocytes.

In addition to anti-inflammatory effects, EpFA also reduce ER-stress and are proposed targets for alleviating neuropathic pain (196). Because OA is characterized by both inflammatory and neuropathic pain (217), a dual approach treating both inflammation and neuropathic pain would improve patient outcomes especially considering that NSAIDs are ineffective in treating neuropathic pain, (218) and current neuropathic pain treatments (such as opioids and pentanoids) have serious addiction potential with debilitating and often deadly side-effects. Additionally, previously published studies demonstrated the pharmacological benefits of targeting dual inhibition of sEHI and COX. For example, in a mouse model of LPS, dual inhibition increased antinociception (128). In addition to synergistic efficacy, others have observed reduced ulcers in mice treated with both the NSAID, diclofenac, and sEHI compared to diclofenac treated mice alone (219, 220). Thus, safer and more effective treatment options are greatly needed, and the combination of sEHI and NSAID could provide a powerful approach to eliminate pain and co-morbidities of patients suffering from OA without deleterious side effects. Targeting OA from two pathways of decreasing PG production, through NSAIDs, as well with sEHI to reduce ER-stress and inflammation in the presence of PG could provide an effective dual approach to reduce inflammatory and neuropathic pain in OA patients.

OA is a debilitating disease for both humans and companion animals. The results of this study identified a lead compound to further investigate the use of sEHI to treat OA in companion animals. In addition, natural disease in dogs is often used as a more appropriate model for human disease than rodent models (221), providing evidence that sEHI is a potential target for human OA as well. A limitation of the study was the high variability observed in the *in vivo* study among each treatment group in the assessments of pain, function and PK, as well as the additional complications in using aged dogs where confounding factors could interfere with the interpretation

of pain and mobility; although the limitations are somewhat offset by using a natural disease state in the animals to be treated. Variability is expected in naturally occurring disease, and as a proof-of-concept study, this study was designed to mimic treatment in a patient population. Future studies will identify mechanistic changes using both *in vitro* and *in vivo* models in rodents and companion animals to identify a detailed characterization of sEH activity in OA. The reduction in pain in the high dose of EC1728 provides justification for continued efforts in developing sEHI alone or in combination with NSAIDs for the treatment of OA in companion animals and humans.

Conflict of Interest

The University of California holds patents on the sEH inhibitors used in this study as well as their use to treat inflammation, inflammatory pain, and neuropathic pain. BD Hammock and CB McReynolds are cofounders and KM Wagner, J Yang and WK Schmidt are employees of EicOsis L.L.C., a startup company advancing sEH inhibitors as potential therapeutics. EicOsis provided funding for studies contracted to InterVivo.

Author Contributions

CBM, SHH, KW, WKS and BDH conceived of the presented idea. SHH synthesized compounds tested in these studies. CBM performed the *in vitro* cell experiments, microsomal stability, PK analysis and analyzed the *in vivo* study results. KW and CM helped supervise the project. JY and DW verified the analytical methods and analyzed the PK samples. DY oversaw the ELISA experiments. BDH provided overall supervision for the project. All authors discussed the results and contributed to the final manuscript.

Supplementary Materials Chapter 3

Supplementary Material Chapter 3. Chemical synthesis of EC3039
EC1728 (*t*-**TUCB**) was synthesized according to the synthetic procedure reported previously (189).

Preparation of *trans*-4-(4-[3-(4-trifluoromethoxy-phenyl)-ureido]-cyclohexyloxy)-benzoic acid (**A**).
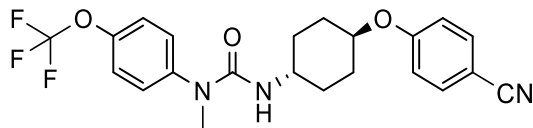
To a solution of N-methyl-4-(trifluoromethoxy)aniline (1.91 g, 10 mmol) and 4-[(trans-4-aminocyclohexyl)oxy]-benzonitrile (2.16 g, 10 mmol) in THF (100 mL) was added triphosgene (1.04 g, 3.5 mol) at 0 °C. The reaction mixture was warmed up to room temperature. After stirring for 2h, water was added, and the reaction mixture was extracted three times with EtOAc. The combined organic layers were dried with MgSO$_4$ and the solvent was removed in vacuo. The remained crude solid was purified by column chromatography to obtain the titled compound (2.6 g, 60% yield). mp 104.0-106.9 °C. ^{1}H NMR (600 MHz, DMSO-d_6) δ 7.73 (d, J = 7 Hz, 2H), 7.36 (d, J = 8 Hz, 2H), 7.32 (d, J = 8 Hz, 2H), 7.10 (d, J = 7 Hz, 2H), 6.13 (d, J = 8 Hz, 1H), 4.41-4.32 (m, 1H), 3.56-3.48 (m, 1H), 3.17 (s, 6H), 2.08-2.01 (m, 2H), 1.87-1.80 (m, 2H), 1.46-1.37 (m, 4H).

Preparation of *trans*-4-(4-[3-methyl-3-(4-trifluoromethoxy-phenyl)-ureido]-cyclohexyloxy)-benzoic acid (*t*-**MTUCB**).
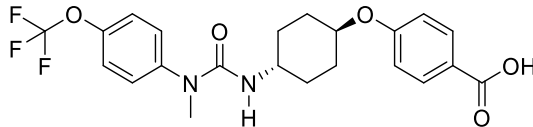
To a solution of the compound **A** (2.5 g, 5.8 mol) in EtOH (58 mL) was added 6N NaOH solution(33.8 mL) at room temperature. The reaction mixture was gently heated up to 90 °C and stirred overnight. The reaction mixture was cooled to 0 °C and acidified with conc. HCl. After evaporating ethanol, the precipitates were filtered and washed with water. The crude solid was purified by column chromatography to obtain the titled compound (2.3 g, 89% yield). mp 92.4-94.7 °C. ^{1}H NMR (400 MHz, DMSO-d_6) δ 12.59 (s, 1H), 7.85 (d, J = 8.8 Hz, 2H), 7.37 (d, J = 9.1 Hz, 2H), 7.32 (d, J = 8.9 Hz, 2H), 7.00 (d, J = 8.8 Hz, 2H), 6.13 (d, J = 7.6 Hz, 1H), 4.39-4.28 (s, 1H), 3.59-3.47 (s, 1H), 3.17 (s, 3H), 2.11-1.99 (s, 2H), 1.89-1.77 (s, 2H), 1.50-1.33 (m, 4H). Anal. Calcd for C$_{22}$H$_{23}$F$_3$N$_2$O$_5$: C, 58.41; H, 5.12; N, 6.19. Found: C, 58.35; H, 5.03; N, 6.09.

Preparation of *trans*-4-(4-[3-(4-trifluoromethoxy-phenyl)-ureido]-cyclohexyloxy)-benzoic-2,3,5,6-d_4 acid (*t*-**TUCB-d_4**).
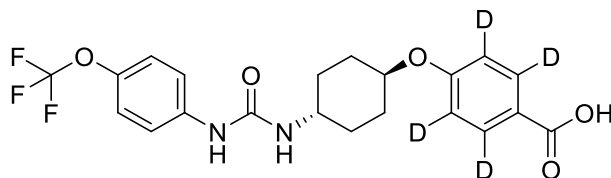
The compound was synthesized according to the synthetic procedure for *t*-TUCB using 4-fluorobenzonitrile-d_4 instead of 4-fluorobenzonitrile (189). ^{1}H NMR (600 MHz, DMSO-d_6) δ

12.58 (s, 1H), 8.52 (s, 1H), 7.47 (d, *J* = 9 Hz, 2H), 7.22 (d, *J* = 9 Hz, 2H), 6.21 (d, *J* = 7 Hz, 1H), 4.49-4.42 (m, 1H), 3.57-3.48 (m, 1H), 2.10-2.02 (m, 2H), 1.96-1.90 (m, 2H), 1.54-1.32 (m, 4H).

S2. LC/MS/MS method for PK analyses of 1728 and 3039

The LC/MS/MS system consisting of Acquity UPLC system and Xevo TQS triple quadrupole system was used to measure the concentrations of inhibitors in the blood. The mobile phases of LC separations are 0.1% of formic acid (FA) in water (Phase A) and 0.1% of formic acid in acetonitrile (Phase B). The gradient of the separation is starting from 30% of phase B in the beginning to 50% of phase B at 2min then ramp to 95% at 2.2 min then came back to 30% of phase B at 3 min. 3 uL of the samples were injected on a 2.1 x 50mm Aquity UPLC BEH C18 1.7 um column. The mass spectrometer was operated under negative ESI mode using multiple reaction monitor (MRM) scan mode with the optimized conditions for the inhibitors. The detail transition parameters are listed in Table S3.1. The conditions for the source were: capillary voltage at 3 kV, desolvation temperature at 300 °C.

Supplementary Data Chapter 3. Table S3.1. The optimized parameters on Waters Xevo TQS system for measuring inhibitors.

Analytes	MRM transition	Cone voltage (V)	Collison Energy (eV)
TAPU	328.1 > 160.0	46	16
CUDA	339.3 > 214.2	22	38
1728	437.2 > 137.0	88	16
3039	451.2 > 260.1	56	16

Supplementary Data Chapter 3. Table S3.2: Signalment for each dog enrolled in the study

DOG #	PERMANENT ID	AGE	SEX	TREATMENT GROUP	RADIOGRAPHIC SCORE
1.1	0006E8F4E4	10.9	M	EC1728 – 1mg/kg	8
1.2	00074FF913	9.8	F	EC1728 – 1mg/kg	2
1.3	0006E94B2D	11.2	F	EC1728 – 1mg/kg	3
1.4	00074F1D08	9.1	F	EC1728 – 1mg/kg	2
1.5	00064CA77C	13.7	M	EC1728 – 1mg/kg	4
1.6	0006E935AA	13.9	F	EC1728 – 1mg/kg	2
1.7	0006894B73	9.5	F	EC1728 – 1mg/kg	7
1.8	0006E96F82	12.8	M	EC1728 – 1mg/kg	1
2.1	00074F1660	8.7	F	EC1728 – 5mg/kg	7
2.2	00074F2D3A	10.2	F	EC1728 – 5mg/kg	5
2.3	00074F1625	9	F	EC1728 – 5mg/kg	6
2.4	0006E8BCDC	12.3	M	EC1728 – 5mg/kg	2
2.5	0006E95DFC	11.3	F	EC1728 – 5mg/kg	10
2.6	0006E8EAEC	12.3	M	EC1728 – 5mg/kg	3
2.7	00074EF48A	9.5	F	EC1728 – 5mg/kg	12
2.8	00064DAD86	13.9	M	EC1728 – 5mg/kg	11
3.1	00071928DC	9.8	M	EC3039 – 1mg/kg	7
3.2	00064D4AC8	13.7	M	EC3039 – 1mg/kg	1
3.3	00064CF01D	14.5	M	EC3039 – 1mg/kg	14
3.4	00074EEABD	7.9	F	EC3039 – 1mg/kg	2
3.5	00074FCAF5	9.8	F	EC3039 – 1mg/kg	18
3.6	00064DC04B	10.7	F	EC3039 – 1mg/kg	8
3.7	0006E8885A	11.4	F	EC3039 – 1mg/kg	9
3.8	00074FFFF7	9.8	F	EC3039 – 1mg/kg	9
4.1	0006E8EFF1	10.2	F	EC3039 – 5mg/kg	5
4.2	0006E96E9B	13.3	F	EC3039 – 5mg/kg	2
4.3	0006E8CF7A	12.9	M	EC3039 – 5mg/kg	4
4.4	00074FC5B5	7.8	F	EC3039 – 5mg/kg	6
4.5	00064E0B44	12.3	F	EC3039 – 5mg/kg	15
4.6	00064E0532	12.3	F	EC3039 – 5mg/kg	16
4.7	0006E91BD9	13.6	M	EC3039 – 5mg/kg	7
4.8	00074FFBF9	12.4	M	EC3039 – 5mg/kg	1

Supplementary Data Chapter 3. Table S3.3: Pain and Function Questionnaire adapted from the Canine Brief Pain Inventory (204)

Pain was scored from 0 (worst pain) to 2 (least pain)

Function was scored from 0 (with great ease) to 5 (with great difficulty)

1. Ease of rising / lying down if observed?
2. General Alertness? (not included in composite score)
3. Ease of initiating walking?
4. General Activity?
5. Willingness to Walk?
6. Willingness to Trot?
7. Willingness to Gallop?
8. Willingness to Step / Jump Over Low Obstacles?
9. Willingness to Climb Stairs?
10. Willingness to Descend Stairs?
11. Willingness to Rear / Jump for Food?
12. Willingness to Jump Down from Step / Perch?
13. Overall Impressions (not included in composite score)
14. Overall Pain assessment (scored 0-4)

Supplementary Data Chapter 3. Table S3.4: Adverse events in dogs dosed with EC1728
A summary of health cases filed over the course of the study can be found below. There was no evidence of treatment-specific adverse events in any group; however, the findings for dog 1.2 (1 mg/kg EC1728) and dog 3.6 (1 mg/kg EC3039) may have impacted the data on days the adverse events were ongoing. However, it is unlikely that this would have substantially impacted the current conclusions.

Date Noted	Study Phase Noted	ID	Description	Findings on Examination	Treatment	Treatment Group / Related
N/A	Pre-Study	1.7	Pre-existing condition of glaucoma	N/A	Azopt TID and Maxidex BID (ongoing)	EC1728 – 1mg/kg / Not Related
2015-09-23	Baseline	Satellite-1F	Yellow discharge right eye	2015-09-23: Mucoid discharge from right eye, minor abrasion beside eye 2015-09-24: Normal tearing, no swelling or discharge from abrasion. Normal.	2015-09-23: Flushed with eye stream. Reassess in 24-48 hours	EC1728 – 1mg/kg / Not Related
N/A	Pre-Study	1.7	Pre-existing condition of allergic dermatitis	N/A	Diphenhydramine 25mg TID (ongoing)	EC1728 – 1mg/kg / Not Related
2015-09-27	Baseline	1.2	Non weight bearing on left hind	2015-09-28: Fully weight bearing. Animal normal	None.	EC1728 – 1mg/kg / Not Related
N/A	Pre-Study	2.8	Pre-existing condition of laceration on left hind	N/A	Clindamycin 150mg BID 2015-09-20 to 2015-10-05	EC1728 – 5mg/kg / Not Related
2015-09-28	Treatment (Day 0)	Satellite-3M	3cm multi nodular mass on inner left mandibular lip	2015-09-28: Firm mass. Multilobulated, irregular, 3cm, pedunculated, on buccal surface mucosa at commissure of upper/lower lip	Remove surgically once study is completed.	EC3039 – 1mg/kg / Not Related

2015-10-02	Treatment (Day 4)	3.6	Raw spot on left hip	2015-10-02: Moist dermatitis	Hibitane ointment and chlorhexidine soak BID 2015-10-02 to 2015-10-07	EC3039 – 1mg/kg / Unlikely Related
2015-10-06	Treatment (Day 8)	Satellite - 4M	Moist dermatitis of ventral neck (suspected clipper burn)	N/A	None started prior to study completion	EC3039 – 5mg/kg / Not Related

Supplementary Data Chapter 3. Table S3.5. EC3039 and EC1728 exposure in the synovial fluid was measured at concentrations above the IC50.

Dogs had higher concentration of sEHI in the synovial fluid compared to concentration in the blood and exceeded the IC_{50} for each compound (EC_{50} of EC3039 = 2 ng/mL and the IC_{50} of EC1728 is 0.4 ng/mL). There was no statistically significant correlation between drug levels and pain or function scores.

A. Summary table of results: synovial fluid and blood concentrations of sEHI in dogs (n=8) administered EC1728

1 mg/kg, po, qd x 5 Compound detected: EC1728 (ng/mL)				5 mg/kg, po, qd x 5 Compound detected: EC1728 (ng/mL)			
	Synovial		**Blood**		**Synovial**		**Blood**
Dog	**D1**	**D5**	**D5**	**Dog**	**D1**	**D5**	**D5**
1.1	483	315	82	2.1	1470	672	228
1.2	111	171	40	2.2	460	668	493
1.3	384	214	36	2.3	nc	2170	244
1.4	917	945	171	2.4	95	80	34
1.5	331	239	31	2.5	2270	1000	206
1.6	206	206	72	2.6	301	1150	348
1.7	455	378	76	2.7	1180	833	314
1.8	232	328	64	2.8	2220	1330	935

nc: not collected

B. Summary table of results: synovial fluid and blood concentrations of sEHI in dogs administered EC3039

1 mg/kg, po, qd x 5						
	Compound detected: EC3039 (ng/mL)			Compound detected: EC1728 (ng/mL)		
	Synovial		Blood	Synovial		Blood
Dog	D1	D5	D5	D1	D5	D5
3.1	3100	1440	346	100	87	12
3.2	1390	586	81	77	69	9
3.3	3430	2190	408	123	111	23
3.4	2100	1930	328	65	100	13
3.5	1220	1630	126	111	111	17
3.6	2710	1480	176	143	80	16
3.7	4100	11900	5340	95	167	17
3.8	3350	1840	347	115	94	12

5 mg/kg, po, qd x 5						
	Compound detected: EC3039 (ng/mL)			Compound detected: EC1728 (ng/mL)		
	Synovial		Blood	Synovial		Blood
Dog	D1	D5	D5	D1	D5	D5
4.1	5220	16100	722	259	320	38
4.2	14300	0	6190	458	50	100
4.3	14700	11700	5650	481	720	79
4.4	9520	5960	929	704	464	115
4.5	5850	5830	859	269	208	62
4.6	13570	4640	672	565	318	71
4.7	14290	9960	5550	250	217	33
4.8	14240	12400	6250	400	360	75

Chapter 4. Plasma linoleate diols are potential biomarkers for severe COVID-19 infections

Cindy McReynolds[1,2], Irene Cortes-Puch[1,2,3], Resmi Ravindran[4], Imran Khan[4], Bruce G. Hammock[5], Pei-an Betty Shih[6], Bruce D. Hammock[1,2,7]*, Jun Yang[1,2]*

[1]Department of Entomology and Nematology, University of California, Davis, CA, USA

[2]EicOsis Human Health Inc., Subsidiary of EicOsis LLC, 1930 5th Street, Suite A, Davis, CA, ISA

[3]Division of Pulmonary, Critical Care, and Sleep Medicine, Department of Internal Medicine, University of California, Davis, CA, USA

[4]Department of Pathology and Laboratory Medicine, University of California, Davis, CA, USA

[5]Department of Veterinary Medicine, Aquatic Health, University of California, Davis, CA

[6]Department of Psychiatry, University of California, San Diego, San Diego, CA, USA

[7]UCD Comprehensive Cancer Center, University of California, Davis, CA, USA

* Correspondence:
Jun Yang
junyang@ucdavis.edu
Bruce D. Hammock
bdhammock@ucdavis.edu

Keywords: linoleate diol, lipid mediators, COVID-19, inflammation, leukotoxin, EpOME, DiHOME, ARDS

Abstract

Polyunsaturated fatty acids are metabolized into regulatory lipids important for initiating inflammatory responses in the event of disease or injury and for signaling the resolution of inflammation and return to homeostasis. The epoxides of linoleic acid (leukotoxins) regulate skin barrier function, perivascular and alveolar permeability and have been associated with poor outcomes in burn patients and in sepsis. It was later reported that blocking metabolism of leukotoxins into the vicinal diols ameliorated the deleterious effects of leukotoxins, suggesting that the leukotoxin diols are contributing to the toxicity. During quantitative profiling of fatty acid chemical mediators (eicosanoids) in COVID-19 patients, we found increases in the regioisomeric leukotoxin diols in plasma samples of hospitalized patients suffering from severe pulmonary involvement. In rodents these leukotoxin diols cause dramatic vascular permeability and are associated with acute adult respiratory like symptoms. Thus, pathways involved in the biosynthesis and degradation of these regulatory lipids should be investigated in larger biomarker studies to determine their significance in COVID-19 disease. In addition, incorporating diols in plasma multi-omics of patients could illuminate the COVID-19 pathological signature along with other lipid mediators and blood chemistry.

Introduction

The pandemic coronavirus disease 2019 (COVID-19), caused by severe acute respiratory syndrome coronavirus 2 (SARS-CoV-2), initiates an aberrant immunological response resulting in a wide range of disease severities ranging from asymptomatic cases to severe cases with rapid progression to acute respiratory distress syndrome (ARDS) and death (222, 223). Patients with severe COVID-19 show evidence of hyperinflammation with increased release of inflammatory cytokines (224). The role of a cytokine release syndrome, or cytokine storm, in COVID-19 has

drawn much attention (225). However, recent reports demonstrate that, although pro-inflammatory cytokine levels are elevated in severe COVID-19 patients, they are lower than levels usually observed in non-COVID ARDS, suggesting additional factors lead to severe outcomes in some patients (226).

One of the key pathways regulating the immune response to infections is the release of regulatory lipid mediators that have dual functions of driving inflammation (*e.g.,* prostaglandins (PGE2)) or promoting resolution of inflammation and return to homeostasis (*e.g.,* long chain epoxy fatty acids (EpFAs)) (227, 228). Recent data indicate a role of dysregulated lipid profiles in COVID-19 and identified cytochrome P450 (CYP) metabolites of polyunsaturated fatty acids (PUFA) as potential biomarkers of disease severity (227, 229).

Linoleic acid (18:2n6, LA) is the primary source of essential long chain n-6 PUFAs. CYP450 enzymes act on linoleate directly to generate linoleic epoxides (epoxyoctadecenoic acids, EpOMEs), which are further metabolized by soluble epoxide hydrolase (sEH) to their corresponding leukotoxin diols (dihydroxyoctadecenoic acids, or DiHOMEs) (**Figure 4.1**). These LA metabolites regulate vascular permeability and stimulate neutrophil chemotaxis (230). The epoxides were originally termed leukotoxins because of their suspected cytotoxic effects and implications in advancing acute and chronic inflammatory diseases and in the pathophysiology of ARDS (231, 232). The deleterious effects of LA metabolites were originally attributed to EpOMEs. It was later discovered that the toxicities attributed to leukotoxins were in fact driven by leukotoxin diols or DiHOMEs, and blocking their formation would alleviate toxicities previously

associated with leukotoxin (16). Despite its potential role in advancing ARDS, the role of these LA metabolites in the pathophysiology of COVID-19 has not been evaluated to date.

In this pilot study, five sequential day plasma samples from six patients with COVID-19 were profiled for lipidomic changes in COVID-19 disease compared to healthy controls. Results indicate that in addition to expected increases in inflammatory prostaglandins and leukotrienes, 12,13 DiHOME and 9,10 DiHOME concentrations are significantly higher in COVID-19 patients compared to healthy controls. This is one of the first studies to focus on oxylipin chemical mediators in COVID-19 disease.

Figure 4.1 Structure of LA, EpOME and DiHOME

Linoleic acid (LA)

CYP450

9,10-EpOME, synonym: 9,10-epoxy-12Z-octadecenoic acid, leukotoxin

12,13-EpOME, , synonym: 12,13 epoxy-9Z-octadecenoic acid, isoleukotoxin

Epoxyoctadecenoic acids (EpOME)

sEH

9,10-DiHOME, synonym: 9,10-dihydroxy-12Z-octadecenoic acid, leukotoxin-diol

12,13-DiHOME, synonym: 12,13-dihydroxy-9Z-octadecenoic acid, isoleukotoxin-diol

Dihydroxyoctadecenoic acids (DiHOME)

Methods

This is a retrospective study using prospectively collected plasma samples and clinical data. For oxylipin analysis, heparinized plasma was collected from six patients with laboratory-confirmed SARS-CoV-2 infection and admitted to the University of California Davis Medical Center in Sacramento, CA and 44 healthy controls carefully chosen from the healthy control arm of a recently completed clinical study. For comparison of cytokines, plasma from healthy volunteers was collected from the California Central Valley Delta Blood Bank (Stockton, CA) prior to the COVID-19 pandemic (n = 75). The methods used for blood collection, plasma processing, use of anti-coagulants/antioxidant/preservatives, and flash-freeze protocol were well-matched between case and control groups. The UC Davis and UC San Diego Institutional Review Boards approved the use of anonymized biospecimens for this study.

Lipid mediator profiling

Plasma (200 µL) samples were aliquoted to a cocktail solution including 600 µL of methanol with 10 µL of 500 nM of surrogate solution including 9 isotope-labeled oxylipins (d4 PGF1a, d4 PGE2, d4 TXB2, d4 LTB4, d6 20 HETE, d11 14,15 DiHETrE, d8 9 HODE, d8 5 HETE, d11 11,12 EpETrE). Before the extraction, the samples were vortexed and centrifuged at 3000 rpm in a biosafety hood. The supernatants were then loaded on prewashed SPE cartridges and washed with two column volumes of 5% MeOH solution before elution by 0.5 mL of MeOH and 1.5 mL of ethyl acetate. The eluents were dried under vacuum using the Nutec MaxiVac vacuum concentrator (Farmingdale, NY USA) before reconstitution with 50 µL of 100 nM CUDA solution in methanol. Then, the extracted samples were analyzed using the UPLC/MS/MS system (Waters Acquity UPLC (Milford, MA, USA) hyphenated to AB Sciex 6500+ QTrap system (Redwood City, CA

USA). The detailed parameters for the UPLC/MS/MS method were described previously (233, 234).

Cytokine multiplex

Plasma cytokines were measured using a multiplex magnetic bead-based cytokine detection kit purchased from Bio-Rad (12007283). Cytokines were measured according to manufacturer's instructions. Data are provided in the supplementary material.

Statistical analysis

To test for differences between the COVID-19 and the control group cytokine levels, cytokine levels were $\log_{10}$ transformed to fit a normal distribution and analyzed in Graphpad Prism (version 8.4.3) using the Wilcoxon rank-sum test with COVID positive and negative status as the main effect.

Lipid mediator results were analyzed using MetaboAnalyst (https://www.metaboanalyst.ca/) and scaled using autoscaling before analysis. Multiple data sets described below were integrated to prioritize the oxylipins as possible biomarkers contributing to the severity of COVID. Oxylipins were analyzed by multiple independent t-tests using patient vs. control as the variable and the two-stage step-up method of Benjamini, Krieger and Yekutieli to determine a false discovery rate (235) to generate the volcano plot.

The lipid mediators were then ranked by their effect sizes (i.e., the fold-difference between mean analyte concentration in each group). The analytes with the largest effect sizes were further evaluated by random effect ANOVA models. We minimized type 1 errors by testing for between-group differences among the analytes with the largest effect sizes and to improve the likelihood of identifying analytes that showed best potential to serve as biomarkers of disease severity. Each

analyte with an effect size above 8 (i.e., analyte concentrations >8-fold different) was used as a response variable. Random effect ANOVAs were run with 'patient' as a random effect to account for the multiple measurements from the same patient, and the fixed effect was 'group' (i.e., COVID positive or control). The $\log_{10}$-transformation of the analyte concentrations was applied. The analysis was done in JMP Pro Version15.

Results

Demographics of patient samples are represented in **Table 4.1**. Seventy-seven lipid mediators were detected from all the patients' samples (oxylipin concentrations are available online: https://doi.org/10.25338/B8M92X). Levels of multiple key pro-inflammatory cytokines and chemokines were significantly higher in patients with COVID-19 than in healthy controls (Supplementary Table S4.1), confirming the activation of the immune response against the virus. Overall, increases were moderate and consistent with those reported in the literature (225).

A volcano plot analysis was performed to evaluate the differences in lipidomic profile between COVID-19 patients and healthy controls (**Figure 4.2A**). The analysis identified 18 differential lipid mediators with statistically significant differences ($p<0.01$) with more than four-fold change between groups.

Oxylipins were ranked according to effect size (**Table 4.2**) between COVID-19 patients and controls. The 9,10 and 12,13 DiHOME metabolites had the biggest effect size (17.94 and 14.12, respectively), followed by PGE2 (12.55). As expected, the epoxides of arachidonic acid (AA) and linolenic acid also increased compared to healthy controls presumably due to biosynthesis and systemic release of free fatty acids from membranes in response to inflammation. The epoxides and diols of the omega-3 fatty acids, EPA and DHA, did not show any increases (effect size <7).

Figure 4.2B demonstrates that changes in the DiHOME concentrations had a more prominent effect in separating patients and controls compared to the EpOMEs. The EpOME/DiHOME ratios also demonstrated case-status predictive effect. The prostaglandins, PGE2 and PGD2, as well as related cyclooxygenase metabolites had large effect sizes but surprisingly were low in concentration in patients with evidence of elevated cytokines. It is worth noting that the large effect size of prostaglandin resulted from a single patient (see online dataset for individual data). Similarly, leukotriene B4 (LTB4, leukocyte aggregating factor) level was surprisingly low for patients with high level of inflammation, marked by elevated cytokines. This finding was also largely driven by the effect of one single patient.

Table 4.1. Clinical characteristics of Sars-Cov-2 patients[1]

Clinical ID/ #Patient ID[2]	Age	Covid19-Symptoms						Onset (d)	Admission	Hospital stay (d)	Airway Procedures Performed	COVID-19 Treatment
RIB0020 #1	<65	SOB[3]	FLS		Dyspnea			5-8		4	none	
RIB0019 #2	<65	SOB[3]	FLS	Fever	Dyspnea	Chest pain	Muscle pain	9-13		13	Supplemental Oxygen	Remdesivir
RIB0012 #3	>65	SOB[4]		Fever	Dyspnea on exertion		Hypoxemia	5-8		16	Supplemental Oxygen	
RIB0016 #4	<65	SOB[4]						9-13	AHRF/Pnu	11	Endotracheal Intubation	
RIB0001 #5	<65		FLS					Several	ARDS/Pnu	26	Endotracheal Intubation	Remdesivir
RIB0004 #6	>65							5-8	ARDS/Pnu	54	Endotracheal Intubation	Sarilumab

[1]All patients were above 45 years of age and had a cough upon admission. Clinical ID/Patient ID2 (patients were assigned a clinical ID at the hospital. For simplification, they were reassigned a number from 1-6. SOB[3] (shortness of breath associate with other respiratory illness); SOB[4] (shortness of breath); FLS (flu-like symptoms); AHRF (Acute Hypoxic Respiratory Failure); ARDS (Acute Respiratory Disease); Pnu (Pneumonia)

Table 4.2. Effect size (mean fold-difference between COVID-positive and control) of EpFA, diols and oxylipins with greater than 8-fold difference (*p<0.0001).

Increased EpFA from the most abundant dietary fatty acids (AA and LA) is expected due release from cellular membranes in response to inflammation. AA epoxides, EpETrE or EETs are anti-inflammatory compounds, but their low concentration and rapid conversion by the sEH is thought to limit their efficacy.

Effect Size of oxylipins compared to healthy controls			
	Effect Size		Effect Size
LA metabolites			
9(10)-EpOME	9.23*	9,10-DiHOME	17.94*
12(13)-EpOME	10.05*	12,13-DiHOME	14.12*
ALA metabolites			
9(10)-EpODE	4.90	9,10-DiHODE	7.36
12(13)-EpODE	3.21	12,13-DiHODE	0.88
15(16)-EpODE	5.39	15,16-DiHODE	0.37
AA metabolites			
5(6)-EpETrE	5.93	5,6-DiHETrE	2.98
8(9)-EpETrE	11.01*	8,9-DiHETrE	1.90
11(12)-EpETrE	11.41*	11,12-DiHETrE	2.07
PGE2	12.55		
DHA metabolites			
		4,5-DiHDPE	0.60
7(8)-EpDPE	1.04	7,8-DiHDPE	5.94
10(11)-EpDPE	0.88	10,11-DiHDPE	0.76
13(14)-EpDPE	0.75	13,14-DiHDPE	0.61
16(17)-EpDPE	0.74	16,17-DiHDPE	0.81
19(20)-EpDPE	3.28	19,20-DiHDPE	0.38
EPA metabolites			
8(9)-EpETE	0.95	8,9-DiHETE	0.93
11(12)-EpETE	1.27	11,12-DiHETE	0.95
14(15)-EpETE	1.03	14,15-DiHETE	0.87
17(18)-EpETE	1.35	17,18-DiHETE	0.43

Figure 4.2. Plasma collected once from healthy COVID-19 negative controls (n=44) and over five sequential days from hospitalized COVID-19 positive patients (n=6).
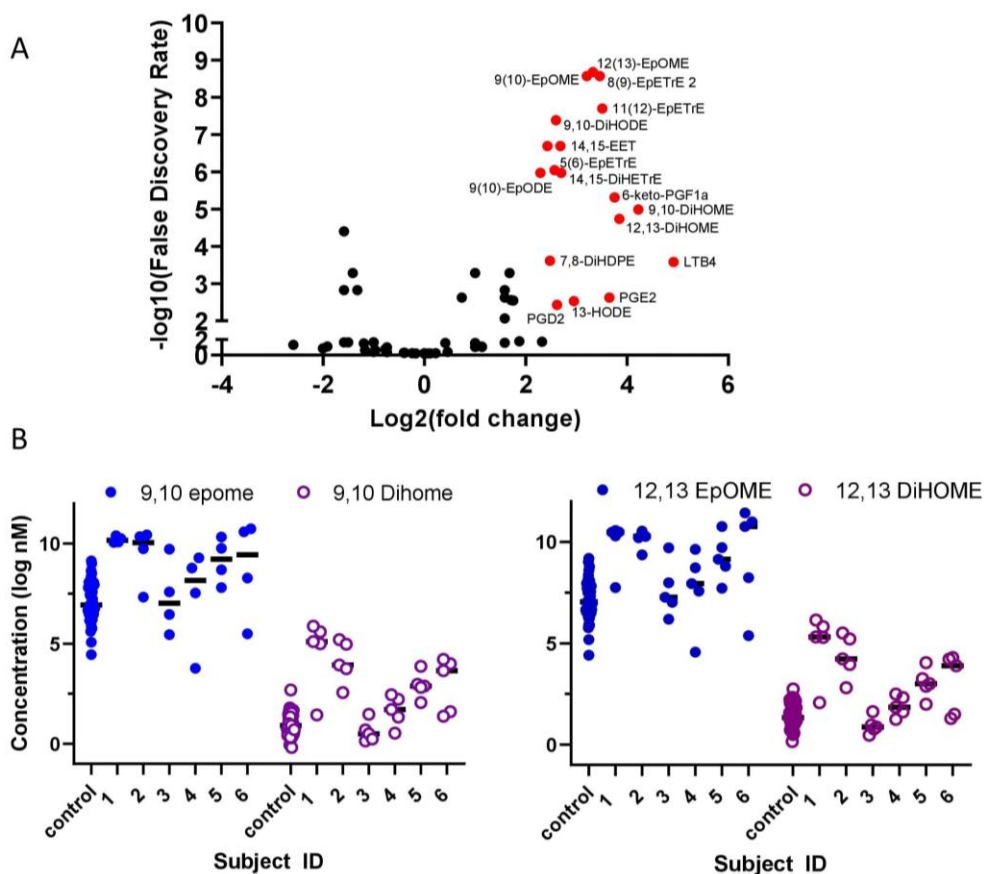
(A) Volcano plot of oxylipins analyzed in COVID-19 patients compared to healthy controls. Red dots identify metabolites that had a >4 fold-change and false discovery rate (p<0.01), 18 compounds in total. To generate the Volcano plot, data from each COVID-19 patient was averaged over the 5-days before averaging as a group and comparing to the average of all control subject data.

(B) Plasma concentration of EpOME and DiHOME in five sequential samples collected from six hospitalized COVID-19 positive patients and control samples collected separately from healthy volunteers (n=44). Data from individual days is represented for each COVID patients and for each individual healthy control. The ratio of EpOME:DiHOME, excluding patient #3 who had low levels of both EpOMES and DiHOMES, was higher in control samples vs. COVID-19 patients on day 1 and steadily increased over time in COVID-19 patients. Overall ratios in COVID-19 patients were 30% lower than healthy controls indicating that DiHOMES increased in greater amounts compared to EpOME (graphical representation of raw data is included in supplementary Figure 4.1).

119

Supplementary Data Chapter 4. Table S4.1. Average cytokine levels ± standard deviation over 5-day sampling period in 6 COVID-19 positive patients and single timepoints in 16 healthy controls.

			COVID negative			COVID positive		
		IP-10	377.51	±	422.00	8,319.04	±	13,197.36
		MCP-1	51.76	±	46.99	198.07	±	151.81
		IL-2R alpha	75.96	±	19.89	228.93	±	221.50
		G-CSF	32.15	±	24.92	243.96	±	185.23
		SCGF-b	65,516.58	±	23,927.79	457,401.32	±	182,805.76
		IL-1ra	1,464.07	±	458.91	6,627.30	±	5,657.16
		IL-18	69.87	±	45.05	218.21	±	165.27
		MIG	652.77	±	1,241.35	5,011.68	±	8,872.44
		RANTES	6,886.20	±	9,986.27	82,607.91	±	119,032.58
		IL-1 alpha	3.64	±	4.86	26.21	±	13.29
		IL-1 beta	1.73	±	2.33	6.62	±	3.10
		IL-2	13.08	±	22.02	8.73	±	3.42
		IL-3	0.01	±	0.02	0.55	±	0.44
		IL-4	1.01	±	0.41	2.30	±	0.82
		IL-5	7.78	±	11.10	8.20	±	5.06
		IL-6	0.41	±	1.28	30.14	±	18.98
		IL-7	4.41	±	3.27	11.95	±	4.90
		IL-8	4.90	±	6.03	57.68	±	38.85
		IL-9	318.33	±	123.79	492.35	±	63.57
		IL-10	9.78	±	12.19	16.75	±	5.56
		IL-12 (p70)	4.45	±	2.32	7.34	±	3.13
		IL-12 (p40)	46.89	±	15.93	99.21	±	58.28
		IL-13	0.91	±	0.46	1.91	±	0.55
		IL-16	94.16	±	26.94	383.52	±	258.54
		PDGF-BB	611.54	±	312.83	4,918.12	±	2,593.90
		MIP-1b	264.54	±	97.06	419.52	±	131.09
		SDF-1a	1,657.55	±	506.14	3,115.42	±	717.18
		MCP-3	0.65	±	0.88	25.38	±	27.26
		LIF	70.61	±	53.20	77.78	±	30.40
		IFN-a2	3.39	±	2.01	9.38	±	4.21
		IFN-g	10.33	±	9.83	50.09	±	33.68
		TNF-a	48.24	±	16.31	128.00	±	53.16
		TNF-b	561.01	±	223.51	840.87	±	91.47
		MIF	4,453.54	±	2,413.46	15,533.21	±	7,131.58
		Basic FGF	3.70	±	0.01	21.34	±	18.93
		MIP-1a	0.37	±	0.56	8.72	±	7.98
		M-CSF	14.02	±	5.30	58.77	±	38.03
		HGF	234.77	±	61.06	6,463.33	±	8,283.03
Significant		SCF	66.05	±	12.63	204.00	±	119.30
		TRAIL	126.49	±	36.31	222.80	±	56.63
		CTACK	400.80	±	134.88	833.03	±	391.99

		Eotaxin	98.23	±	33.87	147.76	±	78.73
		VGEF	61.21	±	158.03	204.95	±	99.50
Not significant		GRO-a	906.44	±	222.88	905.37	±	195.31
		IL-2	8.16	±	22.02	7.83	±	5.39
		IL-5	5.00	±	11.10	5.00	±	11.89
		IL-15	12.70	±	0.00	12.70	±	0.00
		IL-17	2.80	±	0.00	2.80	±	0.00
		b-NGF	0.38	±	0.00	0.38	±	0.00
		GM-CSF	0.50	±	0.10	3.70	±	0.97

Supplementary Data Chapter 4. Figure S1. Individual epoxide and diol levels in patients and controls (A) and calculated EpOME: DiHOME ratios over a 5-day sampling period in COVID-19 patients compared to a single assessment in 44 healthy controls (B).

A.
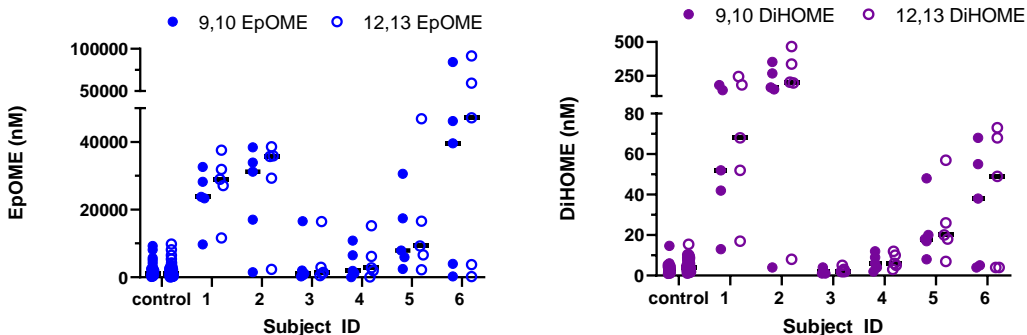
B.
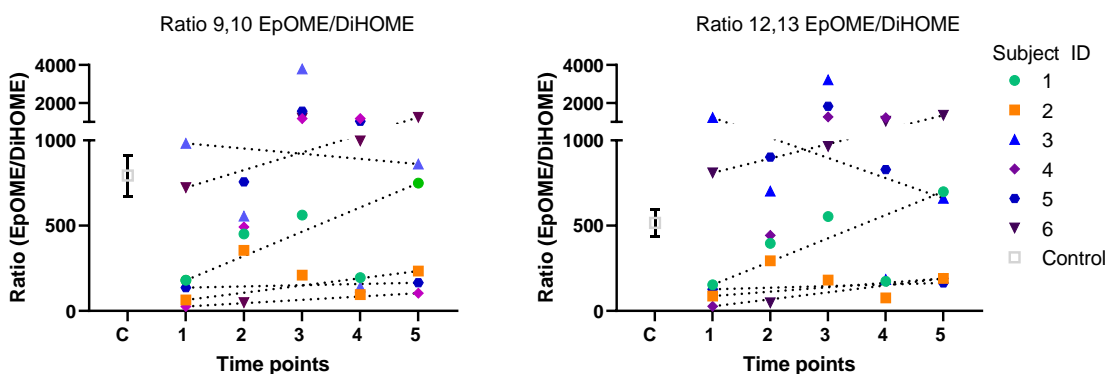
(A) Plasma concentration (nM) of EpOME and DiHOME in five sequential samples collected from six hospitalized COVID-19 positive patients and control samples collected separately from healthy volunteers (n=44). Data from individual days is represented for each COVID patients and for each individual healthy control.

(B) Ratio of EpOME: DiHOME values in healthy controls vs. hospitalized COVID-19 patients. Control values are averaged for one point ± SEM while COVID-19 patient samples are represented in chronological order of sampling after hospital admission. Lower ratios indicate that the DiHOME concentration was higher or the EpOMEs were lower and are commonly used to infer sEH activity [1]. Considering the large increase in EpOMES in COVID-19 patients compared to healthy controls, the decreased valie of the ratios in COVID-19 patients are largely driven by inceased DiHOME concentrations.

[1] D. Stefanovski, P.B. Shih, B.D. Hammock, R.M. Watanabe, and J.H. Youn, Assessment of soluble epoxide hydrolase activity *in vivo*: A metabolomic approach. Prostaglandins & other lipid mediators 148 (2020) 106410.

Discussion

It is clear that the two regioisomeric linoleic acid diols (DiHOMES) had highly elevated concentrations in these COVID-19 positive patients, as did their precursor epoxides (EpOMEs) (**Table 2**). Previous studies show that high levels of the epoxide and diol metabolites of linoleic acid are mitochondrial toxins, stimulate vascular permeability and that injection of either metabolite into mice leads to pulmonary edema and inflammation reminiscent of ARDS (232, 236). However, if inhibitors of the soluble epoxide hydrolase are administered, the edema from EpOMEs is blocked but not that from the DiHOMEs (16), suggesting that DiHOMEs play a role in lung disease and possibly a role in the pathophysiology of COVID-19. In contrast, the EET regioisomers and epoxides of other long chain polyunsaturated fatty acids are under scrutiny as inflammation resolving mediators. Their concentrations are quite low, and the soluble epoxide hydrolase is thought to be largely responsible for converting the biologically active epoxides to their corresponding diols, thereby reducing their inflammation resolving potency. The online dataset represented by the volcano plot in **Figure 4.2A** and the effect sizes in **Table 4.2** do not support these compounds to be associated with severe COVID although increasing epoxides from arachidonic acid (ARA), eicosapentaenoic acid (EPA), and docosahexaenoic acid (DHA) to yield the EET, EEQ, and EDP regioisomers would be predicted to help resolve inflammation (93).

The levels of ARA diols from the corresponding EET epoxides as well as the epoxides and diols of omega-3 fatty acids were low in most subjects with relatively small differences between the COVID positive and control groups. A caution is that the data on omega-3 metabolites in human subjects can be hard to quantify in part because the average dietary levels of omega-3 fatty acids are low. Fatty acid composition, including omega-3 fatty acids, can become quite high due to supplementation. For example, the omega-6 fatty acid LA was once a relatively rare dietary lipid in our evolutionary history but is now a major dietary lipid in the western diet (237). In many

123

western diets the levels of linoleate are far higher than that anticipated from even recent evolutionary history. As an example, the blood levels of the EpOMEs we report here in COVID-19 patients are approximately 10× higher than levels found in ICU-admitted burn patients (238). Thus, the high levels of linoleate substrate would be expected to compete with long chain polyunsaturated fatty acids thus reducing inflammation-resolving epoxides, such as the EETs, EEQs and EDPs, and increasing linoleate epoxides or leukotoxins as shown by our data. Although AA and longer chain omega-3 fatty acid epoxides are better substrates for the sEH, the leukotoxins are still excellent substrates (44). sEH action on leukotoxins leads to metabolic products that are cytotoxic, proinflammatory, and cause extensive perivascular and alveolar edema reminiscent of ARDS in mice (232, 236).

An obvious question remains as to why cells produce a pro-inflammatory metabolite which increases vascular permeability during COVID infection. A possible answer comes from an inspection of the AA cascade where the largely (but not exclusively) pro-inflammatory cyclooxygenase (COX) and lipoxygenase (LOX) pathways are countered by the more recently discovered and largely anti-inflammatory pathway termed the cytochrome CYP450 pathway (239). During inflammation, PUFA are released from cell membranes and are metabolized into epoxides thought to resolve inflammation; however, this process is often dysregulated in patients with severe disease. Specifically, while cytochrome P450 metabolism of PUFA forms mostly anti-inflammatory and inflammation-resolving fatty acid epoxides such as EETs, EDPs and EEQs (from AA, EPA, and DHA respectively), metabolites from LA and other omega-6 PUFAs generated by other enzymes such as COX and LOX form mostly pro-inflammatory compounds. As shown in our results, the COX-generated prostaglandins (e.g. PGE2) and LOX-generated leukotrienes (LTB4) were increased as part of the inflammatory response during COVID-19. The

EpFA resolve effects of these inflammatory eicosanoids directly through downregulation of inflammation, and indirectly by stimulating the production of specific proresolving mediators (SPMs). However, the sEH enzyme is upregulated during inflammation, resulting in conversion of beneficial compounds into inactive or even pro-inflammatory diols. Under normal conditions, CYP450 oxidation of PUFA into EpFA is tightly regulated and occurs at a slower rate than the hydrolysis of EpFA into diols. EpFA are often stored in lipid membranes and are thought to be released during inflammation; however, the rapid conversion by sEH during inflammation limits their concentration *in vivo*.

The high abundance of linoleate as a substrate, coupled with the increased biosynthesis of anti-inflammatory EpFA during severe coronavirus infections and the induction of sEH in an inflammatory state (93) may explain the increased rate of synthesis and concentration of leukotoxin diols observed in COVID-19 patients in our study. This finding raises the possibility that amelioration of COVID-19 symptoms may be achieved in part by reduction of omega-6-rich diet, or an enhanced omega-3 fatty acid intake in patients hospitalized for COVID-19. Linoleate at quite low levels is an essential fatty acid for maintenance of skin barrier function, yet an early study (1958) showed that even with no dietary fat intake, 2% of energy from linoleate was enough to maintain skin barrier function (240). Therefore, reducing linoleate intake or substituting it with 'anti-inflammatory' lipids such as n-3 rich fish oil is unlikely to have a deleterious effect on the long-term health. Indeed, this approach is currently being evaluated through intravenous omega-3 administration in COVID-19 hospitalized patients in the COVID-Omega-F Trial (241). Further benefits from reducing omega-6 fatty acid intake germane to the COVID-Omega-F Trial show increased bioavailability of omega-3 fatty acids with reduced LA consumption (242). Particularly the 'omega' olefins of EPA and DHA are good substrates for epoxidation by relevant cytochrome

P450s (147). Thus, large infusions of omega-3 fatty acids would be predicted to reduce the biosynthesis of the omega-6 EpOMEs by substrate competition. A second prediction is that infusion of omega-3-fatty acids would not lead to a significant increase in cyclooxygenase products because of the substrate preferences of the cyclooxygenases. On the other hand, the anti-inflammatory P450 products are expected to be increased. These EEQ and EDP epoxides also are excellent substrates for the sEH (44) and by competition should reduce the hydration of non-cytotoxic EpOMEs to the DiHOMEs (cytotoxic leukotoxin diols). A reduction in linoleate metabolites could partially explain the difference that omega-3 supplementation had in ARDS related mortality (243). Given the evidence of the role DiHOMEs play in exacerbating ARDS, the possibility that these metabolites could serve as biomarkers for COVID-19 disease is strengthened.

Inhibition of the *in vivo* sEH can also block the toxicity of linoleate epoxides (93) through stabilizing anti-inflammatory long chain epoxy fatty acids and blocking the formation of the leukotoxin diols as demonstrated in our earlier studies (244). This evidence points to the possibility that pharmacological inhibition of the sEH will enhance and synergize with the proresolving effects of omega-3 supplementation in COVID-19 patients, leading to improvement of COVID symptoms.

This was a pilot study designed primarily to inform later experimental designs, and the relatively small sample size limits interpretation. Another limitation is that the small sample size resulted in high variability in disease severity as well as timing of disease onset and resolution which made temporal relationship between blood biomarkers and specific COVID symptoms difficult to evaluate. Our data are novel in that they shed light on a class of lipid mediators that are likely to be important for the pathogenesis of COVID-19 progression. A better understanding of mechanisms involved in COVID-19 pathophysiology is rapidly emerging, and the importance of

LA and its metabolites in this disease is becoming apparent. Recent studies identified that LA

binds to a fatty acid binding pocket in the SARS-CoV-2 spike protein stabilizing its confirmation

in a manner that decreases viral entry into the host cell (245). In support of this finding, Dierckx

et al. demonstrated high LA concentrations associated with lower COVID-19 severity (246).

Neither study monitored LA metabolites therefore making it impossible to understand the

biological roles of the metabolites and how they may impact interpretation from other studies. Our

data described here fill a missing gap of the role bioactive mediators play in COVID-19 and

emphasize a critical need to better understand the relationship between dietary lipids and their

bioactive metabolites. This knowledge will bring about important insights that may lead to

effective strategies to prevent rapidly worsening of COVID-19 symptoms and improved treatment

efficacy. The data support further investigation on the use of DiHOME regioisomers as biological

mediators or biomarkers interacting synergistically through a cross-omic network of cytokines,

other lipid mediators including SPMs like resolvins, and blood chemistry to predict severe

COVID-19 disease.

Conflict of Interest
Drs. Hammock, McReynolds, Cortes-Puch, Yang are partly employed by EicOsis, which is
developing a potent soluble epoxide hydrolase inhibitor for pain relief.

Author Contributions
JY, CM, RR implement the experiments; CM, IC, PBS, BDH, JY wrote and revised the
manuscript; BGH analysed data; IK, PBS, BDH and JY designed the study.

Conclusion

Medical advances over the past 100 years have increased life expectancy overall by approximately 2-fold; yet over the past 5-years starting before the COVID-19 pandemic, both life expectancy and quality of life have decreased due to negative societal trends, such as sedentary lifestyle and poor nutrition, and morbidities associated with chronic diseases (247-250). Although many solutions will be needed to address such a complex problem, access to affordable healthcare, including treatment options with effective outcomes that have limited side effects, will be instrumental in reversing this troubling trend. Despite a desperate need for better treatment options, there are a limited number (between 11-47) of new therapeutics approved by the FDA each year (251). The biggest contributory factor limiting drug development outside of efficacy and safety is cost. A high barrier to safety and efficacy results in only a 10% approval rate for drugs in clinical development, and often these drugs fail after years of development and millions of dollars invested. The estimated cost for drug approval is ~$3B and 12 years to advance from candidate selection through clinical trials (252). Considering the intensive resources invested in drug discovery, it is shocking that approvals generally result in one drug or therapy that treats only one disease. This presents an unsustainable situation given the rising healthcare costs combined with pharma companies high price point for new medicines that are designed to recoup development costs. Additionally, as chronic diseases cause complicated health outcomes with many co-morbidities, multiple pharmaceuticals are often needed to treat each comorbidity or combat the side-effects of a life-sustaining treatment. This creates a situation where a stable patient on life-saving medications risks developing severe complications if a new illness, even as simple as a yeast infection or seasonal allergy, requires a medication that could disrupt the metabolism of the chronic medications onboard. In hospitalized patients, >100,000 people die annually from unintended drug-drug

interactions each year, and over 2.2 million people have a serious adverse drug reaction (253). These facts are not appreciated by the general public and generally suppressed by the medical community and pharmaceutical industry. Thus, therapeutics designed to improve quality of life may contribute to worsening health outcomes.

Chronic pain is an example of a multifaceted disease requiring multi-modal approaches for efficacy. Chronic pain is one of the most important contributors for influencing quality of life (247) and affects over 20% of the US population on average, with some reports suggesting the prevalence is closer to 40% (254). Opioids remain the most prescribed medications for addressing chronic pain, despite serious risks of addiction, toxicity, and contraindications to long-term use due to tolerance and hyperalgesia from repeated use. New pain targets are urgently needed, yet an independent review of new drugs in development lists ~25% as opioid targets. Considering the complicated health of an aging population, novel and safe therapies designed to target multiple diseases are greatly needed. The regulatory lipid cascade studied in this research presents a pathway with multiple druggable targets with the potential for maintaining homeostasis and reversing disease by targeting several mechanisms of action.

Specifically regarding inflammation, blocking inflammatory prostaglandins formed from the metabolism of arachidonic acid (AA) by cyclooxygenase (COX) through Aspirin represents one of the earliest druggable targets in the AA cascade; however, there are many other targets approved and being developed (255, 256), including the stabilization of beneficial lipids described here through inhibition of the sEH. The research detailed above represents various stages in drug discovery: exposure and distribution of a lead compound in target species (Chapter 2), and demonstration of efficacy in a disease model (Chapter 3), associated with developing a novel sEH

inhibitor for the treatment of pain in humans and animals. Demonstration of efficacy in companion animals with naturally occurring disease represents a unique opportunity to increase clinical success because often efficacy observed in laboratory models does not translate to human diseases of complex etiologies. Chapter 4 represents another strategy for improving clinical success by employing biomarker identification in search of new therapeutic opportunities. In this chapter, lipidomic profiles identified the sEH products, 9,10 and 12,13 DiHOME, as increased in a small subset of severe COVID-19 disease. Past literature describing acute respiratory distress syndrome (ARDS) in mice after DiHOME administration suggests that ARDS may be a new target for sEH inhibition (257).

In summary, the regulatory lipid cascade presents a unique opportunity for identifying novel targets for the treatment of disease, and inhibition of the sEH represents a unique pathway for broad application to improve the quality of life for individuals suffering from many diseases. Deploying creative drug discovery, such as biomarker identification and efficacy testing in natural disease, can further improve the chances of translating preclinical compounds into effective drugs.

References:

1. Vane JR. Inhibition of prostaglandin synthesis as a mechanism of action for aspirin-like drugs. Nature: New biology. 1971;231(25):232-5. Epub 1971/06/23. doi: 10.1038/newbio231232a0. PubMed PMID: 5284360.

2. Liu MC, Dube LM, Lancaster J. Acute and chronic effects of a 5-lipoxygenase inhibitor in asthma: a 6-month randomized multicenter trial. Zileuton Study Group. The Journal of allergy and clinical immunology. 1996;98(5 Pt 1):859-71. Epub 1996/11/01. doi: 10.1016/s0091-6749(96)80002-9. PubMed PMID: 8939149.

3. Chopra S, Giovanelli P, Alvarado-Vazquez PA, Alonso S, Song M, Sandoval TA, Chae CS, Tan C, Fonseca MM, Gutierrez S, Jimenez L, Subbaramaiah K, Iwawaki T, Kingsley PJ, Marnett LJ, Kossenkov AV, Crespo MS, Dannenberg AJ, Glimcher LH, Romero-Sandoval EA, Cubillos-Ruiz JR. IRE1alpha-XBP1 signaling in leukocytes controls prostaglandin biosynthesis and pain. Science. 2019;365(6450). Epub 2019/07/20. doi: 10.1126/science.aau6499. PubMed PMID: 31320508.

4. Serhan CN. Pro-resolving lipid mediators are leads for resolution physiology. Nature. 2014;510(7503):92-101. Epub 2014/06/06. doi: 10.1038/nature13479. PubMed PMID: 24899309; PMCID: PMC4263681.

5. McGiff JC, Quilley J. 20-HETE and the kidney: resolution of old problems and new beginnings. The American journal of physiology. 1999;277(3 Pt 2):R607-23. Epub 1999/09/14. PubMed PMID: 10484476.

6. Roman RJ. P-450 metabolites of arachidonic acid in the control of cardiovascular function. Physiological reviews. 2002;82(1):131-85. Epub 2002/01/05. doi: 10.1152/physrev.00021.2001. PubMed PMID: 11773611.

7. Mezentsev A, Mastyugin V, Seta F, Ashkar S, Kemp R, Reddy DS, Falck JR, Dunn MW, Laniado-Schwartzman M. Transfection of cytochrome P4504B1 into the cornea increases angiogenic activity of the limbal vessels. The Journal of pharmacology and experimental therapeutics. 2005;315(1):42-50. Epub 2005/07/13. doi: 10.1124/jpet.105.088211. PubMed PMID: 16009741.

8. Seta F, Patil K, Bellner L, Mezentsev A, Kemp R, Dunn MW, Schwartzman ML. Inhibition of VEGF expression and corneal neovascularization by siRNA targeting cytochrome P450 4B1. Prostaglandins & other lipid mediators. 2007;84(3-4):116-27. Epub 2007/11/10. doi: 10.1016/j.prostaglandins.2007.05.001. PubMed PMID: 17991614; PMCID: PMC2128778.

9. Fromel T, Kohlstedt K, Popp R, Yin X, Awwad K, Barbosa-Sicard E, Thomas AC, Lieberz R, Mayr M, Fleming I. Cytochrome P4502S1: a novel monocyte/macrophage fatty acid epoxygenase in human atherosclerotic plaques. Basic research in cardiology. 2013;108(1):319. Epub 2012/12/12. doi: 10.1007/s00395-012-0319-8. PubMed PMID: 23224081.

10. Inceoglu B, Bettaieb A, Trindade da Silva CA, Lee KS, Haj FG, Hammock BD. Endoplasmic reticulum stress in the peripheral nervous system is a significant driver of neuropathic pain. Proceedings of the National Academy of Sciences of the United States of America. 2015;112(29):9082-7. Epub 2015/07/08. doi: 10.1073/pnas.1510137112. PubMed PMID: 26150506; PMCID: Pmc4517273.

11. Node K, Huo Y, Ruan X, Yang B, Spiecker M, Ley K, Zeldin DC, Liao JK. Anti-inflammatory properties of cytochrome P450 epoxygenase-derived eicosanoids. Science. 1999;285(5431):1276-9. Epub 1999/08/24. doi: 10.1126/science.285.5431.1276. PubMed PMID: 10455056; PMCID: PMC2720027.

12.	Campbell WB, Gebremedhin D, Pratt PF, Harder DR. Identification of epoxyeicosatrienoic acids as endothelium-derived hyperpolarizing factors. Circulation research. 1996;78(3):415-23. Epub 1996/03/01. doi: 10.1161/01.res.78.3.415. PubMed PMID: 8593700.

13.	Weintraub NL, Fang X, Kaduce TL, VanRollins M, Chatterjee P, Spector AA. Epoxide hydrolases regulate epoxyeicosatrienoic acid incorporation into coronary endothelial phospholipids. The American journal of physiology. 1999;277(5):H2098-108. Epub 1999/11/24. doi: 10.1152/ajpheart.1999.277.5.H2098. PubMed PMID: 10564166.

14.	J H. Essential Fatty Acids: Linus Pauling Institute; 2003 [cited 2019]. Available from: https://lpi.oregonstate.edu/mic/other-nutrients/essential-fatty-acids.

15.	Zorn K, Oroz-Guinea I, Brundiek H, Bornscheuer UT. Engineering and application of enzymes for lipid modification, an update. Progress in lipid research. 2016;63:153-64. Epub 2016/06/16. doi: 10.1016/j.plipres.2016.06.001. PubMed PMID: 27301784.

16.	Moghaddam MF, Grant DF, Cheek JM, Greene JF, Williamson KC, Hammock BD. Bioactivation of leukotoxins to their toxic diols by epoxide hydrolase. Nature medicine. 1997;3(5):562-6. Epub 1997/05/01. PubMed PMID: 9142128.

17.	Kopf PG, Zhang DX, Gauthier KM, Nithipatikom K, Yi XY, Falck JR, Campbell WB. Adrenic acid metabolites as endogenous endothelium-derived and zona glomerulosa-derived hyperpolarizing factors. Hypertension. 2010;55(2):547-54. Epub 2009/12/30. doi: 10.1161/hypertensionaha.109.144147. PubMed PMID: 20038752; PMCID: PMC2819927.

18.	Wagner K, Vito S, Inceoglu B, Hammock BD. The role of long chain fatty acids and their epoxide metabolites in nociceptive signaling. Prostaglandins & other lipid mediators. 2014;113-115:2-12. Epub 2014/09/23. doi: 10.1016/j.prostaglandins.2014.09.001. PubMed PMID: 25240260; PMCID: Pmc4254344.

19.	Konkel A, Schunck WH. Role of cytochrome P450 enzymes in the bioactivation of polyunsaturated fatty acids. Biochim Biophys Acta. 2011;1814(1):210-22. Epub 2010/09/28. doi: S1570-9639(10)00258-X [pii]

10.1016/j.bbapap.2010.09.009. PubMed PMID: 20869469.

20.	Potente M, Michaelis UR, Fisslthaler B, Busse R, Fleming I. Cytochrome P450 2C9-induced endothelial cell proliferation involves induction of mitogen-activated protein (MAP) kinase phosphatase-1, inhibition of the c-Jun N-terminal kinase, and up-regulation of cyclin D1. The Journal of biological chemistry. 2002;277(18):15671-6. Epub 2002/02/28. doi: 10.1074/jbc.M110806200. PubMed PMID: 11867622.

21.	Fitzpatrick FA, Ennis MD, Baze ME, Wynalda MA, McGee JE, Liggett WF. Inhibition of cyclooxygenase activity and platelet aggregation by epoxyeicosatrienoic acids. Influence of stereochemistry. The Journal of biological chemistry. 1986;261(32):15334-8. Epub 1986/11/15. PubMed PMID: 3095326.

22.	Fan F, Muroya Y, Roman RJ. Cytochrome P450 eicosanoids in hypertension and renal disease. Current opinion in nephrology and hypertension. 2015;24(1):37-46. Epub 2014/11/27. doi: 10.1097/mnh.0000000000000088. PubMed PMID: 25427230; PMCID: PMC4260681.

23.	Fleming I, Busse R. Endothelium-derived epoxyeicosatrienoic acids and vascular function. Hypertension. 2006;47(4):629-33. Epub 2006/02/24. doi: 10.1161/01.hyp.0000208597.87957.89. PubMed PMID: 16490839.

24.	Roman RJ, Fan F. 20-HETE: Hypertension and Beyond. Hypertension. 2018;72(1):12-8. Epub 2018/05/16. doi: 10.1161/hypertensionaha.118.10269. PubMed PMID: 29760152; PMCID: PMC6002933.

25.   Ulu A, Inceoglu B, Yang J, Singh V, Vito S, Wulff H, Hammock BD. Inhibition of soluble epoxide hydrolase as a novel approach to high dose diazepam induced hypotension. J Clin Toxicol. 2016;6(3). Epub 2017/03/04. doi: 10.4172/2161-0495.1000300. PubMed PMID: 28255523; PMCID: PMC5328659.

26.   McGiff JC, Carroll MA. Cytochrome P450-dependent arachidonate metabolites, renal function and blood pressure regulation. Advances in prostaglandin, thromboxane, and leukotriene research. 1991;21b:675-82. Epub 1991/01/01. PubMed PMID: 1847570.

27.   Imig JD, Pham BT, LeBlanc EA, Reddy KM, Falck JR, Inscho EW. Cytochrome P450 and cyclooxygenase metabolites contribute to the endothelin-1 afferent arteriolar vasoconstrictor and calcium responses. Hypertension. 2000;35(1 Pt 2):307-12. Epub 2000/01/21. doi: 10.1161/01.hyp.35.1.307. PubMed PMID: 10642316.

28.   Liu L, Chen C, Gong W, Li Y, Edin ML, Zeldin DC, Wang DW. Epoxyeicosatrienoic acids attenuate reactive oxygen species level, mitochondrial dysfunction, caspase activation, and apoptosis in carcinoma cells treated with arsenic trioxide. The Journal of pharmacology and experimental therapeutics. 2011;339(2):451-63. Epub 2011/08/19. doi: 10.1124/jpet.111.180505. PubMed PMID: 21846841; PMCID: PMC3199997.

29.   Xu D, Li N, He Y, Timofeyev V, Lu L, Tsai HJ, Kim IH, Tuteja D, Mateo RK, Singapuri A, Davis BB, Low R, Hammock BD, Chiamvimonvat N. Prevention and reversal of cardiac hypertrophy by soluble epoxide hydrolase inhibitors. Proceedings of the National Academy of Sciences of the United States of America. 2006;103(49):18733-8. Epub 2006/11/30. doi: 10.1073/pnas.0609158103. PubMed PMID: 17130447; PMCID: PMC1693731.

30.   Kundu S, Roome T, Bhattacharjee A, Carnevale KA, Yakubenko VP, Zhang R, Hwang SH, Hammock BD, Cathcart MK. Metabolic products of soluble epoxide hydrolase are essential for monocyte chemotaxis to MCP-1 in vitro and in vivo. Journal of lipid research. 2013;54(2):436-47. doi: 10.1194/jlr.M031914. PubMed PMID: 23160182; PMCID: 3588870.

31.   Wagner KM, McReynolds CB, Schmidt WK, Hammock BD. Soluble epoxide hydrolase as a therapeutic target for pain, inflammatory and neurodegenerative diseases. Pharmacol Ther. 2017;180:62-76. Epub 2017/06/24. doi: 10.1016/j.pharmthera.2017.06.006. PubMed PMID: 28642117; PMCID: PMC5677555.

32.   Lin JH, Walter P, Yen TS. Endoplasmic reticulum stress in disease pathogenesis. Annual review of pathology. 2008;3:399-425. Epub 2007/11/28. doi: 10.1146/annurev.pathmechdis.3.121806.151434. PubMed PMID: 18039139; PMCID: PMC3653419.

33.   Fang X, Kaduce TL, Weintraub NL, Harmon S, Teesch LM, Morisseau C, Thompson DA, Hammock BD, Spector AA. Pathways of epoxyeicosatrienoic acid metabolism in endothelial cells. Implications for the vascular effects of soluble epoxide hydrolase inhibition. The Journal of biological chemistry. 2001;276(18):14867-74. Epub 2001/03/30. doi: 10.1074/jbc.M011761200. PubMed PMID: 11278979.

34.   Nelson JW, Subrahmanyan RM, Summers SA, Xiao X, Alkayed NJ. Soluble epoxide hydrolase dimerization is required for hydrolase activity. The Journal of biological chemistry. 2013;288(11):7697-703. Epub 2013/01/31. doi: 10.1074/jbc.M112.429258. PubMed PMID: 23362272; PMCID: PMC3597810.

35.   Morisseau C, Hammock BD. Epoxide hydrolases: mechanisms, inhibitor designs, and biological roles. Annual review of pharmacology and toxicology. 2005;45:311-33. doi: 10.1146/annurev.pharmtox.45.120403.095920. PubMed PMID: 15822179.

36.   Morisseau C. Role of epoxide hydrolases in lipid metabolism. Biochimie. 2013;95(1):91-5. Epub 2012/06/23. doi: 10.1016/j.biochi.2012.06.011. PubMed PMID: 22722082; PMCID: PMC3495083.

37.   Botham KM, Mayes PA. Cholesterol Synthesis, Transport, & Excretion. In: Rodwell VW, Bender DA, Botham KM, Kennelly PJ, Weil PA, editors. Harper's Illustrated Biochemistry, 30e. New York, NY: McGraw-Hill Education; 2016.

38.   Decker M, Adamska M, Cronin A, Di Giallonardo F, Burgener J, Marowsky A, Falck JR, Morisseau C, Hammock BD, Gruzdev A, Zeldin DC, Arand M. EH3 (ABHD9): the first member of a new epoxide hydrolase family with high activity for fatty acid epoxides. Journal of lipid research. 2012;53(10):2038-45. Epub 2012/07/17. doi: 10.1194/jlr.M024448. PubMed PMID: 22798687; PMCID: PMC3435537.

39.   Fornage M, Lee CR, Doris PA, Bray MS, Heiss G, Zeldin DC, Boerwinkle E. The soluble epoxide hydrolase gene harbors sequence variation associated with susceptibility to and protection from incident ischemic stroke. Human molecular genetics. 2005;14(19):2829-37. Epub 2005/08/24. doi: 10.1093/hmg/ddi315. PubMed PMID: 16115816; PMCID: PMC1343524.

40.   Martini RP, Ward J, Siler DA, Eastman JM, Nelson JW, Borkar RN, Alkayed NJ, Dogan A, Cetas JS. Genetic variation in soluble epoxide hydrolase: association with outcome after aneurysmal subarachnoid hemorrhage. Journal of neurosurgery. 2014;121(6):1359-66. Epub 2014/09/13. doi: 10.3171/2014.7.jns131990. PubMed PMID: 25216066; PMCID: PMC4370510.

41.   Morisseau C, Wecksler AT, Deng C, Dong H, Yang J, Lee KS, Kodani SD, Hammock BD. Effect of soluble epoxide hydrolase polymorphism on substrate and inhibitor selectivity and dimer formation. Journal of lipid research. 2014;55(6):1131-8. Epub 2014/04/29. doi: 10.1194/jlr.M049718. PubMed PMID: 24771868; PMCID: PMC4031944.

42.   Przybyla-Zawislak BD, Srivastava PK, Vazquez-Matias J, Mohrenweiser HW, Maxwell JE, Hammock BD, Bradbury JA, Enayetallah AE, Zeldin DC, Grant DF. Polymorphisms in human soluble epoxide hydrolase. Molecular pharmacology. 2003;64(2):482-90. Epub 2003/07/19. doi: 10.1124/mol.64.2.482. PubMed PMID: 12869654.

43.   Morisseau C, Hammock BD. Impact of Soluble Epoxide Hydrolase and Epoxyeicosanoids on Human Health. Annu Rev Pharmacol. 2013;53:37-58. doi: DOI 10.1146/annurev-pharmtox-011112-140244. PubMed PMID: WOS:000323040100003.

44.   Morisseau C, Inceoglu B, Schmelzer K, Tsai HJ, Jinks SL, Hegedus CM, Hammock BD. Naturally occurring monoepoxides of eicosapentaenoic acid and docosahexaenoic acid are bioactive antihyperalgesic lipids. Journal of lipid research. 2010;51(12):3481-90. Epub 2010/07/29. doi: 10.1194/jlr.M006007. PubMed PMID: 20664072; PMCID: PMC2975720.

45.   Ulu A, Harris TR, Morisseau C, Miyabe C, Inoue H, Schuster G, Dong H, Iosif AM, Liu JY, Weiss RH, Chiamvimonvat N, Imig JD, Hammock BD. Anti-inflammatory effects of omega-3 polyunsaturated fatty acids and soluble epoxide hydrolase inhibitors in angiotensin-II-dependent hypertension. Journal of cardiovascular pharmacology. 2013;62(3):285-97. doi: 10.1097/FJC.0b013e318298e460. PubMed PMID: 23676336; PMCID: 3773051.

46.   Scott-Van Zeeland AA, Bloss CS, Tewhey R, Bansal V, Torkamani A, Libiger O, Duvvuri V, Wineinger N, Galvez L, Darst BF, Smith EN, Carson A, Pham P, Phillips T, Villarasa N, Tisch R, Zhang G, Levy S, Murray S, Chen W, Srinivasan S, Berenson G, Brandt H, Crawford S, Crow S, Fichter MM, Halmi KA, Johnson C, Kaplan AS, La Via M, Mitchell JE, Strober M, Rotondo A, Treasure J, Woodside DB, Bulik CM, Keel P, Klump KL, Lilenfeld L, Plotnicov K, Topol EJ, Shih PB, Magistretti P, Bergen AW, Berrettini W, Kaye W, Schork NJ. Evidence for the role of

EPHX2 gene variants in anorexia nervosa. Molecular psychiatry. 2014;19(6):724-32. Epub 2013/09/04. doi: 10.1038/mp.2013.91. PubMed PMID: 23999524; PMCID: PMC3852189.

47.   Shih PB. Integrating multi-omics biomarkers and postprandial metabolism to develop personalized treatment for anorexia nervosa. Prostaglandins & other lipid mediators. 2017;132:69-76. Epub 2017/02/25. doi: 10.1016/j.prostaglandins.2017.02.002. PubMed PMID: 28232135; PMCID: PMC5565718.

48.   Shih PB, Yang J, Morisseau C, German JB, Zeeland AA, Armando AM, Quehenberger O, Bergen AW, Magistretti P, Berrettini W, Halmi KA, Schork N, Hammock BD, Kaye W. Dysregulation of soluble epoxide hydrolase and lipidomic profiles in anorexia nervosa. Molecular psychiatry. 2016;21(4):537-46. Epub 2015/04/01. doi: 10.1038/mp.2015.26. PubMed PMID: 25824304; PMCID: PMC4591075.

49.   Yang J, Shih PB. Fasting and postprandial soluble epoxide hydrolase-associated eicosanoids of remitted patients with eating disorder. Data in brief. 2018;17:334-8. Epub 2018/06/08. doi: 10.1016/j.dib.2018.01.028. PubMed PMID: 29876402; PMCID: PMC5988286.

50.   Sato K, Emi M, Ezura Y, Fujita Y, Takada D, Ishigami T, Umemura S, Xin Y, Wu LL, Larrinaga-Shum S, Stephenson SH, Hunt SC, Hopkins PN. Soluble epoxide hydrolase variant (Glu287Arg) modifies plasma total cholesterol and triglyceride phenotype in familial hypercholesterolemia: intrafamilial association study in an eight-generation hyperlipidemic kindred. Journal of human genetics. 2004;49(1):29-34. Epub 2003/12/16. doi: 10.1007/s10038-003-0103-6. PubMed PMID: 14673705.

51.   Shen L, Peng H, Peng R, Fan Q, Zhao S, Xu D, Morisseau C, Chiamvimonvat N, Hammock BD. Inhibition of soluble epoxide hydrolase in mice promotes reverse cholesterol transport and regression of atherosclerosis. Atherosclerosis. 2015;239(2):557-65. Epub 2015/03/04. doi: 10.1016/j.atherosclerosis.2015.02.014. PubMed PMID: 25733327; PMCID: PMC4527317.

52.   EnayetAllah AE, Luria A, Luo B, Tsai HJ, Sura P, Hammock BD, Grant DF. Opposite regulation of cholesterol levels by the phosphatase and hydrolase domains of soluble epoxide hydrolase. The Journal of biological chemistry. 2008;283(52):36592-8. Epub 2008/11/01. doi: 10.1074/jbc.M806315200. PubMed PMID: 18974052; PMCID: PMC2605982.

53.   Wang N, Tall AR. Regulation and mechanisms of ATP-binding cassette transporter A1-mediated cellular cholesterol efflux. Arteriosclerosis, thrombosis, and vascular biology. 2003;23(7):1178-84. Epub 2003/05/10. doi: 10.1161/01.atv.0000075912.83860.26. PubMed PMID: 12738681.

54.   Campbell WB, Falck JR, Gauthier K. Role of epoxyeicosatrienoic acids as endothelium-derived hyperpolarizing factor in bovine coronary arteries. Medical science monitor : international medical journal of experimental and clinical research. 2001;7(4):578-84. Epub 2001/07/04. PubMed PMID: 11433180.

55.   Sari I, Pinarbasi H, Pinarbasi E, Yildiz C. Association between the soluble epoxide hydrolase gene and preeclampsia. Hypertension in pregnancy. 2017;36(4):315-25. Epub 2017/10/24. doi: 10.1080/10641955.2017.1388390. PubMed PMID: 29058492.

56.   Koerner IP, Jacks R, DeBarber AE, Koop D, Mao P, Grant DF, Alkayed NJ. Polymorphisms in the human soluble epoxide hydrolase gene EPHX2 linked to neuronal survival after ischemic injury. The Journal of neuroscience : the official journal of the Society for Neuroscience. 2007;27(17):4642-9. doi: 10.1523/JNEUROSCI.0056-07.2007. PubMed PMID: 17460077; PMCID: PMC6672984.

57.   Gschwendtner A, Ripke S, Freilinger T, Lichtner P, Muller-Myhsok B, Wichmann HE, Meitinger T, Dichgans M. Genetic variation in soluble epoxide hydrolase (EPHX2) is associated

with an increased risk of ischemic stroke in white Europeans. Stroke. 2008;39(5):1593-6. Epub 2008/03/08. doi: 10.1161/strokeaha.107.502179. PubMed PMID: 18323494.

58.	Lee J, Dahl M, Grande P, Tybjaerg-Hansen A, Nordestgaard BG. Genetically reduced soluble epoxide hydrolase activity and risk of stroke and other cardiovascular disease. Stroke. 2010;41(1):27-33. Epub 2009/11/27. doi: 10.1161/strokeaha.109.567768. PubMed PMID: 19940276.

59.	Fava C, Montagnana M, Danese E, Almgren P, Hedblad B, Engstrom G, Berglund G, Minuz P, Melander O. Homozygosity for the EPHX2 K55R polymorphism increases the long-term risk of ischemic stroke in men: a study in Swedes. Pharmacogenetics and genomics. 2010;20(2):94-103. Epub 2010/01/13. doi: 10.1097/FPC.0b013e3283349ec9. PubMed PMID: 20065888.

60.	Nelson JW, Young JM, Borkar RN, Woltjer RL, Quinn JF, Silbert LC, Grafe MR, Alkayed NJ. Role of soluble epoxide hydrolase in age-related vascular cognitive decline. Prostaglandins & other lipid mediators. 2014;113-115:30-7. Epub 2014/10/04. doi: 10.1016/j.prostaglandins.2014.09.003. PubMed PMID: 25277097; PMCID: PMC4254026.

61.	Václavíková R, Hughes DJ, Souček P. Microsomal epoxide hydrolase 1 (EPHX1): Gene, structure, function, and role in human disease. Gene. 2015;571(1):1-8. Epub 07/26. doi: 10.1016/j.gene.2015.07.071. PubMed PMID: 26216302.

62.	Marowsky A, Burgener J, Falck JR, Fritschy JM, Arand M. Distribution of soluble and microsomal epoxide hydrolase in the mouse brain and its contribution to cerebral epoxyeicosatrienoic acid metabolism. Neuroscience. 2009;163(2):646-61. Epub 06/18. doi: 10.1016/j.neuroscience.2009.06.033. PubMed PMID: 19540314.

63.	Qin XH, Wu Z, Dong JH, Zeng YN, Xiong WC, Liu C, Wang MY, Zhu MZ, Chen WJ, Zhang Y, Huang QY, Zhu XH. Liver Soluble Epoxide Hydrolase Regulates Behavioral and Cellular Effects of Chronic Stress. Cell reports. 2019;29(10):3223-34.e6. Epub 2019/12/05. doi: 10.1016/j.celrep.2019.11.006. PubMed PMID: 31801085.

64.	Sinal CJ, Miyata M, Tohkin M, Nagata K, Bend JR, Gonzalez FJ. Targeted disruption of soluble epoxide hydrolase reveals a role in blood pressure regulation. The Journal of biological chemistry. 2000;275(51):40504-10. Epub 2000/09/26. doi: 10.1074/jbc.M008106200. PubMed PMID: 11001943.

65.	Harris TR, Hammock BD. Soluble epoxide hydrolase: gene structure, expression and deletion. Gene. 2013;526(2):61-74. doi: 10.1016/j.gene.2013.05.008. PubMed PMID: 23701967; PMCID: 3733540.

66.	Atone J, Wagner K, Hashimoto K, Hammock B. Prostaglandins and Other Lipid Mediators Cytochrome P450 derived epoxidized fatty acids as a therapeutic tool against neuroinflammatory diseases. Prostaglandins & other lipid mediators. 2019:106385. Epub 2019/11/08. doi: 10.1016/j.prostaglandins.2019.106385. PubMed PMID: 31698143.

67.	Bettaieb A, Koike S, Hsu MF, Ito Y, Chahed S, Bachaalany S, Gruzdev A, Calvo-Rubio M, Lee KSS, Inceoglu B, Imig JD, Villalba JM, Zeldin DC, Hammock BD, Haj FG. Soluble epoxide hydrolase in podocytes is a significant contributor to renal function under hyperglycemia. Biochimica et biophysica acta General subjects. 2017;1861(11 Pt A):2758-65. Epub 2017/08/02. doi: 10.1016/j.bbagen.2017.07.021. PubMed PMID: 28757338; PMCID: PMC5873293.

68.	Heinricher MM, Maire JJ, Lee D, Nalwalk JW, Hough LB. Physiological basis for inhibition of morphine and improgan antinociception by CC12, a P450 epoxygenase inhibitor. Journal of neurophysiology. 2010;104(6):3222-30. Epub 2010/10/12. doi: 10.1152/jn.00681.2010. PubMed PMID: 20926616; PMCID: PMC3007650.

69.   Conroy JL, Fang C, Gu J, Zeitlin SO, Yang W, Yang J, VanAlstine MA, Nalwalk JW, Albrecht PJ, Mazurkiewicz JE, Snyder-Keller A, Shan Z, Zhang SZ, Wentland MP, Behr M, Knapp BI, Bidlack JM, Zuiderveld OP, Leurs R, Ding X, Hough LB. Opioids activate brain analgesic circuits through cytochrome P450/epoxygenase signaling. Nat Neurosci. 2010;13(3):284-6. doi: 10.1038/nn.2497. PubMed PMID: 20139973; PMCID: PMC2828325.

70.   Hough LB, Nalwalk JW, Yang J, Conroy JL, VanAlstine MA, Yang W, Gargano J, Shan Z, Zhang SZ, Wentland MP, Phillips JG, Knapp BI, Bidlack JM, Zuiderveld OP, Leurs R, Ding X. Brain P450 epoxygenase activity is required for the antinociceptive effects of improgan, a nonopioid analgesic. Pain. 2011;152(4):878-87. Epub 2011/02/15. doi: 10.1016/j.pain.2011.01.001. PubMed PMID: 21316152; PMCID: PMC3065546.

71.   Morris JK, Piccolo BD, John CS, Green ZD, Thyfault JP, Adams SH. Oxylipin Profiling of Alzheimer's Disease in Nondiabetic and Type 2 Diabetic Elderly. Metabolites. 2019;9(9). Epub 2019/09/08. doi: 10.3390/metabo9090177. PubMed PMID: 31491971; PMCID: PMC6780570.

72.   Valdes AM, Ravipati S, Pousinis P, Menni C, Mangino M, Abhishek A, Chapman V, Barrett DA, Doherty M. Omega-6 oxylipins generated by soluble epoxide hydrolase are associated with knee osteoarthritis. Journal of lipid research. 2018;59(9):1763-70. Epub 2018/07/11. doi: 10.1194/jlr.P085118. PubMed PMID: 29986999; PMCID: PMC6121933.

73.   Caligiuri SPB, Aukema HM, Ravandi A, Lavallee R, Guzman R, Pierce GN. Specific plasma oxylipins increase the odds of cardiovascular and cerebrovascular events in patients with peripheral artery disease. Canadian journal of physiology and pharmacology. 2017;95(8):961-8. Epub 2017/07/18. doi: 10.1139/cjpp-2016-0615. PubMed PMID: 28714336.

74.   Theken KN, Schuck RN, Edin ML, Tran B, Ellis K, Bass A, Lih FB, Tomer KB, Poloyac SM, Wu MC, Hinderliter AL, Zeldin DC, Stouffer GA, Lee CR. Evaluation of cytochrome P450-derived eicosanoids in humans with stable atherosclerotic cardiovascular disease. Atherosclerosis. 2012;222(2):530-6. Epub 2012/04/17. doi: 10.1016/j.atherosclerosis.2012.03.022. PubMed PMID: 22503544; PMCID: PMC3361525.

75.   Hennebelle M, Otoki Y, Yang J, Hammock BD, Levitt AJ, Taha AY, Swardfager W. Altered soluble epoxide hydrolase-derived oxylipins in patients with seasonal major depression: An exploratory study. Psychiatry Res. 2017;252:94-101. Epub 2017/03/05. doi: 10.1016/j.psychres.2017.02.056. PubMed PMID: 28259037; PMCID: PMC5611448.

76.   Santos JM, Park JA, Joiakim A, Putt DA, Taylor RN, Kim H. The role of soluble epoxide hydrolase in preeclampsia. Medical hypotheses. 2017;108:81-5. Epub 2017/10/23. doi: 10.1016/j.mehy.2017.07.033. PubMed PMID: 29055406.

77.   Yu D, Hennebelle M, Sahlas DJ, Ramirez J, Gao F, Masellis M, Cogo-Moreira H, Swartz RH, Herrmann N, Chan PC, Pettersen JA, Stuss DT, Black SE, Taha AY, Swardfager W. Soluble Epoxide Hydrolase-Derived Linoleic Acid Oxylipins in Serum Are Associated with Periventricular White Matter Hyperintensities and Vascular Cognitive Impairment. Translational stroke research. 2019;10(5):522-33. Epub 2018/11/18. doi: 10.1007/s12975-018-0672-5. PubMed PMID: 30443886.

78.   Grey A, Bolland M. Clinical trial evidence and use of fish oil supplements. JAMA Intern Med. 2014;174(3):460-2. doi: 10.1001/jamainternmed.2013.12765. PubMed PMID: 24352849.

79.   Rymer C, Gibbs RA, Givens DI. Comparison of algal and fish sources on the oxidative stability of poultry meat and its enrichment with omega-3 polyunsaturated fatty acids. Poultry science. 2010;89(1):150-9. doi: 10.3382/ps.2009-00232. PubMed PMID: 20008813.

80.   Jackowski SA, Alvi AZ, Mirajkar A, Imani Z, Gamalevych Y, Shaikh NA, Jackowski G. Oxidation levels of North American over-the-counter n-3 (omega-3) supplements and the

influence of supplement formulation and delivery form on evaluating oxidative safety. J Nutr Sci. 2015;4:e30-e. doi: 10.1017/jns.2015.21. PubMed PMID: 26688721.

81.   Albert BB, Cameron-Smith D, Hofman PL, Cutfield WS. Oxidation of marine omega-3 supplements and human health. BioMed research international. 2013;2013:464921-. Epub 04/30. doi: 10.1155/2013/464921. PubMed PMID: 23738326.

82.   Hu J, Dziumbla S, Lin J, Bibli SI, Zukunft S, de Mos J, Awwad K, Fromel T, Jungmann A, Devraj K, Cheng Z, Wang L, Fauser S, Eberhart CG, Sodhi A, Hammock BD, Liebner S, Muller OJ, Glaubitz C, Hammes HP, Popp R, Fleming I. Inhibition of soluble epoxide hydrolase prevents diabetic retinopathy. Nature. 2017;552(7684):248-52. Epub 2017/12/07. doi: 10.1038/nature25013. PubMed PMID: 29211719; PMCID: PMC5828869.

83.   Ruparel S, Green D, Chen P, Hargreaves KM. The cytochrome P450 inhibitor, ketoconazole, inhibits oxidized linoleic acid metabolite-mediated peripheral inflammatory pain. Molecular pain. 2012;8:73. Epub 2012/09/26. doi: 10.1186/1744-8069-8-73. PubMed PMID: 23006841; PMCID: PMC3488501.

84.   Goswami SK, Inceoglu B, Yang J, Wan D, Kodani SD, da Silva CA, Morisseau C, Hammock BD. Omeprazole increases the efficacy of a soluble epoxide hydrolase inhibitor in a PGE(2) induced pain model. Toxicology and applied pharmacology. 2015;289(3):419-27. Epub 2015/11/03. doi: 10.1016/j.taap.2015.10.018. PubMed PMID: 26522832; PMCID: PMC4666679.

85.   Hennebelle M, Zhang Z, Metherel AH, Kitson AP, Otoki Y, Richardson CE, Yang J, Lee KSS, Hammock BD, Zhang L, Bazinet RP, Taha AY. Linoleic acid participates in the response to ischemic brain injury through oxidized metabolites that regulate neurotransmission. Scientific reports. 2017;7(1):4342. Epub 2017/07/01. doi: 10.1038/s41598-017-02914-7. PubMed PMID: 28659576; PMCID: PMC5489485.

86.   Ramsden CE, Hennebelle M, Schuster S, Keyes GS, Johnson CD, Kirpich IA, Dahlen JE, Horowitz MS, Zamora D, Feldstein AE, McClain CJ, Muhlhausler BS, Makrides M, Gibson RA, Taha AY. Effects of diets enriched in linoleic acid and its peroxidation products on brain fatty acids, oxylipins, and aldehydes in mice. Biochimica et biophysica acta Molecular and cell biology of lipids. 2018;1863(10):1206-13. Epub 2018/07/28. doi: 10.1016/j.bbalip.2018.07.007. PubMed PMID: 30053599; PMCID: PMC6180905.

87.   Ramsden CE, Ringel A, Feldstein AE, Taha AY, MacIntosh BA, Hibbeln JR, Majchrzak-Hong SF, Faurot KR, Rapoport SI, Cheon Y, Chung YM, Berk M, Mann JD. Lowering dietary linoleic acid reduces bioactive oxidized linoleic acid metabolites in humans. Prostaglandins, leukotrienes, and essential fatty acids. 2012;87(4-5):135-41. Epub 2012/09/11. doi: 10.1016/j.plefa.2012.08.004. PubMed PMID: 22959954; PMCID: PMC3467319.

88.   Vangaveti VN, Jansen H, Kennedy RL, Malabu UH. Hydroxyoctadecadienoic acids: Oxidised derivatives of linoleic acid and their role in inflammation associated with metabolic syndrome and cancer. European journal of pharmacology. 2016;785:70-6. Epub 2015/05/20. doi: 10.1016/j.ejphar.2015.03.096. PubMed PMID: 25987423.

89.   Patwardhan AM, Scotland PE, Akopian AN, Hargreaves KM. Activation of TRPV1 in the spinal cord by oxidized linoleic acid metabolites contributes to inflammatory hyperalgesia. Proceedings of the National Academy of Sciences of the United States of America. 2009;106(44):18820-4. Epub 2009/10/22. doi: 10.1073/pnas.0905415106. PubMed PMID: 19843694; PMCID: PMC2764734.

90.   Henry Krum MUAH. Evaluation of the Effects of Urotensin-II and Soluble Epoxide Hydrolase Inhibitors on Skin Microvessel Tone in Patients With Heart Failure, and in Healthy

Volunteers (NCT00654966) 2011 [cited 2019 October 1]. Available from: https://clinicaltrials.gov/ct2/show/NCT00654966?term=soluble+epoxide+hydrolase&rank=1

91.   Morisseau C, Goodrow MH, Newman JW, Wheelock CE, Dowdy DL, Hammock BD. Structural refinement of inhibitors of urea-based soluble epoxide hydrolases. Biochemical pharmacology. 2002;63(9):1599-608. Epub 2002/05/15. doi: 10.1016/s0006-2952(02)00952-8. PubMed PMID: 12007563.

92.   Tsai HJ, Hwang SH, Morisseau C, Yang J, Jones PD, Kasagami T, Kim IH, Hammock BD. Pharmacokinetic screening of soluble epoxide hydrolase inhibitors in dogs. European journal of pharmaceutical sciences : official journal of the European Federation for Pharmaceutical Sciences. 2010;40(3):222-38. Epub 2010/04/03. doi: 10.1016/j.ejps.2010.03.018. PubMed PMID: 20359531; PMCID: PMC3285443.

93.   Kodani SD, Hammock BD. The 2014 Bernard B. Brodie Award Lecture Epoxide Hydrolases: Drug Metabolism to Therapeutics for Chronic Pain. Drug metabolism and disposition: the biological fate of chemicals. 2015. doi: 10.1124/dmd.115.063339. PubMed PMID: 25762541.

94.   Lee KS, Liu JY, Wagner KM, Pakhomova S, Dong H, Morisseau C, Fu SH, Yang J, Wang P, Ulu A, Mate CA, Nguyen LV, Hwang SH, Edin ML, Mara AA, Wulff H, Newcomer ME, Zeldin DC, Hammock BD. Optimized inhibitors of soluble epoxide hydrolase improve in vitro target residence time and in vivo efficacy. Journal of medicinal chemistry. 2014;57(16):7016-30. doi: 10.1021/jm500694p. PubMed PMID: 25079952; PMCID: 4148150.

95.   Henrick CA, Staal GB, Siddall JB. Alkyl 3,7,11-trimethyl-2,4-dodecadienoates, a new class of potent insect growth regulators with juvenile hormone activity. J Agric Food Chem. 1973;21(3):354-9. Epub 1973/05/01. doi: 10.1021/jf60187a043. PubMed PMID: 4708794.

96.   Tran L, Kompa AR, Wang BH, Krum H. Evaluation of the effects of urotensin II and soluble epoxide hydrolase inhibitor on skin microvessel tone in healthy controls and heart failure patients. Cardiovascular therapeutics. 2012;30(5):295-300. Epub 2011/09/03. doi: 10.1111/j.1755-5922.2011.00282.x. PubMed PMID: 21884016.

97.   Chen D, Whitcomb R, MacIntyre E, Tran V, Do ZN, Sabry J, Patel DV, Anandan SK, Gless R, Webb HK. Pharmacokinetics and pharmacodynamics of AR9281, an inhibitor of soluble epoxide hydrolase, in single- and multiple-dose studies in healthy human subjects. Journal of clinical pharmacology. 2012;52(3):319-28. Epub 2011/03/23. doi: 10.1177/0091270010397049. PubMed PMID: 21422238.

98.   Imig JD, Carpenter MA, Shaw S. The Soluble Epoxide Hydrolase Inhibitor AR9281 Decreases Blood Pressure, Ameliorates Renal Injury and Improves Vascular Function in Hypertension. Pharmaceuticals (Basel, Switzerland). 2009;2(3):217-27. Epub 2009/12/18. doi: 10.3390/ph2030217. PubMed PMID: 27713235; PMCID: PMC3978544.

99.   Lee KS, Morisseau C, Yang J, Wang P, Hwang SH, Hammock BD. Forster resonance energy transfer competitive displacement assay for human soluble epoxide hydrolase. Analytical biochemistry. 2013;434(2):259-68. doi: 10.1016/j.ab.2012.11.015. PubMed PMID: 23219719; PMCID: 3632402.

100.   Podolin PL, Bolognese BJ, Foley JF, Long E, 3rd, Peck B, Umbrecht S, Zhang X, Zhu P, Schwartz B, Xie W, Quinn C, Qi H, Sweitzer S, Chen S, Galop M, Ding Y, Belyanskaya SL, Israel DI, Morgan BA, Behm DJ, Marino JP, Jr., Kurali E, Barnette MS, Mayer RJ, Booth-Genthe CL, Callahan JF. In vitro and in vivo characterization of a novel soluble epoxide hydrolase inhibitor. Prostaglandins & other lipid mediators. 2013;104-105:25-31. doi: 10.1016/j.prostaglandins.2013.02.001. PubMed PMID: 23434473.

101.   Fleming I, Rueben A, Popp R, Fisslthaler B, Schrodt S, Sander A, Haendeler J, Falck JR, Morisseau C, Hammock BD, Busse R. Epoxyeicosatrienoic acids regulate Trp channel dependent Ca2+ signaling and hyperpolarization in endothelial cells. Arteriosclerosis, thrombosis, and vascular biology. 2007;27(12):2612-8. doi: 10.1161/ATVBAHA.107.152074. PubMed PMID: 17872452.

102.   Pozzi A, Macias-Perez I, Abair T, Wei S, Su Y, Zent R, Falck JR, Capdevila JH. Characterization of 5,6- and 8,9-epoxyeicosatrienoic acids (5,6- and 8,9-EET) as potent in vivo angiogenic lipids. The Journal of biological chemistry. 2005;280(29):27138-46. Epub 2005/05/27. doi: 10.1074/jbc.M501730200. PubMed PMID: 15917237.

103.   Panigrahy D, Edin ML, Lee CR, Huang S, Bielenberg DR, Butterfield CE, Barnes CM, Mammoto A, Mammoto T, Luria A, Benny O, Chaponis DM, Dudley AC, Greene ER, Vergilio JA, Pietramaggiori G, Scherer-Pietramaggiori SS, Short SM, Seth M, Lih FB, Tomer KB, Yang J, Schwendener RA, Hammock BD, Falck JR, Manthati VL, Ingber DE, Kaipainen A, D'Amore PA, Kieran MW, Zeldin DC. Epoxyeicosanoids stimulate multiorgan metastasis and tumor dormancy escape in mice. The Journal of clinical investigation. 2012;122(1):178-91. doi: 10.1172/JCI58128. PubMed PMID: 22182838; PMCID: 3248288.

104.   Dai M, Wu L, Wang P, Wen Z, Xu X, Wang DW. CYP2J2 and Its Metabolites EETs Attenuate Insulin Resistance via Regulating Macrophage Polarization in Adipose Tissue. Scientific reports. 2017;7:46743. Epub 2017/04/26. doi: 10.1038/srep46743. PubMed PMID: 28440284; PMCID: PMC5404269.

105.   Li R, Xu X, Chen C, Wang Y, Gruzdev A, Zeldin DC, Wang DW. CYP2J2 attenuates metabolic dysfunction in diabetic mice by reducing hepatic inflammation via the PPARgamma. American journal of physiology Endocrinology and metabolism. 2015;308(4):E270-82. Epub 2014/11/13. doi: 10.1152/ajpendo.00118.2014. PubMed PMID: 25389363; PMCID: PMC4329496.

106.   Yang Y, Dong R, Chen Z, Hu D, Fu M, Tang Y, Wang DW, Xu X, Tu L. Endothelium-specific CYP2J2 overexpression attenuates age-related insulin resistance. Aging Cell. 2018;17(2). Epub 2018/01/11. doi: 10.1111/acel.12718. PubMed PMID: 29318723; PMCID: PMC5847864.

107.   Zarriello S, Tuazon JP, Corey S, Schimmel S, Rajani M, Gorsky A, Incontri D, Hammock BD, Borlongan CV. Humble beginnings with big goals: Small molecule soluble epoxide hydrolase inhibitors for treating CNS disorders. Progress in neurobiology. 2019;172:23-39. Epub 2018/11/18. doi: 10.1016/j.pneurobio.2018.11.001. PubMed PMID: 30447256.

108.   Wagner K, Inceoglu B, Hammock BD. Soluble epoxide hydrolase inhibition, epoxygenated fatty acids and nociception. Prostaglandins & other lipid mediators. 2011;96(1-4):76-83. Epub 2011/08/23. doi: 10.1016/j.prostaglandins.2011.08.001. PubMed PMID: 21854866; PMCID: PMC3215909.

109.   Brostrom L FJ, inventorArachidonic Acid Analogs and Methods for Analgesi Treatment Using Same patent 8,658,632 B2. 2012.

110.   Falck JR, Wallukat G, Puli N, Goli M, Arnold C, Konkel A, Rothe M, Fischer R, Muller DN, Schunck WH. 17(R),18(S)-epoxyeicosatetraenoic acid, a potent eicosapentaenoic acid (EPA) derived regulator of cardiomyocyte contraction: structure-activity relationships and stable analogues. Journal of medicinal chemistry. 2011;54(12):4109-18. Epub 2011/05/20. doi: 10.1021/jm200132q. PubMed PMID: 21591683; PMCID: PMC3122156.

111.   Fraser DA WX, Skjaeret T, Kastelein JP, Schuppan D. A structurally engineered fatty acid, icosabutate, displays optimised absorption, distribution and metabolism properties for targeting hepatic inflammation and normalises elevated liver enzymes in dyslipidemic patients. 2018.

Available from: https://www.northseatherapeutics.com/wp-content/uploads/2018/04/EASL-ILC2018-NST.pdf.

112.   Bays HE, Hallen J, Vige R, Fraser D, Zhou R, Hustvedt SO, Orloff DG, Kastelein JJ. Icosabutate for the treatment of very high triglycerides: A placebo-controlled, randomized, double-blind, 12-week clinical trial. Journal of clinical lipidology. 2016;10(1):181-91.e1-2. Epub 2016/02/20. doi: 10.1016/j.jacl.2015.10.012. PubMed PMID: 26892135.

113.   Bhatt DL, Steg PG, Miller M, Brinton EA, Jacobson TA, Ketchum SB, Doyle RT, Jr., Juliano RA, Jiao L, Granowitz C, Tardif JC, Ballantyne CM. Cardiovascular Risk Reduction with Icosapent Ethyl for Hypertriglyceridemia. The New England journal of medicine. 2019;380(1):11-22. Epub 2018/11/13. doi: 10.1056/NEJMoa1812792. PubMed PMID: 30415628.

114.   Bhatt DL, Steg PG, Miller M, Brinton EA, Jacobson TA, Ketchum SB, Doyle RT, Jr., Juliano RA, Jiao L, Granowitz C, Tardif JC, Gregson J, Pocock SJ, Ballantyne CM. Effects of Icosapent Ethyl on Total Ischemic Events: From REDUCE-IT. Journal of the American College of Cardiology. 2019;73(22):2791-802. Epub 2019/03/23. doi: 10.1016/j.jacc.2019.02.032. PubMed PMID: 30898607.

115.   Wallace JL. How do NSAIDs cause ulcer disease? Bailliere's best practice & research Clinical gastroenterology. 2000;14(1):147-59. Epub 2000/04/05. PubMed PMID: 10749095.

116.   Becker RC. COX-2 inhibitors. Texas Heart Institute journal. 2005;32(3):380-3. Epub 2006/01/06. PubMed PMID: 16392224; PMCID: PMC1336714.

117.   Groenendyk J, Paskevicius T, Urra H, Viricel C, Wang K, Barakat K, Hetz C, Kurgan L, Agellon LB, Michalak M. Cyclosporine A binding to COX-2 reveals a novel signaling pathway that activates the IRE1alpha unfolded protein response sensor. Scientific reports. 2018;8(1):16678. Epub 2018/11/14. doi: 10.1038/s41598-018-34891-w. PubMed PMID: 30420769; PMCID: PMC6232179.

118.   Ghosh R, Alajbegovic A, Gomes AV. NSAIDs and Cardiovascular Diseases: Role of Reactive Oxygen Species. Oxidative medicine and cellular longevity. 2015;2015:536962. Epub 2015/10/13. doi: 10.1155/2015/536962. PubMed PMID: 26457127; PMCID: PMC4592725.

119.   Ohyama K, Shiokawa A, Ito K, Masuyama R, Ichibangase T, Kishikawa N, Imai K, Kuroda N. Toxicoproteomic analysis of a mouse model of nonsteroidal anti-inflammatory drug-induced gastric ulcers. Biochemical and biophysical research communications. 2012;420(1):210-5. Epub 2012/03/20. doi: 10.1016/j.bbrc.2012.03.009. PubMed PMID: 22426477.

120.   Tsutsumi S, Gotoh T, Tomisato W, Mima S, Hoshino T, Hwang HJ, Takenaka H, Tsuchiya T, Mori M, Mizushima T. Endoplasmic reticulum stress response is involved in nonsteroidal anti-inflammatory drug-induced apoptosis. Cell death and differentiation. 2004;11(9):1009-16. Epub 2004/05/08. doi: 10.1038/sj.cdd.4401436. PubMed PMID: 15131590.

121.   Panigrahy D, Greene ER, Pozzi A, Wang DW, Zeldin DC. EET signaling in cancer. Cancer metastasis reviews. 2011;30(3-4):525-40. Epub 2011/10/20. doi: 10.1007/s10555-011-9315-y. PubMed PMID: 22009066; PMCID: PMC3804913.

122.   Lazaar AL, Yang L, Boardley RL, Goyal NS, Robertson J, Baldwin SJ, Newby DE, Wilkinson IB, Tal-Singer R, Mayer RJ, Cheriyan J. Pharmacokinetics, pharmacodynamics and adverse event profile of GSK2256294, a novel soluble epoxide hydrolase inhibitor. British journal of clinical pharmacology. 2016;81(5):971-9. Epub 2015/12/02. doi: 10.1111/bcp.12855. PubMed PMID: 26620151; PMCID: PMC4834590.

123.   Askari A, Thomson SJ, Edin ML, Zeldin DC, Bishop-Bailey D. Roles of the epoxygenase CYP2J2 in the endothelium. Prostaglandins & other lipid mediators. 2013;107:56-63. Epub

2013/03/12. doi: 10.1016/j.prostaglandins.2013.02.003. PubMed PMID: 23474289; PMCID: PMC3711961.

124. Fleming I. The cytochrome P450 pathway in angiogenesis and endothelial cell biology. Cancer metastasis reviews. 2011;30(3-4):541-55. Epub 2011/10/20. doi: 10.1007/s10555-011-9302-3. PubMed PMID: 22009065.

125. Imig JD. Epoxides and soluble epoxide hydrolase in cardiovascular physiology. Physiological reviews. 2012;92(1):101-30. Epub 2012/02/03. doi: 10.1152/physrev.00021.2011. PubMed PMID: 22298653; PMCID: PMC3613253.

126. Rand AA, Rajamani A, Kodani SD, Harris TR, Schlatt L, Barnych B, Passerini AG, Hammock BD. Epoxyeicosatrienoic acid (EET)-stimulated angiogenesis is mediated by epoxy hydroxyeicosatrienoic acids (EHETs) formed from COX-2. Journal of lipid research. 2019. Epub 2019/10/24. doi: 10.1194/jlr.M094219. PubMed PMID: 31641036.

127. Gartung A, Yang J, Sukhatme VP, Bielenberg DR, Fernandes D, Chang J, Schmidt BA, Hwang SH, Zurakowski D, Huang S, Kieran MW, Hammock BD, Panigrahy D. Suppression of chemotherapy-induced cytokine/lipid mediator surge and ovarian cancer by a dual COX-2/sEH inhibitor. Proceedings of the National Academy of Sciences of the United States of America. 2019;116(5):1698-703. Epub 2019/01/17. doi: 10.1073/pnas.1803999116. PubMed PMID: 30647111; PMCID: PMC6358686.

128. Schmelzer KR, Inceoglu B, Kubala L, Kim IH, Jinks SL, Eiserich JP, Hammock BD. Enhancement of antinociception by coadministration of nonsteroidal anti-inflammatory drugs and soluble epoxide hydrolase inhibitors. Proceedings of the National Academy of Sciences of the United States of America. 2006;103(37):13646-51. Epub 2006/09/05. doi: 10.1073/pnas.0605908103. PubMed PMID: 16950874; PMCID: PMC1564210.

129. Sasich LD, Barasain MA, Al Kudsi MA. The cardiovascular risks of etoricoxib (Arcoxia). Annals of Saudi medicine. 2008;28(2):141-2. Epub 2008/04/10. doi: 10.5144/0256-4947.2008.141. PubMed PMID: 18398284; PMCID: PMC6074531.

130. Bruno F, Spaziano G, Liparulo A, Roviezzo F, Nabavi SM, Sureda A, Filosa R, D'Agostino B. Recent advances in the search for novel 5-lipoxygenase inhibitors for the treatment of asthma. European journal of medicinal chemistry. 2018;153:65-72. Epub 2017/11/15. doi: 10.1016/j.ejmech.2017.10.020. PubMed PMID: 29133059.

131. Yang J, Bratt J, Franzi L, Liu JY, Zhang G, Zeki AA, Vogel CF, Williams K, Dong H, Lin Y, Hwang SH, Kenyon NJ, Hammock BD. Soluble epoxide hydrolase inhibitor attenuates inflammation and airway hyperresponsiveness in mice. American journal of respiratory cell and molecular biology. 2015;52(1):46-55. doi: 10.1165/rcmb.2013-0440OC. PubMed PMID: 24922186.

132. Gobel T, Diehl O, Heering J, Merk D, Angioni C, Wittmann SK, Buscato E, Kottke R, Weizel L, Schader T, Maier TJ, Geisslinger G, Schubert-Zsilavecz M, Steinhilber D, Proschak E, Kahnt AS. Zafirlukast Is a Dual Modulator of Human Soluble Epoxide Hydrolase and Peroxisome Proliferator-Activated Receptor gamma. Frontiers in pharmacology. 2019;10:263. Epub 2019/04/06. doi: 10.3389/fphar.2019.00263. PubMed PMID: 30949053; PMCID: PMC6435570.

133. Watkins BA. Diet, endocannabinoids, and health. Nutrition research (New York, NY). 2019;70:32-9. Epub 2019/07/10. doi: 10.1016/j.nutres.2019.06.003. PubMed PMID: 31280882.

134. van Esbroeck ACM, Janssen APA, Cognetta AB, 3rd, Ogasawara D, Shpak G, van der Kroeg M, Kantae V, Baggelaar MP, de Vrij FMS, Deng H, Allara M, Fezza F, Lin Z, van der Wel T, Soethoudt M, Mock ED, den Dulk H, Baak IL, Florea BI, Hendriks G, De Petrocellis L, Overkleeft HS, Hankemeier T, De Zeeuw CI, Di Marzo V, Maccarrone M, Cravatt BF, Kushner

SA, van der Stelt M. Activity-based protein profiling reveals off-target proteins of the FAAH inhibitor BIA 10-2474. Science. 2017;356(6342):1084-7. Epub 2017/06/10. doi: 10.1126/science.aaf7497. PubMed PMID: 28596366; PMCID: PMC5641481.

135. Habib AM, Okorokov AL, Hill MN, Bras JT, Lee MC, Li S, Gossage SJ, van Drimmelen M, Morena M, Houlden H, Ramirez JD, Bennett DLH, Srivastava D, Cox JJ. Microdeletion in a FAAH pseudogene identified in a patient with high anandamide concentrations and pain insensitivity. British journal of anaesthesia. 2019;123(2):e249-e53. Epub 2019/04/02. doi: 10.1016/j.bja.2019.02.019. PubMed PMID: 30929760; PMCID: PMC6676009.

136. Sasso O, Wagner K, Morisseau C, Inceoglu B, Hammock BD, Piomelli D. Peripheral FAAH and soluble epoxide hydrolase inhibitors are synergistically antinociceptive. Pharmacological research. 2015;97:7-15. Epub 2015/04/18. doi: 10.1016/j.phrs.2015.04.001. PubMed PMID: 25882247; PMCID: PMC4464910.

137. Kodani SD, Bhakta S, Hwang SH, Pakhomova S, Newcomer ME, Morisseau C, Hammock BD. Identification and optimization of soluble epoxide hydrolase inhibitors with dual potency towards fatty acid amide hydrolase. Bioorganic & medicinal chemistry letters. 2018. Epub 2018/01/26. doi: 10.1016/j.bmcl.2018.01.003. PubMed PMID: 29366648.

138. Inceoglu B, Wagner K, Schebb NH, Morisseau C, Jinks SL, Ulu A, Hegedus C, Rose T, Brosnan R, Hammock BD. Analgesia mediated by soluble epoxide hydrolase inhibitors is dependent on cAMP. Proceedings of the National Academy of Sciences of the United States of America. 2011;108(12):5093-7. doi: 10.1073/pnas.1101073108. PubMed PMID: 21383170; PMCID: 3064364.

139. Blocher R, Wagner KM, Gopireddy RR, Harris TR, Wu H, Barnych B, Hwang SH, Xiang YK, Proschak E, Morisseau C, Hammock BD. Orally Available Soluble Epoxide Hydrolase/Phosphodiesterase 4 Dual Inhibitor Treats Inflammatory Pain. Journal of medicinal chemistry. 2018;61(8):3541-50. Epub 2018/04/04. doi: 10.1021/acs.jmedchem.7b01804. PubMed PMID: 29614224; PMCID: PMC5933862.

140. Hwang SH, Wecksler AT, Zhang G, Morisseau C, Nguyen LV, Fu SH, Hammock BD. Synthesis and biological evaluation of sorafenib- and regorafenib-like sEH inhibitors. Bioorganic & medicinal chemistry letters. 2013;23(13):3732-7. Epub 05/15. doi: 10.1016/j.bmcl.2013.05.011. PubMed PMID: 23726028.

141. Liang Z, Zhang B, Xu M, Morisseau C, Hwang SH, Hammock BD, Li QX. 1-Trifluoromethoxyphenyl-3-(1-propionylpiperidin-4-yl) Urea, a Selective and Potent Dual Inhibitor of Soluble Epoxide Hydrolase and p38 Kinase Intervenes in Alzheimer's Signaling in Human Nerve Cells. ACS chemical neuroscience. 2019;10(9):4018-30. Epub 2019/08/06. doi: 10.1021/acschemneuro.9b00271. PubMed PMID: 31378059.

142. Reddy AS, Zhang S. Polypharmacology: drug discovery for the future. Expert review of clinical pharmacology. 2013;6(1):41-7. Epub 2013/01/01. doi: 10.1586/ecp.12.74. PubMed PMID: 23272792; PMCID: PMC3809828.

143. Kim JH, Morgan AM, Tai BH, Van DT, Cuong NM, Kim YH. Inhibition of soluble epoxide hydrolase activity by compounds isolated from the aerial parts of Glycosmis stenocarpa. Journal of enzyme inhibition and medicinal chemistry. 2016;31(4):640-4. Epub 2015/10/08. doi: 10.3109/14756366.2015.1057719. PubMed PMID: 26444316.

144. Sun YN, Kim JH, Li W, Jo AR, Yan XT, Yang SY, Kim YH. Soluble epoxide hydrolase inhibitory activity of anthraquinone components from Aloe. Bioorganic & medicinal chemistry. 2015;23(20):6659-65. Epub 2015/09/16. doi: 10.1016/j.bmc.2015.09.003. PubMed PMID: 26372074.

145.   Dimitropoulou C, West L, Field MB, White RE, Reddy LM, Falck JR, Imig JD. Protein phosphatase 2A and Ca2+-activated K+ channels contribute to 11,12-epoxyeicosatrienoic acid analog mediated mesenteric arterial relaxation. Prostaglandins & other lipid mediators. 2007;83(1-2):50-61. Epub 2007/01/30. doi: 10.1016/j.prostaglandins.2006.09.008. PubMed PMID: 17259072.

146.   Shen HC, Hammock BD. Discovery of inhibitors of soluble epoxide hydrolase: a target with multiple potential therapeutic indications. Journal of medicinal chemistry. 2012;55(5):1789-808. doi: 10.1021/jm201468j. PubMed PMID: 22168898; PMCID: 3420824.

147.   Arnold C, Markovic M, Blossey K, Wallukat G, Fischer R, Dechend R, Konkel A, von Schacky C, Luft FC, Muller DN, Rothe M, Schunck WH. Arachidonic acid-metabolizing cytochrome P450 enzymes are targets of {omega}-3 fatty acids. The Journal of biological chemistry. 2010;285(43):32720-33. Epub 2010/08/25. doi: 10.1074/jbc.M110.118406. PubMed PMID: 20732876; PMCID: PMC2963419.

148.   Hutchens MP, Nakano T, Dunlap J, Traystman RJ, Hurn PD, Alkayed NJ. Soluble epoxide hydrolase gene deletion reduces survival after cardiac arrest and cardiopulmonary resuscitation. Resuscitation. 2008;76(1):89-94. Epub 2007/08/31. doi: 10.1016/j.resuscitation.2007.06.031. PubMed PMID: 17728042; PMCID: PMC2585367.

149.   Modric S. Regulatory framework for the availability and use of animal drugs in the United States. Vet Clin North Am Small Anim Pract. 2013;43(5):1005-12. Epub 2013/07/31. doi: 10.1016/j.cvsm.2013.04.001. PubMed PMID: 23890234.

150.   Richardson SJ, Bai A, Kulkarni AA, Moghaddam MF. Efficiency in Drug Discovery: Liver S9 Fraction Assay As a Screen for Metabolic Stability. Drug metabolism letters. 2016;10(2):83-90. Epub 2016/02/24. doi: 10.2174/1872312810666160223121836. PubMed PMID: 26902079; PMCID: PMC5405623.

151.   Court MH. Canine cytochrome P-450 pharmacogenetics. Vet Clin North Am Small Anim Pract. 2013;43(5):1027-38. doi: 10.1016/j.cvsm.2013.05.001. PubMed PMID: 23890236; PMCID: PMC3740394.

152.   Visser M, Weber KL, Lyons LA, Rincon G, Boothe DM, Merritt DA. Identification and quantification of domestic feline cytochrome P450 transcriptome across multiple tissues. J Vet Pharmacol Ther. 2019;42(1):7-15. Epub 2018/09/02. doi: 10.1111/jvp.12708. PubMed PMID: 30171610; PMCID: PMC6322962.

153.   Court MH. Feline drug metabolism and disposition: pharmacokinetic evidence for species differences and molecular mechanisms. Vet Clin North Am Small Anim Pract. 2013;43(5):1039-54. Epub 2013/07/31. doi: 10.1016/j.cvsm.2013.05.002. PubMed PMID: 23890237; PMCID: PMC3811070.

154.   Hugonnard M, Leblond A, Keroack S, Cadoré JL, Troncy E. Attitudes and concerns of French veterinarians towards pain and analgesia in dogs and cats. Veterinary anaesthesia and analgesia. 2004;31(3):154-63. Epub 2004/07/23. doi: 10.1111/j.1467-2987.2004.00175.x. PubMed PMID: 15268686.

155.   Capner CA, Lascelles BD, Waterman-Pearson AE. Current British veterinary attitudes to perioperative analgesia for dogs. The Veterinary record. 1999;145(4):95-9. Epub 1999/08/26. doi: 10.1136/vr.145.4.95. PubMed PMID: 10461733.

156.   Simon BT, Steagall PV. The present and future of opioid analgesics in small animal practice. J Vet Pharmacol Ther. 2017;40(4):315-26. Epub 2016/12/03. doi: 10.1111/jvp.12377. PubMed PMID: 27900781.

157.	Camilleri M, Sanders KM. Opiates, the Pylorus, and Gastroparesis. Gastroenterology. 2020;159(2):414-21. doi: https://doi.org/10.1053/j.gastro.2020.04.072.
158.	Kamata M, Nagahama S, Kakishima K, Sasaki N, Nishimura R. Comparison of behavioral effects of morphine and fentanyl in dogs and cats. The Journal of veterinary medical science. 2012;74(2):231-4. Epub 2011/09/29. doi: 10.1292/jvms.10-0565. PubMed PMID: 21952398.
159.	Clutton RE. Opioid Analgesia in Horses. Veterinary Clinics of North America: Equine Practice. 2010;26(3):493-514. doi: https://doi.org/10.1016/j.cveq.2010.07.002.
160.	(APCC) AAPCC. Announcing: The Top 10 Pet Toxins! 2020 [4/21/2021]. Available from: https://www.aspca.org/news/announcing-top-10-pet-toxins.
161.	Khan SA, McLean MK. Toxicology of frequently encountered nonsteroidal anti-inflammatory drugs in dogs and cats. Vet Clin North Am Small Anim Pract. 2012;42(2):289-306, vi-vii. Epub 2012/03/03. doi: 10.1016/j.cvsm.2012.01.003. PubMed PMID: 22381180.
162.	Knych HK. Nonsteroidal Anti-inflammatory Drug Use in Horses. Veterinary Clinics of North America: Equine Practice. 2017;33(1):1-15. doi: https://doi.org/10.1016/j.cveq.2016.11.001.
163.	Adrian D, Papich MG, Baynes R, Stafford E, Lascelles BDX. The pharmacokinetics of gabapentin in cats. Journal of veterinary internal medicine. 2018;32(6):1996-2002. Epub 2018/10/12. doi: 10.1111/jvim.15313. PubMed PMID: 30307652; PMCID: PMC6271300.
164.	Gold JR, Grubb TL, Green S, Cox S, Villarino NF. Plasma disposition of gabapentin after the intragastric administration of escalating doses to adult horses. Journal of veterinary internal medicine. 2020;34(2):933-40. Epub 2020/02/09. doi: 10.1111/jvim.15724. PubMed PMID: 32034928; PMCID: PMC7096665.
165.	Guedes AGP, Meadows JM, Pypendop BH, Johnson EG, Zaffarano B. Assessment of the effects of gabapentin on activity levels and owner-perceived mobility impairment and quality of life in osteoarthritic geriatric cats. Journal of the American Veterinary Medical Association. 2018;253(5):579-85. Epub 2018/08/16. doi: 10.2460/javma.253.5.579. PubMed PMID: 30110208.
166.	Philbrick A. Pain Management in Companion Animals. America's Pharmacist [Internet]. 2015; APJUL15-CE:[43-52 pp.]. Available from: http://www.ncpa.co/issues/APJUL15-CE.pdf.
167.	Peck C. The adverse effect profile of gabapentin in dogs. A retrospective questionnaire study. Uppsala: Swedish University of Agricultural Sciences; 2017.
168.	Wagner K, Inceoglu B, Gill SS, Hammock BD. Epoxygenated fatty acids and soluble epoxide hydrolase inhibition: novel mediators of pain reduction. J Agric Food Chem. 2011;59(7):2816-24. doi: 10.1021/jf102559q. PubMed PMID: 20958046; PMCID: 3483885.
169.	McReynolds C, Morisseau C, Wagner K, Hammock B. Epoxy Fatty Acids Are Promising Targets for Treatment of Pain, Cardiovascular Disease and Other Indications Characterized by Mitochondrial Dysfunction, Endoplasmic Stress and Inflammation. Advances in experimental medicine and biology. 2020;1274:71-99. Epub 2020/09/08. doi: 10.1007/978-3-030-50621-6_5. PubMed PMID: 32894508; PMCID: PMC7737916.
170.	Shihadih DS, Harris TR, Kodani SD, Hwang SH, Lee KSS, Mavangira V, Hamamoto B, Guedes A, Hammock BD, Morisseau C. Selection of Potent Inhibitors of Soluble Epoxide Hydrolase for Usage in Veterinary Medicine. Frontiers in veterinary science. 2020;7:580. Epub 2020/10/03. doi: 10.3389/fvets.2020.00580. PubMed PMID: 33005645; PMCID: PMC7479175.
171.	Guedes A, Galuppo L, Hood D, Hwang SH, Morisseau C, Hammock BD. Soluble epoxide hydrolase activity and pharmacologic inhibition in horses with chronic severe laminitis. Equine veterinary journal. 2017;49(3):345-51. Epub 2016/06/25. doi: 10.1111/evj.12603. PubMed PMID: 27338788; PMCID: PMC5580818.

172.   McReynolds CB, Hwang SH, Yang J, Wan D, Wagner K, Morisseau C, Li D, Schmidt WK, Hammock BD. Pharmaceutical Effects of Inhibiting the Soluble Epoxide Hydrolase in Canine Osteoarthritis. Frontiers in pharmacology. 2019;10:533. Epub 2019/06/20. doi: 10.3389/fphar.2019.00533. PubMed PMID: 31214021; PMCID: PMC6554663.

173.   Wagner K, Inceoglu B, Dong H, Yang J, Hwang SH, Jones P, Morisseau C, Hammock BD. Comparative efficacy of 3 soluble epoxide hydrolase inhibitors in rat neuropathic and inflammatory pain models. European journal of pharmacology. 2013;700(1-3):93-101. Epub 2013/01/02. doi: 10.1016/j.ejphar.2012.12.015. PubMed PMID: 23276668; PMCID: PMC3578047.

174.   Wagner K, Yang J, Inceoglu B, Hammock BD. Soluble epoxide hydrolase inhibition is antinociceptive in a mouse model of diabetic neuropathy. The journal of pain : official journal of the American Pain Society. 2014;15(9):907-14. Epub 2014/06/14. doi: 10.1016/j.jpain.2014.05.008. PubMed PMID: 24924124; PMCID: PMC4150748.

175.   Jones PD, Wolf NM, Morisseau C, Whetstone P, Hock B, Hammock BD. Fluorescent substrates for soluble epoxide hydrolase and application to inhibition studies. Analytical biochemistry. 2005;343(1):66-75. doi: 10.1016/j.ab.2005.03.041. PubMed PMID: 15963942; PMCID: 1447601.

176.   Ulu A, Appt S, Morisseau C, Hwang SH, Jones PD, Rose TE, Dong H, Lango J, Yang J, Tsai HJ, Miyabe C, Fortenbach C, Adams MR, Hammock BD. Pharmacokinetics and in vivo potency of soluble epoxide hydrolase inhibitors in cynomolgus monkeys. British journal of pharmacology. 2012;165(5):1401-12. doi: 10.1111/j.1476-5381.2011.01641.x. PubMed PMID: 21880036; PMCID: 3372725.

177.   Guedes AGP, Aristizabal F, Sole A, Adedeji A, Brosnan R, Knych H, Yang J, Hwang SH, Morisseau C, Hammock BD. Pharmacokinetics and antinociceptive effects of the soluble epoxide hydrolase inhibitor t-TUCB in horses with experimentally induced radiocarpal synovitis. J Vet Pharmacol Ther. 2018;41(2):230-8. Epub 2017/10/27. doi: 10.1111/jvp.12463. PubMed PMID: 29067696; PMCID: PMC5920688.

178.   Sams RA. Principles of drug disposition in the horse. The Veterinary clinics of North America Equine practice. 1987;3(1):221-50. Epub 1987/04/01. doi: 10.1016/s0749-0739(17)30699-5. PubMed PMID: 3555729.

179.   Visser M, Zaya MJ, Locuson CW, Boothe DM, Merritt DA. Comparison of predicted intrinsic hepatic clearance of 30 pharmaceuticals in canine and feline liver microsomes. Xenobiotica; the fate of foreign compounds in biological systems. 2019;49(2):177-86. Epub 2018/02/07. doi: 10.1080/00498254.2018.1437933. PubMed PMID: 29405805.

180.   Lautz LS, Jeddi MZ, Girolami F, Nebbia C, Dorne JLCM. Metabolism and pharmacokinetics of pharmaceuticals in cats (Felix sylvestris catus) and implications for the risk assessment of feed additives and contaminants. Toxicology letters. 2021;338:114-27. doi: https://doi.org/10.1016/j.toxlet.2020.11.014.

181.   Liu JY, Lin YP, Qiu H, Morisseau C, Rose TE, Hwang SH, Chiamvimonvat N, Hammock BD. Substituted phenyl groups improve the pharmacokinetic profile and anti-inflammatory effect of urea-based soluble epoxide hydrolase inhibitors in murine models. European journal of pharmaceutical sciences : official journal of the European Federation for Pharmaceutical Sciences. 2013;48(4-5):619-27. Epub 2013/01/08. doi: 10.1016/j.ejps.2012.12.013. PubMed PMID: 23291046; PMCID: PMC3596469.

182.   Hammock BD, McReynolds CB, Wagner K, Buckpitt A, Cortes-Puch I, Croston G, Lee KSS, Yang J, Schmidt WK, Hwang SH. Movement to the Clinic of Soluble Epoxide Hydrolase

Inhibitor EC5026 as an Analgesic for Neuropathic Pain and for Use as a Nonaddictive Opioid Alternative. Journal of medicinal chemistry. 2021. doi: 10.1021/acs.jmedchem.0c01886. PubMed PMID: 33550801.

183.   Lautz LS, Jeddi MZ, Girolami F, Nebbia C, Dorne J. Metabolism and pharmacokinetics of pharmaceuticals in cats (Felix sylvestris catus) and implications for the risk assessment of feed additives and contaminants. Toxicology letters. 2021;338:114-27. Epub 2020/12/01. doi: 10.1016/j.toxlet.2020.11.014. PubMed PMID: 33253781.

184.   Shugarts S, Benet LZ. The role of transporters in the pharmacokinetics of orally administered drugs. Pharmaceutical research. 2009;26(9):2039-54. Epub 2009/07/02. doi: 10.1007/s11095-009-9924-0. PubMed PMID: 19568696; PMCID: PMC2719753.

185.   Wu CY, Benet LZ. Predicting drug disposition via application of BCS: transport/absorption/ elimination interplay and development of a biopharmaceutics drug disposition classification system. Pharmaceutical research. 2005;22(1):11-23. Epub 2005/03/18. doi: 10.1007/s11095-004-9004-4. PubMed PMID: 15771225.

186.   Goh LB, Spears KJ, Yao D, Ayrton A, Morgan P, Roland Wolf C, Friedberg T. Endogenous drug transporters in in vitro and in vivo models for the prediction of drug disposition in man. Biochemical pharmacology. 2002;64(11):1569-78. Epub 2002/11/14. doi: 10.1016/s0006-2952(02)01355-2. PubMed PMID: 12429346.

187.   Cho SM, Park SW, Kim NH, Park JA, Yi H, Cho HJ, Park KH, Hwang I, Shin HC. Expression of intestinal transporter genes in beagle dogs. Experimental and therapeutic medicine. 2013;5(1):308-14. Epub 2012/12/20. doi: 10.3892/etm.2012.777. PubMed PMID: 23251289; PMCID: PMC3524273.

188.   An G, Lee KSS, Yang J, Hammock BD. Target-Mediated Drug Disposition-A Class Effect of Soluble Epoxide Hydrolase Inhibitors. Journal of clinical pharmacology. 2021;61(4):531-7. Epub 2020/10/21. doi: 10.1002/jcph.1763. PubMed PMID: 33078430; PMCID: PMC7969377.

189.   Hwang SH, Tsai HJ, Liu JY, Morisseau C, Hammock BD. Orally bioavailable potent soluble epoxide hydrolase inhibitors. Journal of medicinal chemistry. 2007;50(16):3825-40. Epub 2007/07/10. doi: 10.1021/jm070270t. PubMed PMID: 17616115; PMCID: PMC2596069.

190.   Pecic S, Zeki AA, Xu X, Jin GY, Zhang S, Kodani S, Halim M, Morisseau C, Hammock BD, Deng SX. Novel piperidine-derived amide sEH inhibitors as mediators of lipid metabolism with improved stability. Prostaglandins & other lipid mediators. 2018;136:90-5. Epub 2018/03/24. doi: 10.1016/j.prostaglandins.2018.02.004. PubMed PMID: 29567338; PMCID: PMC5970965.

191.   Mahmood I, Martinez M, Hunter RP. Interspecies allometric scaling. Part I: prediction of clearance in large animals. J Vet Pharmacol Ther. 2006;29(5):415-23. Epub 2006/09/09. doi: 10.1111/j.1365-2885.2006.00786.x. PubMed PMID: 16958787.

192.   Tanaka T, Hishitani Y, Ogata A. Monoclonal antibodies in rheumatoid arthritis: comparative effectiveness of tocilizumab with tumor necrosis factor inhibitors. Biologics. 2014;8:141-53. Epub 2014/04/18. doi: 10.2147/btt.s37509. PubMed PMID: 24741293; PMCID: PMC3984066.

193.   Ivers N, Dhalla IA, Allan GM. Opioids for osteoarthritis pain: benefits and risks. Can Fam Physician. 2012;58(12):e708. PubMed PMID: 23242901; PMCID: PMC3520677.

194.   da Costa BR, Reichenbach S, Keller N, Nartey L, Wandel S, Juni P, Trelle S. Effectiveness of non-steroidal anti-inflammatory drugs for the treatment of pain in knee and hip osteoarthritis: a network meta-analysis. Lancet. 2017;390(10090):e21-e33. Epub 2017/07/13. doi: 10.1016/s0140-6736(17)31744-0. PubMed PMID: 28699595.

195.   Marcum ZA, Hanlon JT. Recognizing the Risks of Chronic Nonsteroidal Anti-Inflammatory Drug Use in Older Adults. The annals of long-term care : the official journal of the American Medical Directors Association. 2010;18(9):24-7. Epub 2010/01/01. PubMed PMID: 21857795; PMCID: PMC3158445.

196.   Inceoglu B, Bettaieb A, Haj FG, Gomes AV, Hammock BD. Modulation of mitochondrial dysfunction and endoplasmic reticulum stress are key mechanisms for the wide-ranging actions of epoxy fatty acids and soluble epoxide hydrolase inhibitors. Prostaglandins & other lipid mediators. 2017;133:68-78. Epub 2017/08/30. doi: 10.1016/j.prostaglandins.2017.08.003. PubMed PMID: 28847566.

197.   Shimizu T. Lipid mediators in health and disease: enzymes and receptors as therapeutic targets for the regulation of immunity and inflammation. Annual review of pharmacology and toxicology. 2009;49:123-50. doi: 10.1146/annurev.pharmtox.011008.145616. PubMed PMID: 18834304.

198.   Wagner K, Gilda J, Yang J, Wan D, Morisseau C, Gomes AV, Hammock BD. Soluble epoxide hydrolase inhibition alleviates neuropathy in Akita (Ins2 Akita) mice. Behavioural brain research. 2017;326:69-76. Epub 2017/03/06. doi: 10.1016/j.bbr.2017.02.048. PubMed PMID: 28259677; PMCID: PMC5409858.

199.   Kodani SD, Wan D, Wagner KM, Hwang SH, Morisseau C, Hammock BD. Design and Potency of Dual Soluble Epoxide Hydrolase/Fatty Acid Amide Hydrolase Inhibitors. ACS omega. 2018;3(10):14076-86. Epub 2018/11/10. doi: 10.1021/acsomega.8b01625. PubMed PMID: 30411058; PMCID: PMC6210075 are authors on a patent own by the University of California for compounds presented in this text (WO2017160861). BDH, KMW and SSH are part of Eicosis L.L.C., a company developing sEH inhibitors for clinical trials.

200.   Wolf NM, Morisseau C, Jones PD, Hock B, Hammock BD. Development of a high-throughput screen for soluble epoxide hydrolase inhibition. Analytical biochemistry. 2006;355(1):71-80. doi: 10.1016/j.ab.2006.04.045. PubMed PMID: 16729954; PMCID: 1964503.

201.   O'Brien J, Wilson I, Orton T, Pognan F. Investigation of the Alamar Blue (resazurin) fluorescent dye for the assessment of mammalian cell cytotoxicity. European journal of biochemistry / FEBS. 2000;267(17):5421-6. Epub 2000/08/22. PubMed PMID: 10951200.

202.   Larson EM, Doughman DJ, Gregerson DS, Obritsch WF. A new, simple, nonradioactive, nontoxic in vitro assay to monitor corneal endothelial cell viability. Investigative ophthalmology & visual science. 1997;38(10):1929-33. Epub 1997/10/23. PubMed PMID: 9331256.

203.   Li D, Cui Y, Morisseau C, Gee SJ, Bever CS, Liu X, Wu J, Hammock BD, Ying Y. Nanobody Based Immunoassay for Human Soluble Epoxide Hydrolase Detection Using Polymeric Horseradish Peroxidase (PolyHRP) for Signal Enhancement: The Rediscovery of PolyHRP? Analytical chemistry. 2017;89(11):6248-56. Epub 2017/05/04. doi: 10.1021/acs.analchem.7b01247. PubMed PMID: 28460522; PMCID: PMC5611449.

204.   Brown DC, Boston RC, Coyne JC, Farrar JT. Development and psychometric testing of an instrument designed to measure chronic pain in dogs with osteoarthritis. American journal of veterinary research. 2007;68(6):631-7. Epub 2007/06/05. doi: 10.2460/ajvr.68.6.631. PubMed PMID: 17542696; PMCID: PMC2907349.

205.   Chu KA, Yalkowsky SH. An interesting relationship between drug absorption and melting point. International journal of pharmaceutics. 2009;373(1-2):24-40. Epub 2009/05/12. doi: 10.1016/j.ijpharm.2009.01.026. PubMed PMID: 19429285.

206.   Ito S. Pharmacokinetics 101. Paediatrics & child health. 2011;16(9):535-6. Epub 2012/11/02. PubMed PMID: 23115489; PMCID: PMC3223885.

207. McNulty AL, Rothfusz NE, Leddy HA, Guilak F. Synovial fluid concentrations and relative potency of interleukin-1 alpha and beta in cartilage and meniscus degradation. Journal of orthopaedic research : official publication of the Orthopaedic Research Society. 2013;31(7):1039-45. Epub 2013/03/14. doi: 10.1002/jor.22334. PubMed PMID: 23483596; PMCID: PMC4037157.

208. Attur MG, Patel IR, Patel RN, Abramson SB, Amin AR. Autocrine production of IL-1 beta by human osteoarthritis-affected cartilage and differential regulation of endogenous nitric oxide, IL-6, prostaglandin E2, and IL-8. Proceedings of the Association of American Physicians. 1998;110(1):65-72. Epub 1998/02/14. PubMed PMID: 9460084.

209. Hinson RM, Williams JA, Shacter E. Elevated interleukin 6 is induced by prostaglandin E2 in a murine model of inflammation: possible role of cyclooxygenase-2. Proceedings of the National Academy of Sciences of the United States of America. 1996;93(10):4885-90. Epub 1996/05/14. PubMed PMID: 8643498; PMCID: PMC39374.

210. Gomez GA, Morisseau C, Hammock BD, Christianson DW. Human soluble epoxide hydrolase: structural basis of inhibition by 4-(3-cyclohexylureido)-carboxylic acids. Protein science : a publication of the Protein Society. 2006;15(1):58-64. doi: 10.1110/ps.051720206. PubMed PMID: 16322563; PMCID: 1762130.

211. Tonge PJ. Drug-Target Kinetics in Drug Discovery. ACS chemical neuroscience. 2018;9(1):29-39. Epub 2017/06/24. doi: 10.1021/acschemneuro.7b00185. PubMed PMID: 28640596; PMCID: PMC5767540.

212. Johnson CI, Argyle DJ, Clements DN. In vitro models for the study of osteoarthritis. Veterinary journal. 2016;209:40-9. Epub 2016/02/03. doi: 10.1016/j.tvjl.2015.07.011. PubMed PMID: 26831151.

213. Akkiraju H, Nohe A. Role of Chondrocytes in Cartilage Formation, Progression of Osteoarthritis and Cartilage Regeneration. Journal of developmental biology. 2015;3(4):177-92. Epub 2016/06/28. doi: 10.3390/jdb3040177. PubMed PMID: 27347486; PMCID: PMC4916494.

214. Kapoor M, Martel-Pelletier J, Lajeunesse D, Pelletier JP, Fahmi H. Role of proinflammatory cytokines in the pathophysiology of osteoarthritis. Nature reviews Rheumatology. 2011;7(1):33-42. Epub 2010/12/02. doi: 10.1038/nrrheum.2010.196. PubMed PMID: 21119608.

215. Pelletier JP, McCollum R, Cloutier JM, Martel-Pelletier J. Synthesis of metalloproteases and interleukin 6 (IL-6) in human osteoarthritic synovial membrane is an IL-1 mediated process. The Journal of rheumatology Supplement. 1995;43:109-14. Epub 1995/02/01. PubMed PMID: 7752112.

216. Daheshia M, Yao JQ. The interleukin 1beta pathway in the pathogenesis of osteoarthritis. The Journal of rheumatology. 2008;35(12):2306-12. Epub 2008/10/18. PubMed PMID: 18925684.

217. Dimitroulas T, Duarte RV, Behura A, Kitas GD, Raphael JH. Neuropathic pain in osteoarthritis: a review of pathophysiological mechanisms and implications for treatment. Seminars in arthritis and rheumatism. 2014;44(2):145-54. Epub 2014/06/15. doi: 10.1016/j.semarthrit.2014.05.011. PubMed PMID: 24928208.

218. Rasmussen-Barr E, Held U, Grooten WJ, Roelofs PD, Koes BW, van Tulder MW, Wertli MM. Non-steroidal anti-inflammatory drugs for sciatica. The Cochrane database of systematic reviews. 2016;10:Cd012382. Epub 2016/11/02. doi: 10.1002/14651858.cd012382. PubMed PMID: 27743405.

219. Goswami SK, Rand AA, Wan D, Yang J, Inceoglu B, Thomas M, Morisseau C, Yang GY, Hammock BD. Pharmacological inhibition of soluble epoxide hydrolase or genetic deletion

reduces diclofenac-induced gastric ulcers. Life sciences. 2017;180:114-22. Epub 2017/05/20. doi: 10.1016/j.lfs.2017.05.018. PubMed PMID: 28522175; PMCID: PMC5659729.

220.   Goswami SK, Wan D, Yang J, Trindade da Silva CA, Morisseau C, Kodani SD, Yang GY, Inceoglu B, Hammock BD. Anti-Ulcer Efficacy of Soluble Epoxide Hydrolase Inhibitor TPPU on Diclofenac-Induced Intestinal Ulcers. The Journal of pharmacology and experimental therapeutics. 2016;357(3):529-36. Epub 2016/03/19. doi: 10.1124/jpet.116.232108. PubMed PMID: 26989141; PMCID: Pmc4885505.

221.   Hoffman JM, Creevy KE, Franks A, O'Neill DG, Promislow DEL. The companion dog as a model for human aging and mortality. Aging Cell. 2018;17(3):e12737. doi: 10.1111/acel.12737. PubMed PMID: 29457329; PMCID: PMC5946068.

222.   Arentz M, Yim E, Klaff L, Lokhandwala S, Riedo FX, Chong M, Lee M. Characteristics and Outcomes of 21 Critically Ill Patients With COVID-19 in Washington State. JAMA : the journal of the American Medical Association. 2020;323(16):1612-4. doi: 10.1001/jama.2020.4326. PubMed PMID: 32191259; PMCID: PMC7082763.

223.   Du Y, Tu L, Zhu P, Mu M, Wang R, Yang P, Wang X, Hu C, Ping R, Hu P, Li T, Cao F, Chang C, Hu Q, Jin Y, Xu G. Clinical Features of 85 Fatal Cases of COVID-19 from Wuhan. A Retrospective Observational Study. American journal of respiratory and critical care medicine. 2020;201(11):1372-9. doi: 10.1164/rccm.202003-0543OC. PubMed PMID: 32242738; PMCID: PMC7258652.

224.   Pedersen SF, Ho YC. SARS-CoV-2: a storm is raging. Journal of Clinical Investigation. 2020;130(5):2202-5. doi: 10.1172/Jci137647. PubMed PMID: WOS:000571121100013.

225.   Mehta P, McAuley DF, Brown M, Sanchez E, Tattersall RS, Manson JJ, Hlh Across Speciality Collaboration UK. COVID-19: consider cytokine storm syndromes and immunosuppression. Lancet. 2020;395(10229):1033-4. doi: 10.1016/S0140-6736(20)30628-0. PubMed PMID: 32192578; PMCID: PMC7270045.

226.   Sinha P, Matthay MA, Calfee CS. Is a "Cytokine Storm" Relevant to COVID-19? JAMA Intern Med. 2020;180(9):1152-4. doi: 10.1001/jamainternmed.2020.3313. PubMed PMID: 32602883.

227.   Hammock BD, Wang W, Gilligan MM, Panigrahy D. Eicosanoids: The Overlooked Storm in Coronavirus Disease 2019 (COVID-19)? The American journal of pathology. 2020;190(9):1782-8. Epub 2020/07/11. doi: 10.1016/j.ajpath.2020.06.010. PubMed PMID: 32650004; PMCID: PMC7340586.

228.   Dennis EA, Norris PC. Eicosanoid storm in infection and inflammation. Nature reviews Immunology. 2015;15(8):511-23. Epub 2015/07/04. doi: 10.1038/nri3859. PubMed PMID: 26139350; PMCID: PMC4606863.

229.   Schwarz B, Sharma L, Roberts L, Peng X, Bermejo S, Leighton I, Massana AC, Farhadian S, Ko A, DelaCruz C, Bosio CM. Severe SARS-CoV-2 infection in humans is defined by a shift in the serum lipidome resulting in dysregulation of eicosanoid immune mediators. medRxiv. 2020. doi: 10.1101/2020.07.09.20149849. PubMed PMID: 32676616; PMCID: 7359541.

230.   Hildreth K, Kodani SD, Hammock BD, Zhao L. Cytochrome P450-derived linoleic acid metabolites EpOMEs and DiHOMEs: a review of recent studies. J Nutr Biochem. 2020;86:108484. Epub 2020/08/23. doi: 10.1016/j.jnutbio.2020.108484. PubMed PMID: 32827665; PMCID: PMC7606796.

231.   Sugiyama S, Hayakawa M, Nagai S, Ajioka M, Ozawa T. Leukotoxin, 9, 10-epoxy-12-octadecenoate, causes cardiac failure in dogs. Life sciences. 1987;40(3):225-31. Epub 1987/01/19. doi: 10.1016/0024-3205(87)90336-5. PubMed PMID: 3796222.

232. Zheng J, Plopper CG, Lakritz J, Storms DH, Hammock BD. Leukotoxin-diol: a putative toxic mediator involved in acute respiratory distress syndrome. American journal of respiratory cell and molecular biology. 2001;25(4):434-8. doi: 10.1165/ajrcmb.25.4.4104. PubMed PMID: 11694448.

233. Yang J, Bruun DA, Wang C, Wan D, McReynolds CB, Phu K, Inceoglu B, Lein PJ, Hammock BD. Lipidomes of brain from rats acutely intoxicated with diisopropylfluorophosphate identifies potential therapeutic targets. Toxicology and applied pharmacology. 2019;382:114749. Epub 2019/09/16. doi: 10.1016/j.taap.2019.114749. PubMed PMID: 31521729; PMCID: PMC6957308.

234. Yang J, Schmelzer K, Georgi K, Hammock BD. Quantitative profiling method for oxylipin metabolome by liquid chromatography electrospray ionization tandem mass spectrometry. Analytical chemistry. 2009;81(19):8085-93. doi: 10.1021/ac901282n. PubMed PMID: 19715299; PMCID: 3290520.

235. Benjamini Y, Krieger AM, Yekutieli D. Adaptive linear step-up procedures that control the false discovery rate. Biometrika. 2006;93(3):491-507. doi: 10.1093/biomet/93.3.491.

236. Greene JF, Hammock BD. Toxicity of linoleic acid metabolites. Advances in experimental medicine and biology. 1999;469:471-7. Epub 2000/02/10. PubMed PMID: 10667370.

237. Deol P, Fahrmann J, Yang J, Evans JR, Rizo A, Grapov D, Salemi M, Wanichthanarak K, Fiehn O, Phinney B, Hammock BD, Sladek FM. Omega-6 and omega-3 oxylipins are implicated in soybean oil-induced obesity in mice. Scientific reports. 2017;7(1):12488. Epub 2017/10/04. doi: 10.1038/s41598-017-12624-9. PubMed PMID: 28970503.

238. Kosaka K, Suzuki K, Hayakawa M, Sugiyama S, Ozawa T. Leukotoxin, a linoleate epoxide: its implication in the late death of patients with extensive burns. Molecular and cellular biochemistry. 1994;139(2):141-8. Epub 1994/10/26. doi: 10.1007/bf01081737. PubMed PMID: 7862104.

239. Kodani SD, Hammock BD. The 2014 Bernard B. Brodie award lecture-epoxide hydrolases: drug metabolism to therapeutics for chronic pain. Drug metabolism and disposition: the biological fate of chemicals. 2015;43(5):788-802. Epub 2015/03/13. doi: 10.1124/dmd.115.063339. PubMed PMID: 25762541; PMCID: Pmc4407705.

240. Hansen AE, Haggard ME, Boelsche AN, Adam DJ, Wiese HF. Essential fatty acids in infant nutrition. III. Clinical manifestations of linoleic acid deficiency. The Journal of nutrition. 1958;66(4):565-76. Epub 1958/12/10. doi: 10.1093/jn/66.4.565. PubMed PMID: 13621281.

241. Arnardottir H, Pawelzik S-C, Öhlund Wistbacka U, Artiach G, Hofmann R, Reinholdsson I, Braunschweig F, Tornvall P, Religa D, Bäck M. Stimulating the Resolution of Inflammation Through Omega-3 Polyunsaturated Fatty Acids in COVID-19: Rationale for the COVID-Omega-F Trial. Frontiers in physiology. 2021;11(1748). doi: 10.3389/fphys.2020.624657.

242. Taha AY, Cheon Y, Faurot KF, Macintosh B, Majchrzak-Hong SF, Mann JD, Hibbeln JR, Ringel A, Ramsden CE. Dietary omega-6 fatty acid lowering increases bioavailability of omega-3 polyunsaturated fatty acids in human plasma lipid pools. Prostaglandins, leukotrienes, and essential fatty acids. 2014;90(5):151-7. Epub 2014/03/29. doi: 10.1016/j.plefa.2014.02.003. PubMed PMID: 24675168; PMCID: PMC4035030.

243. Langlois PL, D'Aragon F, Hardy G, Manzanares W. Omega-3 polyunsaturated fatty acids in critically ill patients with acute respiratory distress syndrome: A systematic review and meta-analysis. Nutrition (Burbank, Los Angeles County, Calif). 2019;61:84-92. Epub 2019/02/01. doi: 10.1016/j.nut.2018.10.026. PubMed PMID: 30703574.

244. Grant DF, Greene JF, Pinot F, Borhan B, Moghaddam MF, Hammock BD, McCutchen B, Ohkawa H, Luo G, Guenthner TM. Development of an in situ toxicity assay system using recombinant baculoviruses. Biochemical pharmacology. 1996;51(4):503-15. PubMed PMID: 8619897.

245. Toelzer C, Gupta K, Yadav SKN, Borucu U, Davidson AD, Kavanagh Williamson M, Shoemark DK, Garzoni F, Staufer O, Milligan R, Capin J, Mulholland AJ, Spatz J, Fitzgerald D, Berger I, Schaffitzel C. Free fatty acid binding pocket in the locked structure of SARS-CoV-2 spike protein. Science. 2020;370(6517):725-30. doi: 10.1126/science.abd3255. PubMed PMID: 32958580.

246. Dierckx T, van Elslande J, Salmela H, Decru B, Wauters E, Gunst J, Van Herck Y, Wauters J, Stessel B, Vermeersch P. The metabolic fingerprint of COVID-19 severity. medRxiv. 2020:2020.11.09.20228221. doi: 10.1101/2020.11.09.20228221.

247. Heyworth IT, Hazell ML, Linehan MF, Frank TL. How do common chronic conditions affect health-related quality of life? The British journal of general practice : the journal of the Royal College of General Practitioners. 2009;59(568):e353-8. Epub 2009/08/07. doi: 10.3399/bjgp09X453990. PubMed PMID: 19656444; PMCID: PMC2765853.

248. Samiei Siboni F, Alimoradi Z, Atashi V, Alipour M, Khatooni M. Quality of Life in Different Chronic Diseases and Its Related Factors. International journal of preventive medicine. 2019;10:65. Epub 2019/06/15. doi: 10.4103/ijpvm.IJPVM_429_17. PubMed PMID: 31198500; PMCID: PMC6547796.

249. Pesce NL. The U.S. dropped majorly on the index that measures well-being — here's where it ranks now 2020 [cited 2021 1/18/2021]. Available from: https://www.marketwatch.com/story/the-us-drops-to-no-28-on-this-global-well-being-index-2020-09-10.

250. O'Neill A. Life expectancy in the United States, 1860-2020 2020 [cited 2021]. Available from: https://www.statista.com/statistics/1040079/life-expectancy-united-states-all-time/.

251. Baedeker M, Ringel M, Schulze U. 2020 FDA approvals: momentum kept despite COVID-19, but value falls. Nature reviews Drug discovery. 2021. Epub 2021/01/17. doi: 10.1038/d41573-021-00016-8. PubMed PMID: 33452492.

252. Vincent Rajkumar S. The high cost of prescription drugs: causes and solutions. Blood Cancer J. 2020;10(6):71. doi: 10.1038/s41408-020-0338-x. PubMed PMID: 32576816; PMCID: PMC7311400.

253. FDA. Preventable Adverse Drug Reactions: A Focus on Drug Interactions 2018 [1/23/2021]. Available from: https://www.fda.gov/drugs/drug-interactions-labeling/preventable-adverse-drug-reactions-focus-drug-interactions#:~:text=These%20studies%20estimate%20that%206.7,a%20fatality%20rate%20of%200.32%25.&text=If%20these%20estimates%20are%20correct,causing%20over%20106%2C000%20deaths%20annually.

254. Pitcher MH, Von Korff M, Bushnell MC, Porter L. Prevalence and Profile of High-Impact Chronic Pain in the United States. The journal of pain : official journal of the American Pain Society. 2019;20(2):146-60. Epub 2018/08/11. doi: 10.1016/j.jpain.2018.07.006. PubMed PMID: 30096445.

255. Kihara Y. Introduction: Druggable Lipid Signaling Pathways. Advances in experimental medicine and biology. 2020;1274:1-4. doi: 10.1007/978-3-030-50621-6_1. PubMed PMID: 32894504.

256.	Evans JF, Hutchinson JH. Seeing the future of bioactive lipid drug targets. Nature chemical biology. 2010;6(7):476-9. doi: 10.1038/nchembio.394. PubMed PMID: 20559310.

257.	Zheng J, Plopper CG, Lakritz J, Storms DH, Hammock BD. Leukotoxin-diol - A putative toxic mediator involved in acute respiratory distress syndrome. American journal of respiratory cell and molecular biology. 2001;25(4):434-8. doi: DOI 10.1165/ajrcmb.25.4.4104. PubMed PMID: WOS:000172114600007.